Assessing a Ten-Fold Increase in the Chesapeake Bay Native Oyster Population

A Report to the EPA Chesapeake Bay Program

July 2005

Carl F. Cerco and Mark R. Noel

US Army Engineer Research and Development Center, Vicksburg MS

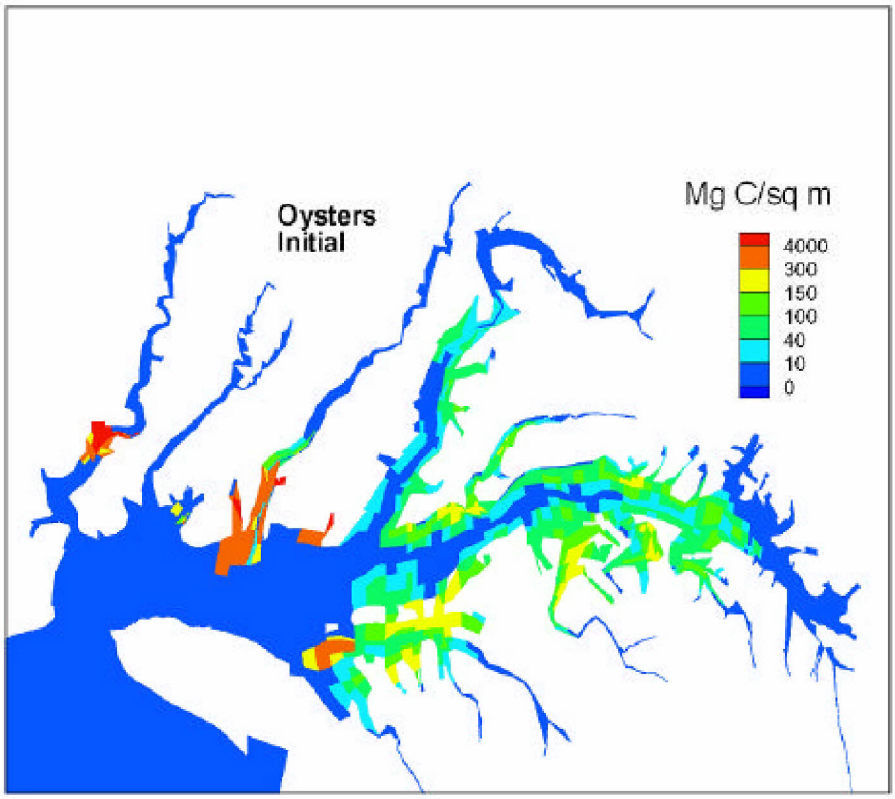

Abstract

The Chesapeake Bay Environmental Model Package (CBEMP) was used to assess the environmental benefits of a ten-fold increase in native oysters in Chesapeake Bay. The CBEMP consists of a coupled system of models including a three-dimensional hydrodynamic model, a three-dimensional eutrophication model, and a sediment diagenesis model. The existing CBEMP benthos submodel was modified to specifically represent the Virginia oyster, *Crassostrea virginica*. The ten-fold oyster restoration is computed to increase summer-average, bottom, dissolved oxygen in the deep waters of the bay (depth > 12.9 m) by 0.25 g m^{-3}. Summer-average system-wide surface chlorophyll declines by 1 mg m^{-3}. Filtration of phytoplankton from the water column produces net removal of 30,000 kg d^{-1} nitrogen through sediment denitrification and sediment retention. A significant benefit of oyster restoration is enhancement of submerged aquatic vegetation. Calculated summer-average biomass improves by 25% for a ten-fold increase in oyster biomass. Oyster restoration is most beneficial in shallow regions with limited exchange rather than in regions of great depth, large volume and spatial extent.

Point of Contact

Carl F. Cerco, PhD, PE
Research Hydrologist
Mail Stop EP-W
US Army ERDC
3909 Halls Ferry Road
Vicksburg MS 39180 USA
601-634-4207 (voice)
601-634-3129 (fax)
cercoc@wes.army.mil

1 Introduction

More than twenty years ago, grazing by benthos was implicated as a controlling process on phytoplankton concentration in tidal waters (Cloern 1982, Cohen et al. 1984). Officer et al. (1982) identified criteria for regimes in which benthic control is possible. They were:

1. Shallow water depths in the range of 2 to 10 m;
2. A large and widespread benthic filter feeding population;
3. Partially-enclosed regions of substantial size with poor hydrodynamic exchange;
4. Adequate nutrient supplies; and
5. Regions that show relatively constant and low phytoplankton levels.

A link between decimation of the oyster population and deteriorating water quality in Chesapeake Bay was proposed by Newell (1988). Newell calculated the 19th century oyster population could filter the entire volume of the bay in less than a week and suggested an increase in the oyster population could significantly improve water quality by removing large quantities of particulate carbon. Gerritsen et al. (1994) largely countered Newell's suggestion. They noted that benthic filter feeders can be dominant consumers in shallow portions of the bay but are suppressed in deeper portions. Processes leading to suppression include hydrodynamic limits and hypoxia. Gerritsen et al. concluded that use of filter-feeding bivalves to improve water quality in large estuaries is limited by the depth and width of the estuary.

Recent research on the role of oysters in Chesapeake Bay has focused on processes by which oysters influence their immediate environment rather than on system-wide effects. Newell et al. (2002) provided experimental evidence that denitrification of nitrogen in oyster feces may enhance nitrogen removal in estuaries. They examined the effect of light on algal biomass and nutrient fluxes at the sediment-water interface and suggested that clarification of the water column by filter feeders may provoke a shift to an ecosystem dominated by benthic primary production. Porter et al. (2004) placed oysters in experimental mesocosms. Their work largely supported the suggestions by Newell et al. (2002). The found that oysters shifted processes to the sediment by decreasing phytoplankton biomass and increasing light penetration to the bottom. Increased

light penetration stimulated microphytobenthos, which diminished nutrient regeneration from the sediments. They found, however, that high bottom shear stress eroded the microphytobenthos and cautioned that, under high bottom shear conditions, nutrient regeneration from the sediments may increase. Most recently, Newell and Koch (2004) employed a model to examine the interactions between oysters, turbidity, and seagrass density. They predicted that restoration of oysters has the potential to reduce turbidity in shallow estuaries and facilitate efforts to restore seagrasses.

Our own interest in oysters stems from the "Chesapeake 2000" agreement. The agreement, signed by the executives of the Commonwealth of Pennsylvania, the State of Maryland, the Commonwealth of Virginia, the District of Columbia, the US Environmental Protection Agency, and the Chesapeake Bay Commission, rededicates the individuals and entities to the "restoration and protection of the ecological integrity, productivity, and beneficial uses of the Chesapeake Bay system." The agreement sets specific goals including:

> Restore, enhance and protect the finfish, shellfish and other living resources, their habitats and ecological relationships to sustain all fisheries and provide for a balanced ecosystem.

The agreement lists methods to achieve this goal including:

> By 2010, achieve, at a minimum, a tenfold increase in native oysters in the Chesapeake Bay, based on a 1994 baseline.

and

> By 2004, assess the effects of different population levels of filter feeders such as menhaden, oysters and clams on Bay water quality and habitat.

The environmental effects of a ten-fold increase in population of native oysters were assessed by incorporating oysters into the Chesapeake Bay Environmental Model Package (CBEMP), a comprehensive mathematical model of physical and eutrophication processes in the bay and its tidal tributaries. This report is the primary documentation for the assessment.

The Chesapeake Bay Environmental Model Package

Three models are at the heart of the CBEMP. Distributed flows and loads from the watershed are computed with a highly-modified version of the HSPF model (Bicknell et al. 1996). These flows are input to the CH3D-WES hydrodynamic model (Johnson et al. 1993) that computes three-dimensional intra-tidal transport. Computed loads and transport are input to the CE-QUAL-ICM eutrophication model (Cerco and Cole 1993) which computes algal biomass, nutrient cycling, and dissolved oxygen, as well as numerous additional constituents and processes. The eutrophication model incorporates a predictive sediment diagenesis component (DiToro and Fitzpatrick 1993).

The first coupling of these models simulated the period 1984-1986. Emphasis in the model application was on examination of bottom-water anoxia. Circa 1992, management emphasis shifted from dissolved oxygen, a living-resource indicator, to living resources themselves. In response, the computational grid was refined to emphasize resource-rich areas (Wang and Johnson 2000) and living resources including benthos (Meyers et al. 2000), zooplankton (Cerco and Meyers 2000), and submerged aquatic vegetation (Cerco and Moore 2001) were added to the model. The simulation period was extended from 1985 to 1994.

Model improvements to address the issues raised by the Chesapeake 2000 Agreement started soon after the agreement was signed. The computational grid was further refined and plans were made to incorporate new living resources into the model. At the same time, regulatory forces were shaping the direction of management efforts. Regulatory agencies in Maryland listed the state's portion of Chesapeake Bay as "impaired." The US Environmental Protection Agency added bay waters within Virginia to the impaired list. Impairments in the bay were defined as low dissolved oxygen, excessive chlorophyll concentration, and diminished water clarity. Management emphasis shifted from living resources back to living-resource indicators: dissolved oxygen, chlorophyll, and clarity. A model recalibration was undertaken, with emphasis on improved accuracy in the computation of the three key indicators.

A revision of the CBEMP was delivered in 2002 (Cerco and Noel 2004) and used in development of the most recent nutrient and solids load allocations in the bay. This version of the model is used to examine the impact of the tenfold increase in native oysters. The 2002 CBEMP employs nutrient and solids loads from Phase 4.3 of the watershed model (Linker et al. 2000). (Documentation may be found on the Chesapeake Bay Program web site http://www.chesapeakebay.net/modsc.htm.) Nutrient and solids loads are computed on a daily basis for 94 sub-watersheds of the 166,000 km^2 Chesapeake Bay watershed and are routed to individual model cells based on local watershed characteristics and on drainage area contributing to the cell. The hydrodynamic and eutrophication models operate on a grid of 13,000 cells. The grid contains 2,900 surface cells ($\approx$4 km^2) and employs non-orthogonal curvilinear coordinates in the horizontal plane. Z coordinates are used in the vertical direction, which is up to 19 layers deep. Depth of the surface cells is 2.1 m at mean tide and varies as a function of tide, wind, and other forcing functions. Depth of sub-surface cells is fixed at 1.5 m. A band of littoral cells, 2.1 m deep at mean tide, adjoins the shoreline throughout most of the system. Ten years, 1985-1994, are simulated continuously using time steps of $\approx$5 minutes (hydrodynamic model) and $\approx$15 minutes (eutrophication model).

References

Bicknell, B., Imhoff, J., Kittle, J., Donigian, A., Johanson, R., and Barnwell, T. (1996). "Hydrologic simulation program - FORTRAN user's manual for release 11," United States Environmental Protection Agency Environmental Research Laboratory, Athens GA.

Cerco, C., and Cole, T. (1993). "Three-dimensional eutrophication model of Chesapeake Bay," *Journal of Environmental Engineering*, 119(6), 1006-10025.

Cerco, C., and Meyers, M. (2000). "Tributary refinements to the Chesapeake Bay Model," *Journal of Environmental Engineering*, 126(2), 164-174.

Cerco, C., and Moore, K. (2001). "System-wide submerged aquatic vegetation model for Chesapeake Bay," *Estuaries*, 24(4), 522-534.

Cerco, C., and Noel, M. (2004). "The 2002 Chesapeake Bay eutrophication model," EPA 903-R-04-004, Chesapeake Bay Program Office, US Environmental Protection Agency, Annapolis, MD.

Cloern, J. (1982). "Does the benthos control phytoplankton biomass in south San Francisco Bay?," *Marine Ecology Progress Series*, 9, 191-202.

Cohen, R., Dresler, P., Phillips, E., and Cory, R. (1984). "The effect of the Asiatic clam, *Corbicula fluminea*, on phytoplankton of the Potomac River, Maryland," *Limnology and Oceanography*, 29(1), 170-180.

DiToro, D., and Fitzpatrick, J. (1993). "Chesapeake Bay sediment flux model," Contract Report EL-93-2, US Army Engineer Waterways Experiment Station, Vicksburg, MS.

Gerritsen, J., Holland, A., and Irvine, D. (1994). "Suspension-feeding bivalves and the fate of primary production: An estuarine model applied to Chesapeake Bay," *Estuaries*, 17(2), 403-416.

Johnson, B., Kim, K., Heath, R., Hsieh, B., and Butler, L. (1993). "Validation of a three-dimensional hydrodynamic model of Chesapeake Bay," *Journal of Hydraulic Engineering*, 199(1), 2-20.

Linker, L., Shenk, G., Dennis, R., and Sweeney, J. (2000). "Cross-media models of the Chesapeake Bay watershed and airshed," *Water Quality and Ecosystem Modeling*, 1(1-4), 91-122.

Meyers, M., DiToro, D., and Lowe, S. (2000). "Coupling suspension feeders to the Chesapeake Bay eutrophication model," *Water Quality and Ecosystem Modeling*, 1(1-4), 123-140.

Newell, R. (1988). "Ecological changes in Chesapeake Bay: Are they the result of overharvesting the American oyster (*Crassostrea virginica*)?," *Understanding the estuary – Advances in Chesapeake Bay Research.* Publication 129, Chesapeake Research Consortium, Baltimore, 536-546.

Newell, R., Cornwell, J., and Owens, M. (2002). "Influence of simulated bivalve biodeposition and microphytobenthos on sediment nitrogen dynamics," Limnology and Oceanography, 47(5), 1367-1379.

Newell, R., and Koch, E. (2004). "Modeling seagrass density and distribution in response to changes in turbidity stemming from bivalve filtration and seagrass sediment stabilization," *Estuaries*, 27(5), 793-806.

Officer, C., Smayda, T., and Mann, R. (1982). "Benthic filter feeding: A natural eutrophication control," *Marine Ecology Progress Series*, 9, 203-210.

Porter, E., Cornwell, J., and Sanford, L. (2004). "Effect of oysters *Crassostrea virginica* and bottom shear velocity on benthic pelagic coupling and estuarine water quality," *Marine Ecology Progress Series*, 271, 61-75.

Wang, H., and Johnson, B. (2000). "Validation and application of the second-generation three-dimensional hydrodynamic model of Chesapeake Bay," *Water Quality and Ecosystem Modeling*, 1(1-4), 51-90.

2 The Oyster Model

Introduction

The ultimate aim of eutrophication modeling is to preserve precious living resources. Usually, the modeling process involves the simulation of living-resource indicators such as dissolved oxygen. For the "Virginia Tributary Refinements" phase of the Chesapeake Bay modeling (Cerco et al. 2002), a decision was made to initiate direct interactive simulation of three living resource groups: zooplankton, benthos, and SAV.

Benthos were included in the model because they are an important food source for crabs, finfish, and other economically and ecologically significant biota. In addition, benthos can exert a substantial influence on water quality through their filtering of overlying water. Benthos within the model were divided into two groups: deposit feeders and filter feeders (Figure 1). The deposit-feeding group represents benthos that live within bottom sediments and feed on deposited material. The filter-feeding group represents benthos that live at the sediment surface and feed by filtering overlying water. The primary reference for the benthos model (HydroQual, 2000) is available on-line at http://www.chesapeakebay.net/modsc.htm. Less comprehensive descriptions may be found in Cerco and Meyers (2000) and in Meyers at al. (2000).

The benthos model incorporates three filter-feeding groups: 1) *Rangea cuneata*, which inhabit oligohaline and lower mesohaline portions of the system; 2) *Macoma baltica*, which inhabit mesohaline portions of the system; and 3) *Corbicula fluminea*, which are found in the tidal fresh portion of the Potomac. These organisms were selected based on their dominance of total filter-feeding biomass and on their widespread distribution. The distributions of the organisms within the model grid were assigned based on observations from the Chesapeake Bay benthic monitoring program (http://www.chesapeakebay.net/data/index.htm). Oysters were neglected in the initial application of the benthos model. The primary reasoning was that oyster biomass was considered negligible relative to the most abundant organisms.

Oysters

The oyster model builds on the concepts established in the benthos model. The existing benthos model was left untouched. The code was duplicated and one portion was modified for specific application to native

oysters, *Crassostrea virginica*. The original model assigned one of the three species exclusively to a model cell. In the revised model, oysters may coexist and compete with the other filter feeders. The fundamental state variable is oyster carbon, quantified as mass per unit area. The minimum area represented is the quadrilateral model cell, which is typically 1 to 2 km on a side. Oyster biomass and processes are averaged over the cell area. Oysters filter particulate matter, including carbon, nitrogen, phosphorus, silica, and inorganic solids from the water column. Particulate matter is deposited in the sediments as feces and pseudofeces. Respiration removes dissolved oxygen from the water column while excretion returns dissolved nitrogen and phosphorus.

Particulate carbon is removed from the water column by the filtration process. Filtration rate is affected by temperature, salinity, suspended solids concentration, and dissolved oxygen. The amount of carbon filtered may exceed the oyster's ingestion capacity. In that case, the excess of filtration over ingestion is deposited in the sediments as pseudofeces (Figure 2). A portion of the carbon ingested is refractory or otherwise unavailable for nutrition. The unassimilated fraction is deposited in the sediments as feces. Biomass accumulation (or diminishment) is determined by the difference between carbon assimilated and lost through respiration and mortality. Respiration losses remove dissolved oxygen from the water column. Mortality losses are deposited to the sediments as particulate carbon.

The nutrients nitrogen and phosphorus constitute a constant fraction of oyster biomass. Particulate nitrogen and phosphorus, filtered from the water column, are subject to ingestion and assimilation. Assimilated nutrients that are not accumulated in biomass or lost to the sediments through mortality are excreted to the water column in dissolved inorganic form. All filtered particulate silica is deposited to the sediments or excreted to the water column. A fraction (~ 10%) of filtered inorganic solids is deposited to the sediments. The fraction is determined by the net settling velocity specified in the suspended solids algorithms. The remainder is considered to be resuspended.

The mass-balance equation for oyster biomass is:

$$\frac{dO}{dt} = \alpha \cdot Fr \cdot POC \cdot IF \cdot (1 - RF) \cdot O - BM \cdot O - \beta \cdot O \quad \textbf{(1)}$$

in which:

O = oyster biomass (g C m^{-2})
a = assimilation efficiency ($0 < a < 1$)
Fr = filtration rate (m^3 g^{-1} oyster carbon d^{-1})
POC = particulate organic carbon in overlying water (g m^{-3})
IF = fraction ingested ($0 < IF < 1$)
RF = respiratory fraction ($0 < RF < 1$)
BM = basal metabolic rate (d^{-1})
ß = specific mortality rate (d^{-1})
t = time (d)

The assimilation efficiency is specified individually for each form of particulate organic matter in the water column. The respiratory fraction represents active respiratory losses associated with feeding activity. Basal metabolism represents passive respiratory losses.

Filtration

Filtration rate is represented in the model as a maximum or optimal rate that is modified by ambient temperature, suspended solids, salinity, and dissolved oxygen:

$$Fr = f(T) \cdot f(TSS) \cdot f(S) \cdot f(DO) \cdot Fr\max \qquad \textbf{(2)}$$

in which:

f(T) = effect of temperature on filtration rate ($0 \leq f(T) \leq 1$)
f(TSS) = effect of suspended solids on filtration rate ($0 \leq f(TSS) \leq 1$)
f(S) = effect of salinity on filtration rate ($0 \leq f(S) \leq 1$)
f(DO) = effect of dissolved oxygen on filtration rate ($0 \leq f(DO) \leq 1$)
Frmax = maximum filtration rate ($m^3\ g^{-1}$ oyster carbon d^{-1})

Bivalve filtration rate, quantified as water volume cleared of particles per unit biomass per unit time (Winter 1978), is typically derived from observed rates of particle removal from water overlying a known bivalve biomass (Doering et al. 1986, Doering and Oviatt 1986, Riisgard 1988, Newell and Koch 2004). Since particle retention depends on particle size and composition (Riisgard 1988, Langdon and Newell 1990), correct quantification of filtration requires a particle distribution that represents the natural distribution in the study system (Doering and Oviatt 1986). Filtration rate for our model was based primarily on measures (Jordan 1987) conducted in a laboratory flume maintained at ambient conditions in the adjacent Choptank River, a mesohaline Chesapeake Bay tributary that supports a population of native oysters. These were supplemented with laboratory measures conducted on oysters removed from the same system (Newell and Koch 2004). Jordan reported weight-specific biodeposition rate as a function of temperature, suspended solids concentration and salinity. The biodeposition rate represents a minimum value for filtration since all deposited material is first filtered. Filtration rate was derived:

$$Fr = WBR / TSS \qquad \textbf{(3)}$$

in which:

WBR = weight-specific biodeposition rate (mg g^{-1} dry oyster weight hr^{-1})
TSS = total suspended solids concentration (mg L^{-1})

Filtration rate was converted from L g^{-1} DW h^{-1} to model units based on a carbon-to-dry-weight ratio of 0.5.

The observed rates indicate a strong dependence of filtration on temperature (Figure 3) although the range of filtration rates observed at any

temperature indicate the influence of other factors as well. The maximum filtration rate and the temperature dependence for use in the model are indicated by a curve drawn across the highest filtration rates at any temperature:

$$Fr = Fr\max \cdot e^{-Ktg \cdot (T-Topt)^2} \qquad \textbf{(4)}$$

in which:

Frmax = maximum filtration rate (0.55 m^3 g^{-1} oyster carbon d^{-1})
Ktg = effect of temperature on filtration (0.015 $^{\circ}C^{-2}$)
T = temperature for optimal filtration (27 $^{\circ}C$)

Suspended Solids Effects. The deleterious effect of high suspended solids concentrations on oyster filtration rate has been long recognized although the solids concentrations induced in classic experiments, 10^2 to 10^3 g m^{-3} (Loosanoff and Tommers 1948), are extreme relative to concentrations commonly observed in Chesapeake Bay. We formed our solids function by recasting Jordan's data to show filtration rate as a function of suspended solids concentration (Figure 4). The experiments indicate three regions. Filtration rate was depressed when solids were below ~ 5 gm m^{-3} and above ~ 25 gm m^{-3}, relative to filtration rate when solids were between these two levels. The observations suggest oysters reduce their filtration rate when food is unavailable or when filtration at the maximum rate removes vastly more particles than the oysters can ingest. We visually fit a piecewise function to Jordan's data (Figure 4) supplemented with an approximation of Loosanoff and Tommers' results:

$f(TSS) = 0.1$ when TSS < 5 g m^{-3}
$f(TSS) = 1.0$ when 5 g m^{-3} < TSS < 25 g m^{-3}
$f(TSS) = 0.2$ when 25 g m^{-3} < TSS < 100 g m^{-3}
$f(TSS) = 0.0$ when TSS > 100 g m^{-3}

Salinity Effects. Oysters reduce their filtration rate when ambient salinity falls below ~20% of the oceanic value (Loosanoff 1953) and cease filtering when salinity falls below ~10% of the oceanic value. The form and parameterization of a relationship to describe these experiments is arbitrary. We selected a functional form (Figure 5) used extensively elsewhere in the CBEMP:

$$f(S) = 0.5 \cdot \left(1 + \tanh\left(S - KHsoy\right)\right) \qquad \textbf{(5)}$$

in which:

S = salinity (ppt)
KHsoy = salinity at which filtration rate is halved (7.5 ppt)

Dissolved Oxygen. Hypoxic conditions (dissolved oxygen < 2 g m^{-3}) have a profound effect on the macrobenthic community of Chesapeake Bay. Effects range from alteration in predation pressure (Nestlerode and Diaz 1998) to species shifts (Dauer et al. 1992) to near total faunal depletion (Holland et al. 1977). In the context of the benthos model, effects of hypoxia are expressed through a

reduction in filtration rate and increased mortality. The general function from the benthos model (Figure 6), based on effects from marine species, was adapted unchanged for the oyster model:

$$f(DO) = \frac{1}{1 + \exp\left(1.1 \cdot \frac{DO_{hx} - DO}{DO_{hx} - DO_{qx}}\right)} \qquad \textbf{(6)}$$

in which:

DO = dissolved oxygen in overlying water (g m^{-3})
DO_{hx} = dissolved oxygen concentration at which value of function is one-half (1.0 g m^{-3})
DO_{qx} = dissolved oxygen concentration at which value of function is one-fourth (0.7 g m^{-3})

This logistic function has the same shape as the tanh function used to quantify salinity effects (Figure 5). The use of two parameters, DO_{hx} and DO_{qx}, allows more freedom in specifying the shape of the function than the tanh function, based on the single parameter KHsoy, allows.

Ingestion

Oyster ingestion capacity must be derived indirectly from sparse observations and reports. In the report on his experiments, Jordan (1987) states "at moderate and high temperatures and low seston concentration (< 4 mg/L) nearly all biodeposits were feces" (page 54). This statement indicates no pseudofeces was produced; all organic matter filtered was ingested. Elsewhere in Jordan (1987) we find that ~ 75% of seston is organic matter and the filtration rate at 4 g seston m^{-3} is ~ 0.1 m^{-3} g^{-1} oyster C d^{-1} (Figure 4). The ingestion rate must be at least the amount of organic matter filtered. Conversion to model units indicates an ingestion rate of:

$$\frac{4\ g\ seston}{m^{-3}} \cdot \frac{0.75\ organic}{total} \cdot \frac{g\ C}{2.5\ g\ seston} \cdot \frac{0.1\ m^3}{g\ C\ d} = \frac{0.12\ g\ C\ ingested}{g\ oyster\ C\ d}$$

Tenore and Dunstan (1973) present a figure showing feeding rate and biodeposition. The difference between feeding and deposition must be ingestion. The largest observed difference is 19 mg C g^{-1} DW d^{-1} or 0.038 g C ingested g^{-1} oyster C d^{-1} (utilizing a carbon-to-dry-weight ratio of 0.5). No pseudofeces was produced during their experiments so the derived ingestion rate is not necessarily a maximum value.

In reporting on the removal of algae from suspension, Epifanio and Ewart (1977) noted that large amounts of pseudofeces were produced when algal suspensions exceeded 12 µg mL^{-1}. These results indicate the amount removed from the water column when algal suspensions were less than 12 µg mL^{-1}, ~ 4 to 17 mg algal DW g^{-1} oyster total weight d^{-1}, was ingested. The 15 g total weight

oysters in Epifanio and Ewart's experiments has a dry weight of 0.27 g (Dame 1972). The minimum ingestion rate is then:

$$\frac{4\ mg\ algal\ DW}{g\ oyster\ TW} \cdot \frac{15\ g\ TW}{0.27\ g\ DW} \cdot \frac{g\ oyster\ DW}{0.5\ g\ oyster\ C} \cdot \frac{g\ algal\ C}{2500\ mg\ DW} = \frac{0.18\ g\ C\ ingested}{g\ oyster\ C\ d}$$

Analogous unit conversions yield 0.76 g C ingested g^{-1} oyster C d^{-1} for a removal rate of 17 mg algal DW g^{-1} oyster total weight d^{-1}.

Summary of these analyses indicates the order of magnitude for ingestion rate is 0.1 g C ingested g^{-1} oyster C d^{-1}. The value 0.12 g C ingested g^{-1} oyster C d^{-1} was employed in the model based on our evaluation of Jordan's experiments.

Assimilation

The fraction of ingested carbon assimilated by oysters depends on the carbon source. The assimilation of macrophyte detritus can be as low as 3% (Langdon and Newell 1990) while the assimilation of viable microphytobenthos is 70% to 90% (Cognie et al.). Tenore and Dunstan (1973) observed that oysters assimilated 77% to 88% of a mixed algal culture. Specification of assimilation for the oyster model is shaped by the nature of the eutrophication model. The eutrophication model considers three forms of particulate organic carbon: phytoplankton, labile particulate organic carbon, and refractory particulate organic carbon. Assimilation of phytoplankton is specified as 75%, based on citations above. The labile and refractory particulate organic carbon are detrital components. These are mapped to three G classes of organic matter (Westrich and Berner 1984) employed in the sediment diagenesis model (DiToro 2001). The G1, labile, class has half-life of 20 days. The G2, refractory, class has a half-life of one year. The G3 class is inert within time scales considered by the model. Model labile particulate organic carbon maps to the G1 class and is assigned an assimilation efficiency of 75%, corresponding to phytoplankton. Model refractory particulate organic carbon combines the G2 and G3 classes and is assigned an assimilation efficiency of zero.

Respiration

Two forms of respiration are considered: active respiration, associated with acquiring and assimilating food, and passive respiration (or basal metabolism). This division of respiration is consistent with models of predators ranging from zooplankton (Steele and Mullin 1977) to fish (Hewett and Johnson 1987). Active respiration is considered to be a constant fraction of assimilated food. Basal metabolism is represented as a constant fraction of biomass, modified by ambient temperature:

$$BM = BMr \cdot e^{KTbmr \cdot (T - Tr)} \qquad (7)$$

in which:

BM = basal metabolism (d^{-1})
BMr = basal metabolism at reference temperature (d^{-1})

T = temperature (°C)
Tr = reference temperature (°C)
KTbmr = constant that relates metabolism to temperature ($°C^{-1}$)

The rate of basal metabolism depends on organism biomass (Winter 1978, Shumway and Koehn 1982). The average oyster in Jordan's (1987) experiments, upon which our filtration rates are based, is 2.1 g DW. Allometric relationships (Shumway and Koehn 1982) indicate basal metabolism for a 2.1 g DW oyster at 20 °C is 0.002 to 0.005 d^{-1}, depending on salinity. A graphical summary presented by Winter (1978) indicates metabolic rate for a 2 g DW oyster at 20 °C is 0.009 d^{-1}. Winter noted a 1 g DW mussel requires 1.5% of its dry tissue weight daily as a maintenance ration. Based on these reports, the value 0.008 d^{-1} was employed for basal metabolism at a reference temperature of 20 °C. Parameter KTbmr was assigned the value 0.069 $°C^{-1}$, equivalent to a Q10 of 2, typical of measured rates in oysters (Shumway and Koehn 1982).

The respiratory fraction was assigned through comparison of computed oxygen consumption with metabolism in active oyster reefs (Boucher and Boucher-Rodoni 1988, Dame et al. 1992). The value RF = 0.1 was determined. A comparable value of 0.172 (specific dynamic activity coefficient) was assigned to herbivorous fish in Chesapeake Bay (Luo et al. 2001).

Mortality

The model considers two forms of mortality. These are mortality due to hypoxia and a term that considers all other sources of mortality including disease and harvest. Although bivalves incorporate physiological responses that render them tolerant to hypoxia, extended periods of anoxia result in near-extinction (Holland et al. 1977, Josefson and Widbom 1988). Casting the results of experiments and observations into a relationship that quantitatively relates mortality to dissolved oxygen concentration incorporates a good deal of uncertainty in functional form and parameterization. The effect of hypoxia on oyster mortality, adopted from the benthos model, employs two concepts. The first is the time to death under complete anoxia. This time to death is converted to a first-order mortality rate via the relationship:

$$hmr = \frac{\ln(1/100)}{ttd} \qquad \textbf{(8)}$$

in which:

hmr = mortality due to hypoxia (d^{-1})
ttd = time to death for 99% of the population (14 d)

The mitigating effect on mortality of dissolved oxygen concentration greater than zero is quantified through multiplication by $(1 - f(DO))$ in which $f(DO)$ is the logistic function that expresses the effects of hypoxia on filtration rate (Equation 6). This functionality increases mortality as dissolved oxygen concentrations become low enough to affect filtration rate (Figure 6). When dissolved oxygen is depleted, filtration rate approaches zero and mortality is at its

maximum. As parameterized in the model, effects on filtration and mortality are negligible until dissolved oxygen falls below ~ 2 g m^{-3} (Figure 6). The time to death for 99% of the population exceeds 90 days when dissolved oxygen exceeds 1.4 g m^{-3} (Figure 7). Under this scheme, some fraction of the oyster population can survive an entire summer of hypoxia provided dissolved oxygen exceeds 1.4 g m^{-3}. No significant portion of the oyster population will survive summer hypoxia for dissolved oxygen concentrations below 1.4 g m^{-3}.

Mortality from all other sources, primarily disease and harvest, is represented by a spatially uniform and temporally constant first-order term. Magnitude of the term is specified to produce various system-wide population levels with the model. The order of magnitude can be derived from Jordan et al. (2002) who reported the 1990 total mortality of "market stock" oysters in northern Chesapeake Bay was 0.94 yr^{-1} (or 0.0026 d^{-1}). Of this total, 0.22 yr^{-1} (or 0.0006 d^{-1}) was natural mortality. The balance was fishing mortality.

Nutrients

Model oysters are composed of carbon, nitrogen, and phosphorus in constant ratios. In the original benthos model (HydroQual 2000), the carbon-to-nitrogen mass ratio of bivalves was set at 5.67:1; the phosphorus-to-carbon mass ratio was 45:1. Composition data for bivalves is not abundant. Calculations by Jordan (1987), based on earlier work by Kuenzler (1961) and Newell (1982), yield a carbon-to-nitrogen mass ratio between 4.8:1 and 6.9:1 and a phosphorus-to-carbon mass ratio of 66:1. The nitrogen composition values encompass the value used in the model. The phosphorus composition value differs from the model but no context exists to judge if the difference is significant.

The oyster model differs substantially from the original benthos model in the way nutrients are assimilated and processed. In the original model, nutrients are assimilated and excreted in constant ratios equivalent to the oyster composition. If assimilated carbon is in excess relative to assimilated nitrogen or phosphorus, the excess carbon is converted to feces and the bivalves are effectively nutrient limited. Computed bivalve growth is:

$$G = \min\left[Cassim, Nassim \cdot SFCN, Passim \cdot SFCP\right] \qquad \textbf{(9)}$$

in which:

G = bivalve biomass accumulation (g C m^{-2} d^{-1})
Cassim = carbon assimilation rate (g C m^{-2} d^{-1})
Nassim = nitrogen assimilation rate (g N m^{-2} d^{-1})
SFCN = bivalve carbon-to-nitrogen ratio (g C g^{-1} N)
Passim = phosphorus assimilation rate (g P m^{-2} d^{-1})
SFCP = bivalve carbon-to-nitrogen ratio (g P g^{-1} N)

If the carbon-to-nitrogen ratio in assimilated food, Cassim/Nassim, exceeds the ratio in bivalve composition, SFCN, then biomass accumulation is proportional to the rate of nitrogen assimilation. Similarly, when the ratio Cassim/Passim > SFCP, biomass accumulation is proportional to phosphorus assimilation. The

algal phosphorus-to-carbon ratio in the eutrophication model (Cerco and Noel 2004) is 57:1 for spring diatoms and 80:1 for other algae. Since these ratios exceed SFCP, growth of bivalves feeding on algae will be limited by the phosphorus content of the algae rather than the amount of carbon assimilated.

Algal composition does not provide a complete picture of the tendency for nutrient limitation of bivalve growth since modeled bivalves utilize detritus as well as algae. Initial applications of the oyster model indicated, however, that phosphorus limitation of oyster growth did occur. Nutrient limitation was eliminated through two methods. First, oyster phosphorus composition was thinned out; carbon-to-phosphorus ratio was increased to 90:1. More significantly, a mass balance approach to nutrient utilization and excretion was adopted. Biomass accumulation was modeled as carbon assimilation less respiration loss while nutrient excretion was calculated as the amount of assimilated nutrients not required for biomass accumulation.

Model Parameters

Parameter values for the oyster model are summarized in Table 1.

Table 1
Parameters for Oyster Model

Parameter	Definition	Value	Units
Frmax	maximum filtration rate	0.55	$m^3\ g^{-1}$ oyster carbon d^{-1}
Topt	optimum temperature for filtration	27	°C
Ktg	constant that controls temperature dependence of filtration	0.015	$°C^{-2}$
KHsoy	salinity at which filtration rate is halved	7.5	ppt
BMR	base metabolism rate at 20 °C	0.008	d^{-1}
KTbmr	constant that controls temperature dependence of metabolism	0.069	$°C^{-1}$
Tr	reference temperature for specification of metabolism	20	°C
RF	respiratory fraction	0.1	$0 \leq RF \leq 1$
DO_{hx}	dissolved oxygen concentration at which value of logistic function is one-half	1.0	$g\ m^{-3}$
DO_{qx}	dissolved oxygen concentration at which value of logistic function is one-quarter	0.7	$g\ m^{-3}$
ttd	time to death for 99% of the population	14	d
a_{alg}	assimilation efficiency for phytoplankton	0.75	$0 < a < 1$
a_{lab}	assimilation efficiency for labile organic matter	0.75	$0 < a < 1$
a_{ref}	assimilation efficiency for refractory organic matter	0.0	$0 < a < 1$
Imax	maximum ingestion rate	0.12	g prey C g^{-1} C d^{-1}
SFCN	carbon-to-nitrogen ratio	6	g C g^{-1} N
SFCP	carbon-to-phosphorus ratio	90	g C g^{-1} P

References

Boucher, G., and Boucher-Rodoni, R. (1988). "In situ measurement of respiratory metabolism and nitrogen fluxes at the interface of oyster beds," *Marine Ecology Progress Series*, 44, 229-238.

Cerco, C., and Meyers, M. (2000). "Tributary refinements to the Chesapeake Bay Model," *Journal of Environmental Engineering*, 126(2), 164-174.

Cerco, C., Johnson, B., and Wang, H. (2002). "Tributary refinements to the Chesapeake Bay model, ERDC TR-02-4, US Army Engineer Research and Development Center, Vicksburg, MS.

Cerco, C., and Noel, M. (2004). "The 2002 Chesapeake Bay eutrophication model," EPA 903-R-04-004, Chesapeake Bay Program Office, US Environmental Protection Agency, Annapolis, MD.

Cognie, B., Barille, L., and Rince, Y. (2001). "Selective feeding of the oyster *Crassostrea gigas* fed on a natural microphytobenthos assemblage," *Estuaries*, 24(1), 126-131.

Dame, R., (1972). "Comparison of various allometric relationships in intertidal and subtidal American oysters," *Fishery Bulletin*, 70(4), 1121-1126.

Dame, R., Spurrier, J., and Zingmark, R. (1992). "In situ metabolism of an oyster reef," *Journal of Experimental Marine Biology and Ecology*, 164, 147-159.

Dauer, D., Rodi, A., and Ranasinghe, J. (1992). "Effects of low dissolved oxygen events on the macrobenthos of the lower Chesapeake Bay," *Estuaries*, 15(3), 384-391.

DiToro, D. (2001). *Sediment Flux Modeling*, John Wiley and Sons, New York.

Doering, P., and Oviatt, C. (1986). "Application of filtration rate models to field populations of bivalves: an assessment using experimental mesocosms," *Marine Ecology Progress Series*, 31, 265-275.

Doering, P., Oviatt, C., and Kelly, J. (1986). "The effects of the filter-feeding clam *Mercenaria mercenaria* on carbon cycling in experimental ecosystems," *Journal of Marine Research*, 44, 839-861.

Epifanio, C., and Ewart, J. (1977). "Maximum ration of four algal diets for the oyster *Crassostrea virginica* Gmelin," *Aquaculture*, 11, 13-29.

Hewett, S., and Johnson, B. (1997). "A generalized bioenergetics model of fish growth for microcomputers," WIS-SG-87-245, Wisconsin Sea Grant College Program, University of Wisconsin, Madison.

Holland, A., Mountford, N., and Mihursky, J. (1977). "Temporal variation in upper bay mesohaline benthic communities: I. The 9-m mud habitat," *Chesapeake Science*, 18(4), 370-378.

HydroQual. (2000). "Development of a suspension feeding and deposit feeding benthos model for Chesapeake Bay," produced by HydroQual Inc. under contract to the U.S. Army Engineer Research and Development Center, Vicksburg MS.

Jordan, S. (1987). "Sedimentation and remineralization associated with biodeposition by the American oyster *Crassostrea virginica* (Gmelin)," Ph.D. diss., University of Maryland, College Park.

Jordan, S., Greenhawk, K., McCollough, C., Vanisko, J., and Homer, M. (2002). "Oyster biomass, abundance, and harvest in northern Chesapeake Bay: Trends and forecasts," *Journal of Shellfish Research*, 21(2), 733-741.

Josefson, A., and Widbom, B. (1988). "Differential response of benthic macrofauna and meiofauna to hypoxia in the Gullmar Fjord Basin," *Marine Biology*, 100, 31-40.

Kuenzler, E. (1961). "Phosphorus budget of a mussel population," *Limnology and Oceanography*, 6, 400-415.

Langdon, C., and Newell, R. (1990). "Utilization of detritus and bacteria as food sources by two bivalve suspension-feeders, the oyster *Crassostrea virginica* and the mussel *Geukensia demissa*," *Marine Ecology Progress Series*, 58, 299-310.

Loosanoff, V., and Tommers, F. (1948). "Effect of suspended silt and other substances on rate of feeding of oysters," *Science*, 107, 69-70.

Loosanoff, V. (1953). "Behavior of oysters in water of low salinities," *Proceedings of the National Shellfish Association*, 43:135-151.

Luo, J., Hartman, K., Brandt, S., Cerco, C., and Rippetoe, T. (2001). "A spatially-explicit approach for estimating carrying capacity: An application for the Atlantic menhaden (*Brevoortia tyrannus*) in Chesapeake Bay," *Estuaries*, 24(4), 545-556.

Meyers, M., DiToro, D., and Lowe, S. (2000). "Coupling suspension feeders to the Chesapeake Bay eutrophication model," *Water Quality and Ecosystem Modeling*, 1, 123-140.

Nestlerode, J., and Diaz, R. (1998). "Effects of periodic environmental hypoxia on predation of a tethered ploychaete, *Glycera Americana*: implications for trophic dynamics," *Marine Ecology Progress Series*, 172, 185-195.

Newell, R. (1982). "An evaluation of the wet oxidation technique for use in determining the energy content of seston samples," *Canadian Journal of Fisheries and Aquatic Science*, 39, 1383-1388.

Newell, R., and Koch, E. (2004). "Modeling seagrass density and distribution in response to changes in turbidity stemming from bivalve filtration and seagrass sediment stabilization," *Estuaries*, 27(5), 793-806.

Riisgard, H. (1988). "Eficiency of particle retention and filtration rate in 6 species of Northeast American bivalves," *Marine Ecology Progress Series*, 45, 217-223.

Shumway, S., and Koehn, R. (1982). "Oxygen consumption in the American oyster *Crassostrea virginica*," *Marine Ecology Progress Series*, 9, 59-68.

Steele, J., and Mullin, M. (1977). "Zooplankton dynamics." *The sea*. E. Goldberg, I. McCave, J. O'Brien, J. Steele eds., Volume 6, Wiley-Interscience, New York, 857-890.

Tenore, K., and Dunstan, W. (1973). "Comparison of feeding and biodeposition of three bivalves at different food levels," *Marine Biology*, 21, 190-195.

Westrich, J., and Berner, R. (1984). "The role of sedimentary organic matter in bacterial sulfate reduction: The G model tested," *Limnology and Oceanography*, 29, 236-249.

Winter, J. (1978). "A review of the knowledge of suspension-feeding in lamellibranchiate bivalves, with special reference to artificial aquaculture systems," *Aquaculture*, 13, 1-33.

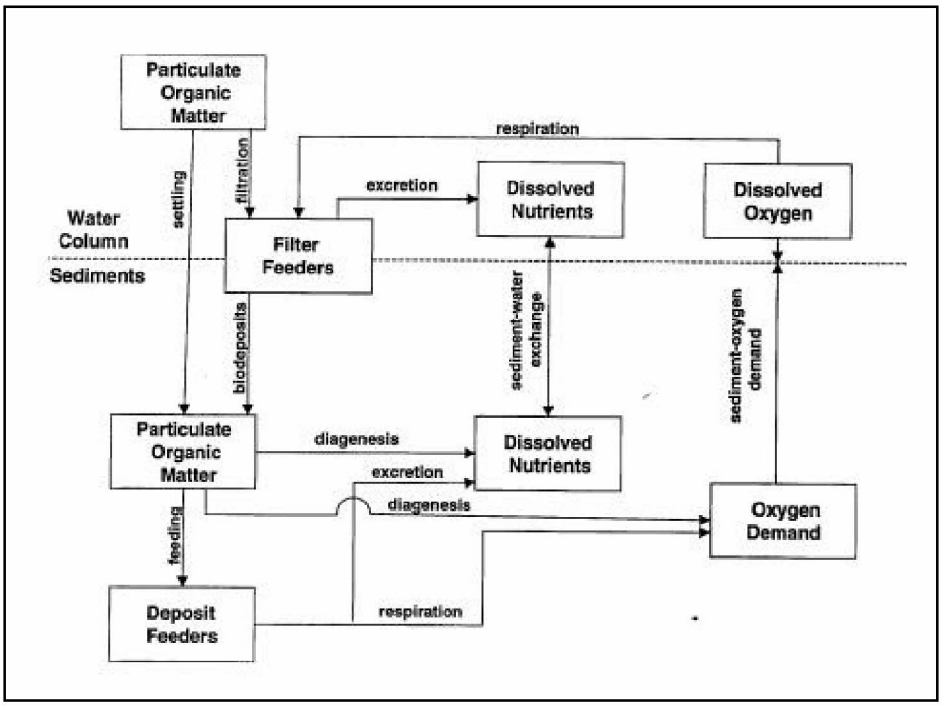

Figure 1. Benthos model schematic.

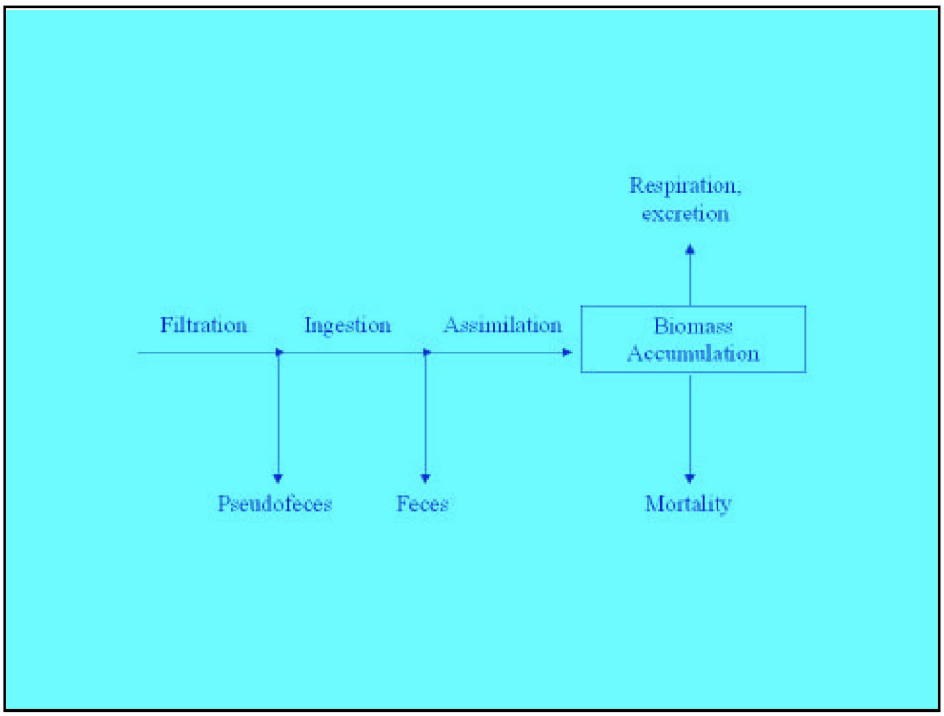

Figure 2. Processes affecting filtered material.

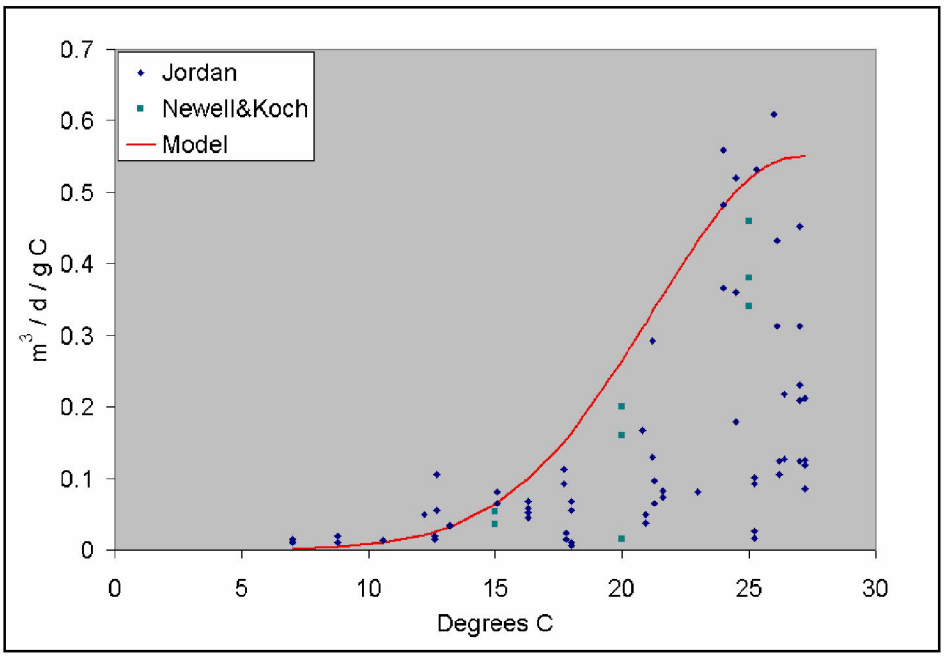

Figure 3. Effect of Temperature on filtration rate.

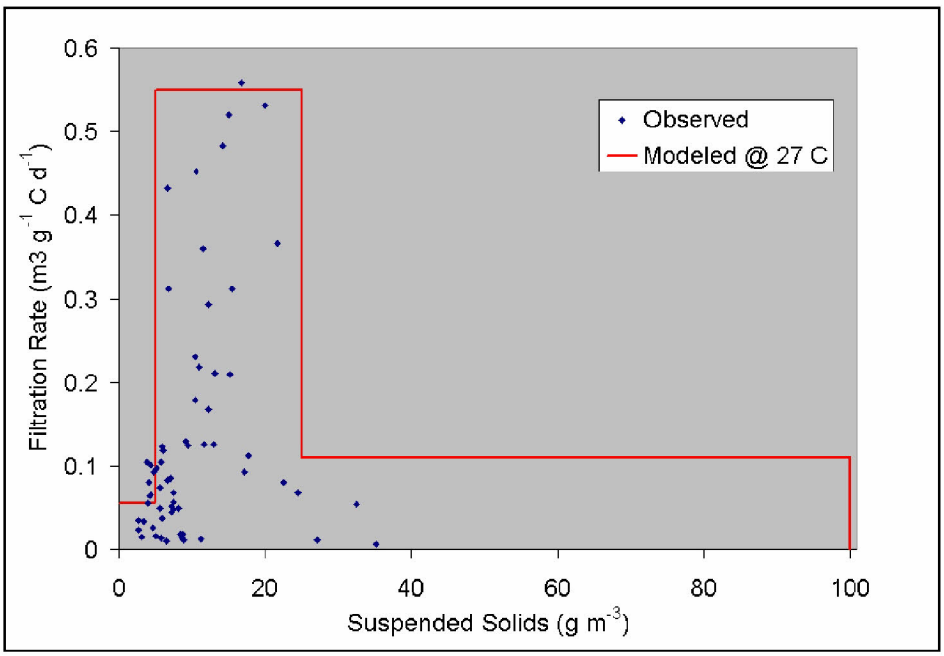

Figure 4. Effect of suspended solids on filtration rate.

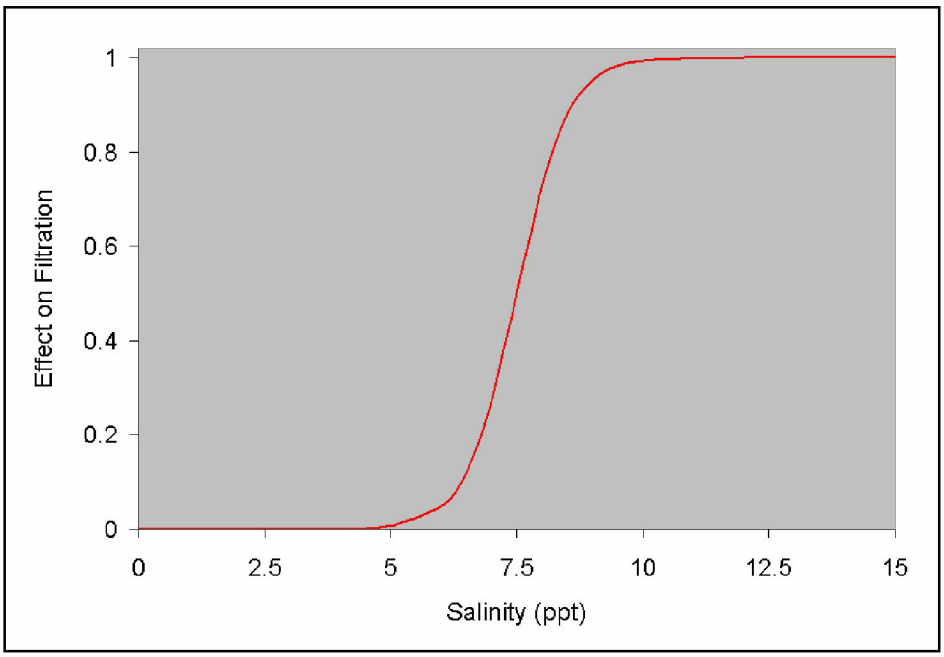

Figure 5. Effect of salinity on filtration rate.

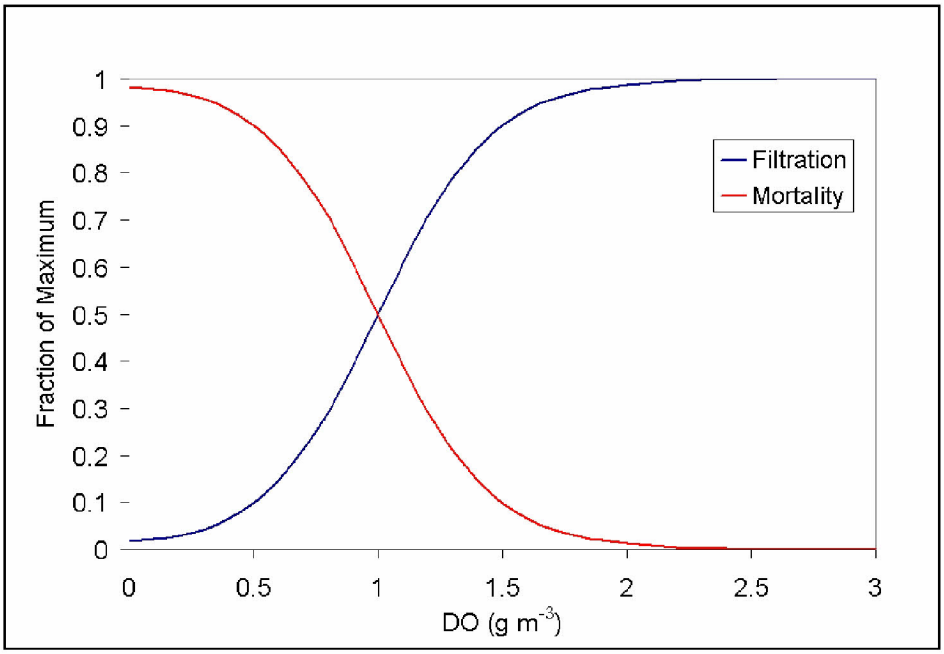

Figure 6. Effect of dissolved oxygen on filtration and mortality rates.

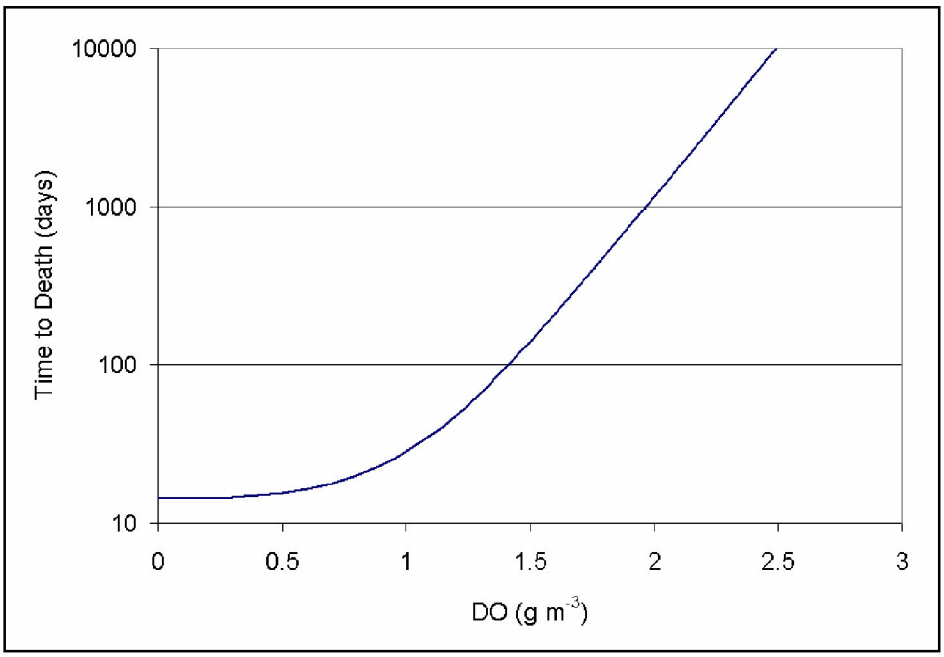

Figure 7. Effect of dissolved oxygen on time to death for 99% of population.

3 Biomass Estimates

Introduction

The Chesapeake 2000 Agreement calls for a tenfold increase in native oysters in the Chesapeake Bay, based on a 1994 baseline. At the commencement of this study, no estimate of the baseline oyster population existed. Evaluation of the existing population and its distribution was required before the effects of proposed increases could be examined. Since our model is based on mass balance, population estimates took the form of mass rather than number of individuals. We use the terms "biomass" to indicate total weight of oysters e.g. kg C and "density" to indicate weight per unit area e.g. g C m^{-2}.

Existing Biomass

Virginia

Density estimates for Virginia were provided by Dr. Roger Mann, of Virginia Institute of Marine Science (VIMS), in October 2003. Estimates were based on patent tong surveys. The EPA Chesapeake Bay Program Office (CBPO) provided VIMS with model grid coordinates. Patent tong samples were averaged for each model cell and results were provided as g DW/m^{-2}. Number of samples per cell varied from 4 to more than 50. Estimates were provided for one to five individual years in the interval 1998-2002. The coefficient of variation (CV, defined as standard deviation/mean) for inter-annual density estimates in individual cells (one or two km on a side) ranged from 0.11 to 1.67 with a median value of 0.69. The CV of the inter-annual total biomass was 0.088. The area of cells containing oysters was 377 km^2.

Maryland

Biomass and spatial distribution for Maryland were based on the recommendation of Dr. Roger Newell of the University of Maryland Center for Environmental Science. Dr. Newell recommended recent biomass estimates (Jordan et al. 2002) should be uniformly distributed across the historical oyster habitat denoted in the "Yates" surveys (Yates 1911). The areas and locations of named oyster bars were obtained by the CBPO and bar areas were assigned to model cells. Total area of named oyster bars was 1330 km^2. Mean biomass for the period 1991-2000, 5.7 x 10^8 g DW, was obtained from Jordan et al. (2002). A mean density of 0.43 g DW m^{-2} (total biomass / total area) was assigned to the

bar area in each model cell. Since the bar area was usually less than the cell area, cell density was adjusted so that biomass per cell matched biomass of bars within the cell. The area of cells containing oysters was 3696 km^2.

Other Filter Feeders

Examination of the effects of oyster restoration requires consideration of existing filter feeders. Observations from the bay-wide benthic database (http://www.chesapeakebay.net/data/index.htm) were analyzed by HydroQual (2000) as part of the initial benthos modeling effort. The analysis indicates suspension feeding bivalves are distributed primarily in the upper bay and tributaries (Figure 1). Average bivalve densities in the upper bay are commonly an order of magnitude or more greater than the present density of oysters. The arithmetic densities computed by HydroQual are perhaps influenced by a few large density values; median densities might present a more realistic picture. Still, the data support the decision to neglect Maryland oysters in the original benthos model. In the lower bay, the existing oyster density is substantial relative to other bivalves in the lower Rappahannock River and in a limited portion of the James River. The decision to neglect existing oysters in these rivers should be revisited. Recent research (Thompson and Schaffner 2001) indicates polycheate filter feeders, with reported densities ~ 6 g C m^{-2}, may also play a substantial role in the lower bay.

Summary

The oyster density and distribution are distinctly different in the Maryland and Virginia portions of the bay (Figure 2). In the northern, Maryland, portion, lower densities are distributed over a wide area. In the southern, Virginia, portion, high densities are concentrated in limited areas, primarily in the lower James and Rappahannock Rivers. Oyster biomass in Virginia is five times the biomass in Maryland (Table 1) but distributed across an order of magnitude less area. We were puzzled by the limited distribution in Virginia, especially since maps and other information we obtained indicated a wider distribution of lease holdings and restoration areas. We were assured by Dr. Roger Mann that much of the leased area is unproductive and that biomass outside the areas reported to us is negligible. Our estimate of Maryland biomass is roughly half the biomass from two other independent estimates (Table 1). Our estimate of Virginia biomass is three times the biomass from an alternate independent estimate (Table 1).

Modeled Biomass

Model oyster density is dynamically computed based on environmental conditions including temperature, dissolved oxygen, salinity, and food supply. The densities are not specified as model inputs. Rather, they must be calculated as a function of model parameters and computed conditions. The calculation, rather than specification, of density ensures that oysters are not placed where conditions do not support their specified density. We initially attempted to calculate target oyster densities through dynamic variation of the mortality function. Mortality in each model cell was adjusted upwards or downwards as

Table 1
Oyster Biomass Estimates

Source	Maryland, kg C	Virginia, kg C	Comments
This study	287,000	1,170,000	Maryland from Jordan et al (2002). Virginia from Roger Mann (personal communication).
Newell (1988)	550,000	400,000	
Uphoff (2002)	570,000		Year 2000 exploitable biomass based on skipjack catch per effort

calculated density exceeded or fell below specified levels. This process successfully capped density at target levels but many cells would not support existing density or a tenfold increase. The problem originated with the attempt to calculate target densities within individual cells. The calculated conditions in many cells would not support the target densities. Consequently, we switched to a strategy in which a bay-wide target biomass was specified. A uniform bay-wide mortality rate was prescribed that produced the target biomass. The mortality rate was obtained through a trial-and-error process in which various rates were prescribed and the calculated biomass was examined.

The spatial distributions of biomass and density are conveniently examined through aggregation of individual model cells into Chesapeake Bay Program Segments (CBPS). Program segments are subdivisions of the bay determined by mean salinity, natural boundaries, and other features. Our analysis is based on the original (circa 1993) segmentation (Table 2, Figure 3) in which the bay is divided in 35 segments with a median area of 150 km^2.

Computed density and biomass vary on intra-annual and inter-annual bases (Figure 4). Variations within the annual cycle are largely driven by temperature. Highest densities are computed in late summer and in fall, after a season of filtering at peak rates (Figure 5). Variations from year to year (Figure 6) are largely driven by runoff. Variations in runoff may enhance or diminish computed biomass, depending on local factors. Years with high runoff coincide with large nutrient loads that result in high phytoplankton abundance. The advantages produced by abundant food may be offset, however, by increased anoxia and by sub-optimal salinity.

Baseline Estimates

First-order estimates of the density and biomass of existing bivalve filter feeders can be obtained from the latest application of the CBEMP (Cerco and Noel 2004). This benthos component of this model was originally calibrated to match the observed density in the bay-wide benthic database (HydroQual 2000). Subsequent review (Schaffner et al. 2002) indicated the model tends to over-predict suspension-feeding density in the lower to mid-bay (where density is low) and under-predicts or approximates suspension-feeding density in the upper bay

and tributaries (where density is high). Still, the model biomass is a useful baseline, especially in the absence of alternate bay-wide abundance estimates.

Table 2
Chesapeake Bay Program Segments that Support Oysters

CBPS	Designation	State
CB2	Upper Chesapeake Bay	Maryland
CB3	Upper Central Chesapeake Bay	Maryland
CB4	Upper Middle Chesapeake Bay	Maryland
CB5	Lower Chesapeake Bay	Maryland - Virginia
CB6	Western Lower Chesapeake Bay	Virginia
CB7	Eastern Lower Chesapeake Bay	Virginia
EE1	Eastern Bay	Maryland
EE2	Lower Choptank River	Maryland
EE3	Tangier Sound	Maryland - Virginia
ET4	Chester River	Maryland
ET5	Choptank River	Maryland
ET6	Nanticoke River	Maryland
ET7	Wicomico River	Maryland
ET8	Manokin River	Maryland
ET9	Big Annemessex River	Maryland
LE1	Lower Patuxent River	Maryland
LE2	Lower Potomac River	Maryland
LE3	Lower Rappahannock River	Virginia
LE5	Lower James River	Virginia
RET1	Middle Patuxent River	Maryland
RET2	Middle Potomac River	Maryland
WE4	Mobjack Bay	Virginia
WT6	Magothy River	Maryland
WT7	Severn River	Maryland
WT8	South River	Maryland

Autumn is the season when individual oysters attain maximum biomass and when most population surveys, on which our estimates are based, are conducted. For comparison with estimates of existing oysters, we averaged the calculated autumn (September – November) bivalve density and biomass from ten years (1985 – 1994). The density comparisons are averaged across total bottom area in each CBPS. The resulting densities are less than individual observations or averages across oyster bars since area not suited for bivalves is included in the average. In most portions of the bay, the calculated density of existing bivalve filter feeders vastly exceeds the estimated density of oysters (Figure 7). Notable exceptions are in the Rappahannock (LE3) and James (LE5) where existing oysters exceed other bivalve filter feeders. Oysters also predominate in two Eastern Shore tributaries (ET8, ET9) and in the lower

western shore of the mainstem (CB6). These segments are characterized by the virtual absence of other bivalves rather than by abundant oysters, however. Biomass comparisons (Figure 8) reflect the density comparisons. Oyster biomass exceeds other bivalve biomass in the lower Rappahannock and James Rivers. Oysters are virtually the only bivalves in the two noted Eastern shore tributaries (ET8, ET9) and in the lower western shore of the bay (CB6).

These comparisons have implications for the overall modeling effort and for the present work. As noted previously, the decision to ignore oysters in the model, until now, was a valid one, with the exception of the lower Rappahannock and James Rivers. For the present study, the model runs with no oysters provide an acceptable baseline for comparison with tenfold population increase since the oysters comprise only a small fraction of filter-feeding biomass throughout most of the bay.

Tenfold Increase

The model run for examination of the tenfold population increase, called for in the Chesapeake 2000 Agreement, was determined through a recursive process in which mortality rate was varied until the desired biomass was obtained. Intra- and inter-annual variations in computed biomass made an exact multiplier of existing oyster biomass impossible to obtain. We settled on comparison of computed autumn (September – November) biomass with population estimates since most surveys are conducted in the fall. We compared the mean of ten computed years, 1985-1994, with the estimates of existing population. We settled on a first-order mortality rate of 0.015 d^{-1}, which produced a mean biomass 13-times the estimated existing biomass (Table 3). Biomass in individual years varied by roughly 50% above and below the mean. We refer to this run as the "tenfold increase" although the magnitude and spatial distribution of the increase varies. The southern, Virginia, portion of the bay receives only a fourfold biomass increase while the northern, Maryland, portion increases nearly 50-times. The disparity in multipliers reflects the disparity in initial biomass distribution. An implication of this model run is that, under existing conditions, the northern portion of the bay suffers higher mortality from harvest and disease than the southern portion since imposition of a uniform mortality rate results in greater biomass in the north than in the south. Estimates of the present population indicate the opposite trend. With the tenfold increase, oysters become the dominant filter feeders in the system (Figures 9, 10) although other bivalves predominate in a few segments that provide marginal oyster habitat. Also worth noting is a decline in bivalve biomass, as much as 50%, throughout much of the bay (Figure 11).

Historical Biomass

As one part of sensitivity analyses, we computed the biomass of oysters with no mortality from harvest or predation. Limitations to biomass in this run were food availability, respiration, and mortality from hypoxia. The computed biomass (Table 3) that resulted approached the pre-1870 biomass estimated by Newell (1988). This run is documented as an example of improvements that could result from full restoration of historic oyster biomass.

Table 3 Estimated and Modeled Oyster Biomass, kg C			
	Maryland	**Virginia**	**Total**
Existing, estimated	287,005	1,099,339	1,386,344
Historic (Newell 1988)			94,000,000
Tenfold, model	14,107,500	4,374,953	18,482,453
Historic, model	69,749,506	17,165,230	86,914,736

Equivalent Settling and Removal Rates

The influence of oysters on the environment is a function of their density, filtration rate, and local geometry. The product of density and filtration rate has units of length/time (velocity) and is denoted here as "Equivalent Settling Rate":

$$Woys = \frac{1}{A} \cdot \int O \cdot Fr \, dA \qquad (1)$$

in which:

Woys = equivalent settling rate (m d^{-1})
A = area over which rate is computed (m^2)
O = oyster density (g C m^{-2})
Fr = filtration rate (m^3 g^{-1} oyster carbon d^{-1})

The equivalent settling rate can be viewed as the velocity at which particles are transferred from the water column into the oyster bed. Higher velocities indicate more rapid removal. However, the distance to be covered (depth) affects removal as well as velocity. Geometry is brought into the characterization through calculation of "Equivalent Removal Rate":

$$Roys = \frac{1}{A} \cdot \int \frac{1}{D} \cdot O \cdot Fr \, dA \qquad (2)$$

in which:

Roys = equivalent removal rate (d^{-1})
D = local depth (m)

The equivalent removal rate can be viewed as a decay rate of material in the water column. High removal rates indicate the bivalves clear the water column rapidly. The inverse of the equivalent removal rate is an "Equivalent Residence Time": the time required for the bivalves to filter the water column once.

Under existing conditions, highest settling rates are in smaller tributaries; lower settling rates prevail in the mainstem bay and in the portions of major western tributaries that adjoin the bay (Figure 12). The tenfold biomass increase

(Figure 13) and the historic biomass (Figure 14) shift the highest settling rates to the lower portions of the western tributaries and to the upper mainstem of the bay. Median settling velocity increases by an order of magnitude from present modeled conditions to historical conditions (Table 4).

Under existing conditions, the ranking of residence times corresponds to the ranking of settling rates (Figure 15). Shortest residence times (highest turnover rates) are in tributaries. More lengthy residence times prevail in the lower portions of western tributaries and in the mainstem bay. The effects of geometry influence the rankings under conditions of oyster restoration (Figures 16, 17). Several of the large-volume segments which rank high in terms of settling rate rank lower when their depth is incorporated into the index of potential bivalve influence. Overall, the median residence time of individual CBPS's diminishes from 18 days under computed existing conditions to less than three days under historic oyster densities (Table 4).

Table 4
Median Settling Rates, Removal Rates, and Residence Times

	Settling, m d^{-1}	Removal, d^{-1}	Residence, d
Existing Conditions	0.15	0.04	18.3
Tenfold Oyster Increase	0.62	0.19	5.3
Historic Conditions	1.44	0.38	2.6

References

Cerco, C., and Noel, M. (2004). "The 2002 Chesapeake Bay eutrophication model," EPA 903-R-04-004, Chesapeake Bay Program Office, US Environmental Protection Agency, Annapolis, MD.

HydroQual. (2000). "Development of a suspension feeding and deposit feeding benthos model for Chesapeake Bay," produced by HydroQual Inc. under contract to the U.S. Army Engineer Research and Development Center, Vicksburg MS.

Jordan, S., Greenhawk, K., McCollough, C., Vanisko, J., and Homer, M. (2002). "Oyster biomass, abundance, and harvest in northern Chesapeake Bay: Trends and forecasts," *Journal of Shellfish Research*, 21(2), 733-741.

Newell, R. (1988). "Ecological changes in Chesapeake Bay: Are they the result of overharvesting the American oyster (*Crassostrea virginica*)?," *Understanding the estuary – Advances in Chesapeake Bay Research.* Publication 129, Chesapeake Research Consortium, Baltimore, 536-546.

Schaffner, L., Friedrichs, C., and Dauer, D. (2002). "Review of the benthic processes model with recommendations for future modeling efforts," A Report from the Benthic Process Model Review Team, EPA Chesapeake Bay Program, Annapolis MD. (Available at http://www.chesapeakebay.net/modsc.htm)

Thompson, M., and Schaffner, L. (2001). "Population biology and secondary production of the suspension feeding polychaete *Chaetopterus* cf. *variopedatus*: Implications for benthic-pelagic coupling in lower Chesapeake Bay," *Limnology and Oceanography*, 46(8), 1899-1907.

Uphoff, J. (2002). "Biomass dynamic modeling of oysters in Maryland," Maryland Department of Natural Resources, Annapolis. (Unpublished manuscript provided by the author).

Yates, C. (1911). "Survey of the oyster bars by county of the State of Maryland," Department of Commerce and Labor, Coast and Geodetic Survey, Washington DC.

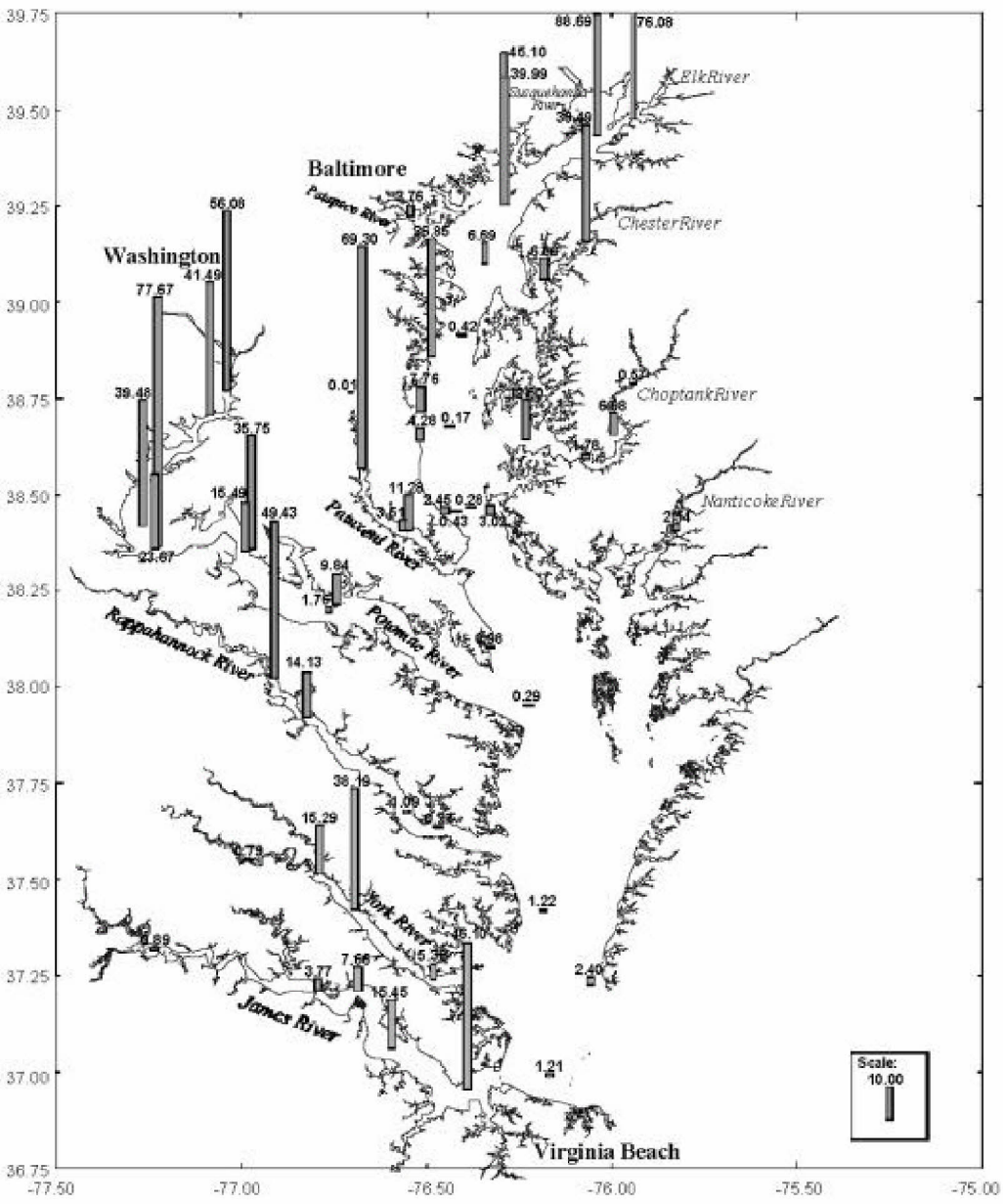

Figure 1. Density of existing bivalve filter feeders (from HydroQual 2000)

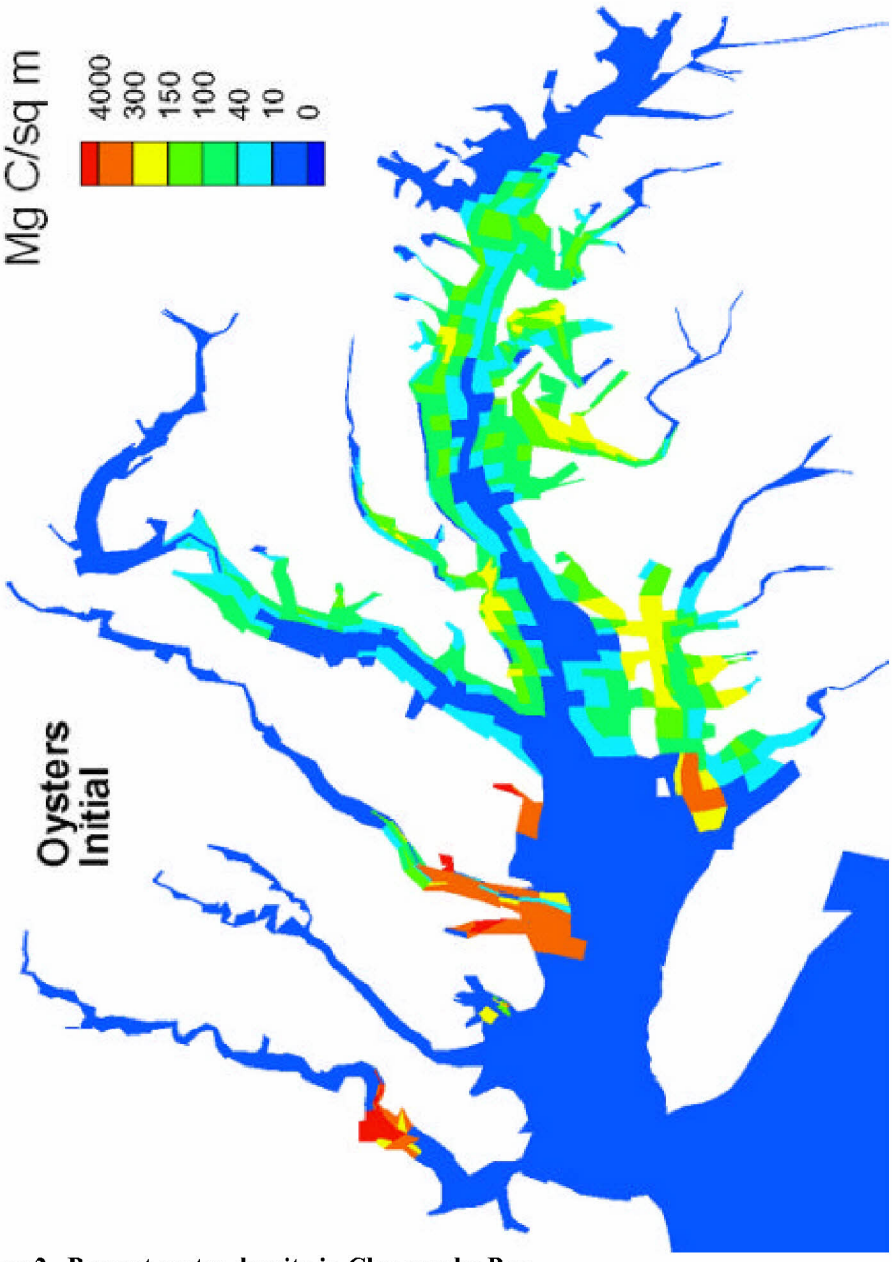

Figure 2. Present oyster density in Chesapeake Bay

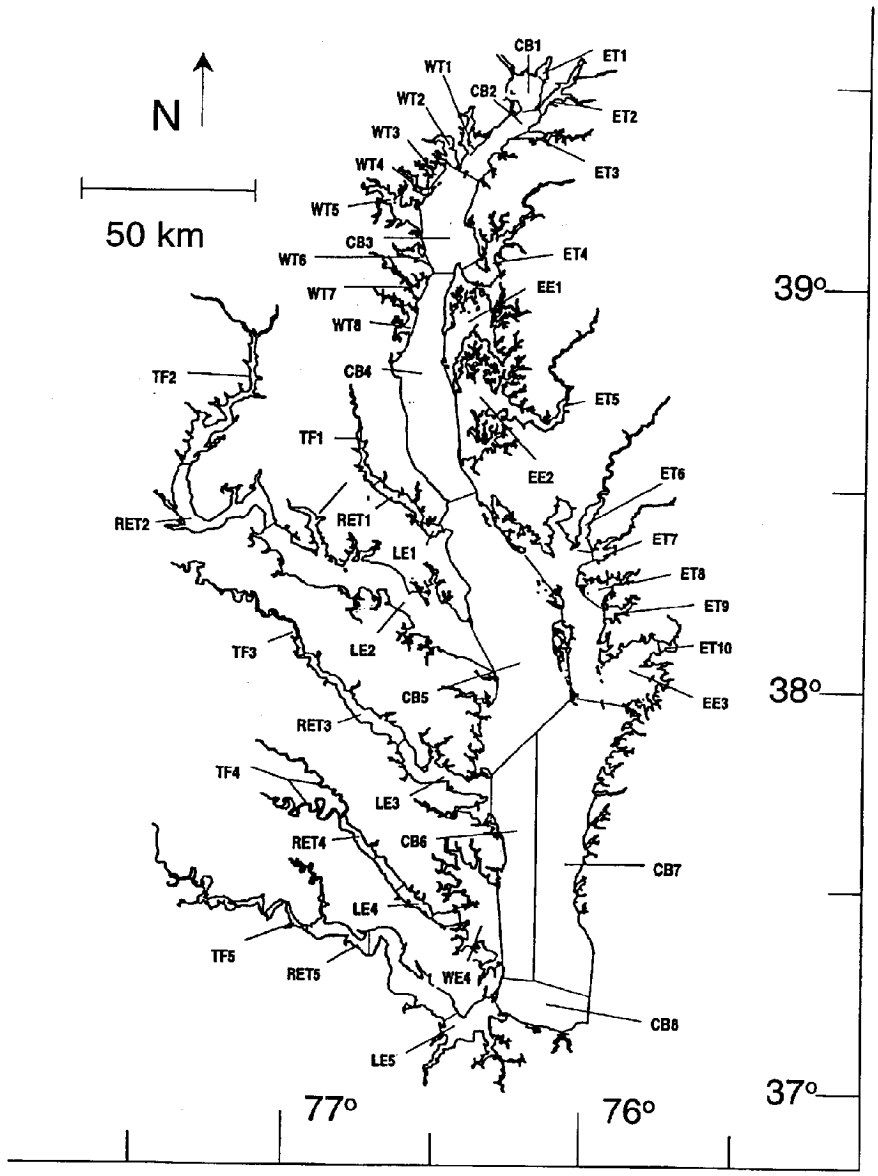

Figure 3. Chesapeake Bay Program Segments

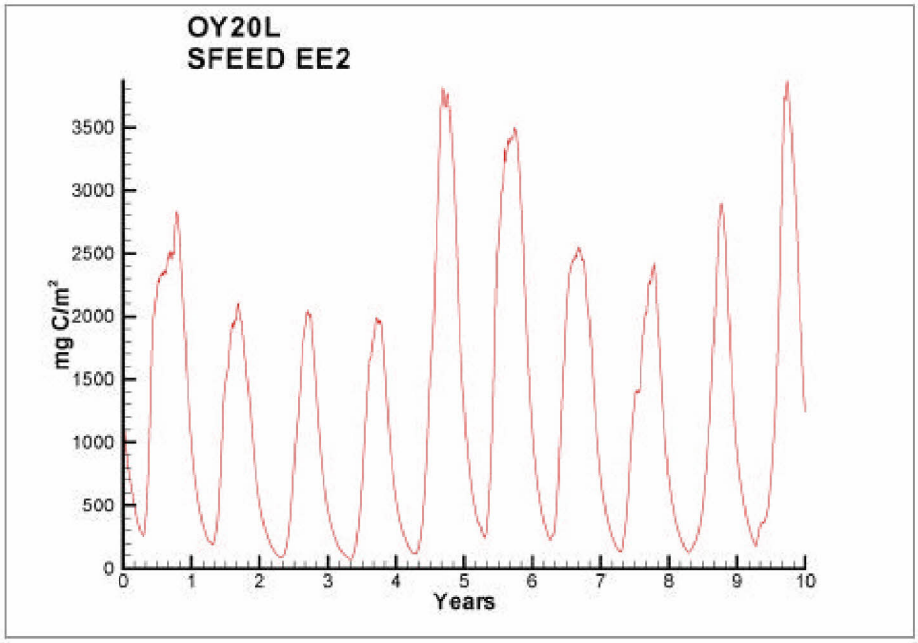

Figure 4. Calculated oyster density in the lower Choptank River, 1985-1994

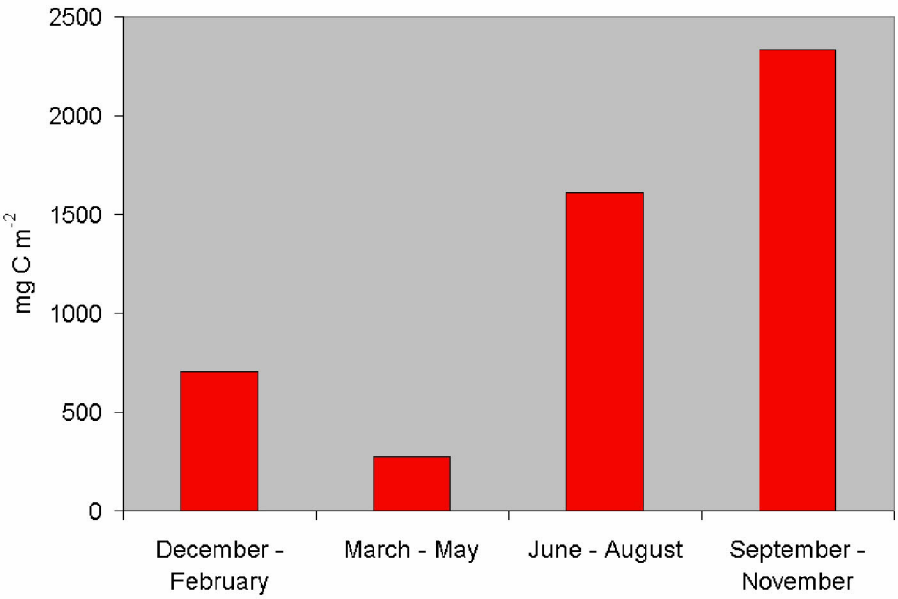

Figure 5. Seasonal-average calculated oyster density in the lower Choptank River

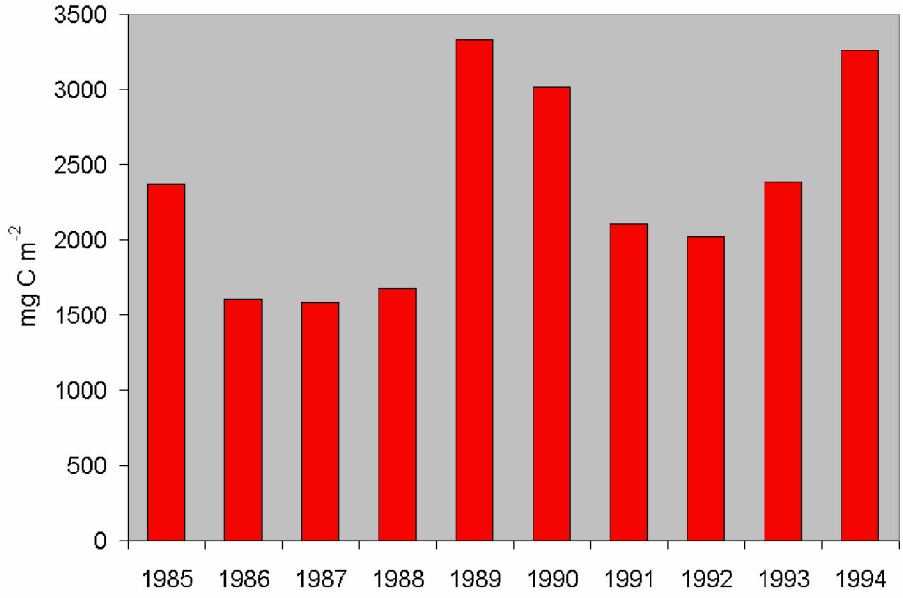

Figure 6. Calculated autumn oyster density in lower Choptank River

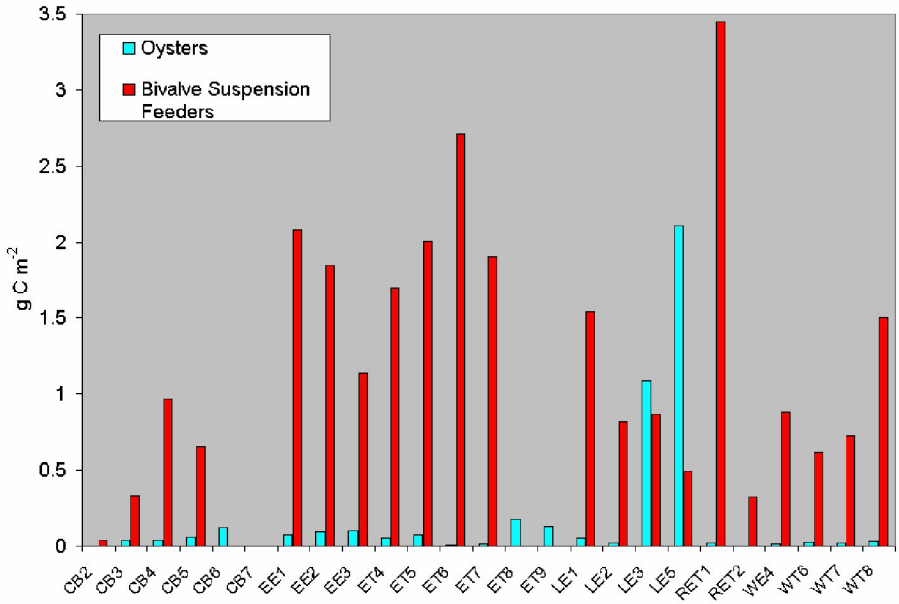

Figure 7. Estimated density of existing oysters and bivalve filter feeders

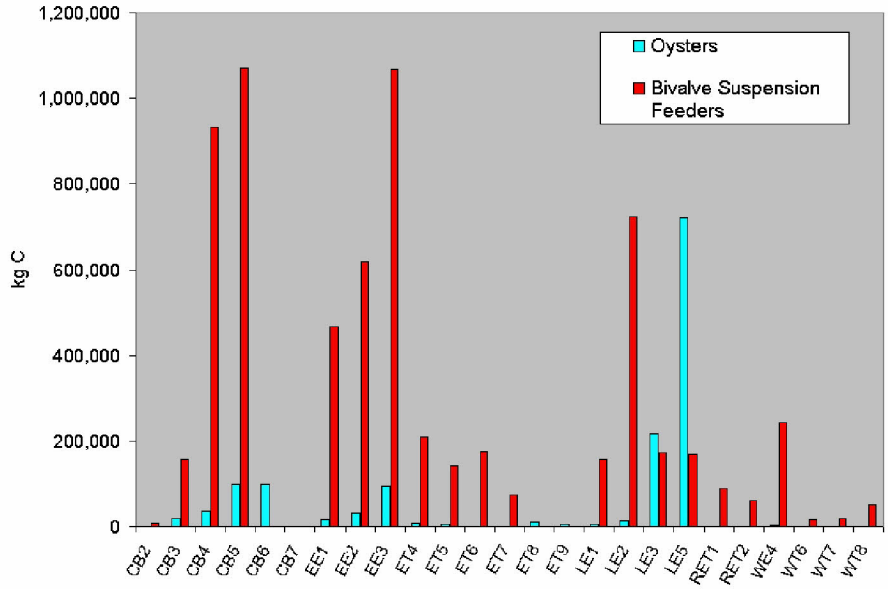

Figure 8. Estimated biomass of existing oysters and bivalve filter feeders

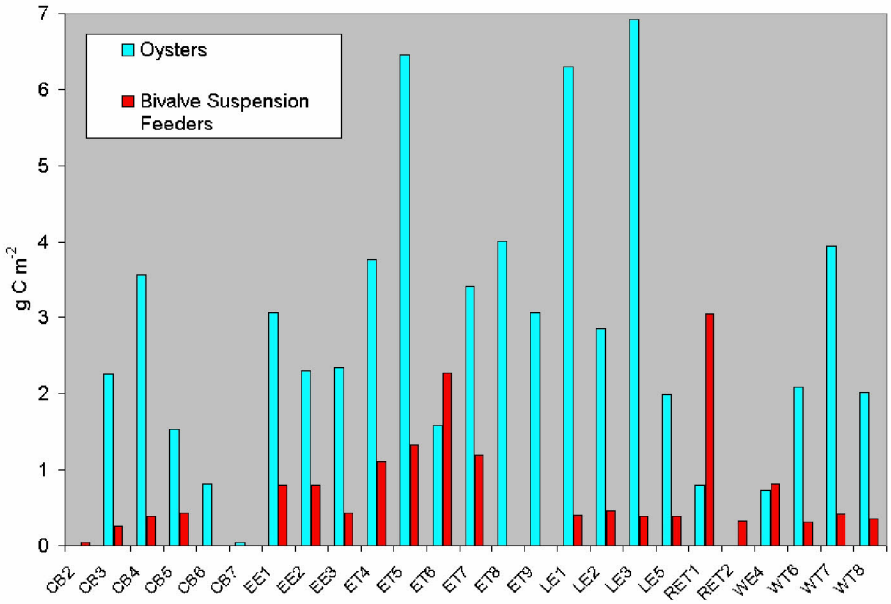

Figure 9. Calculated density of oysters and bivalve filter feeders under the nominal tenfold increase in oyster biomass

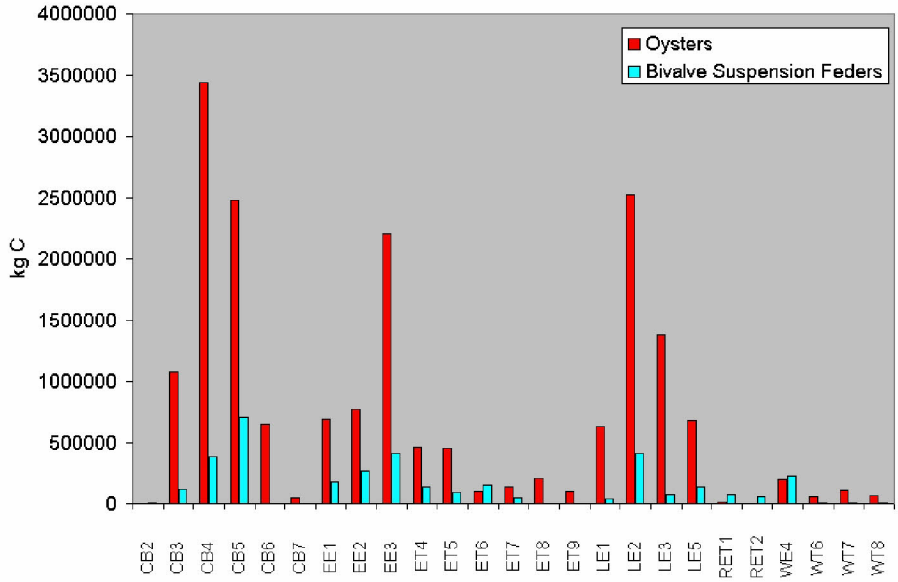

Figure 10. Calculated biomass of oysters and bivalve filter feeders under the nominal tenfold increase in oyster biomass

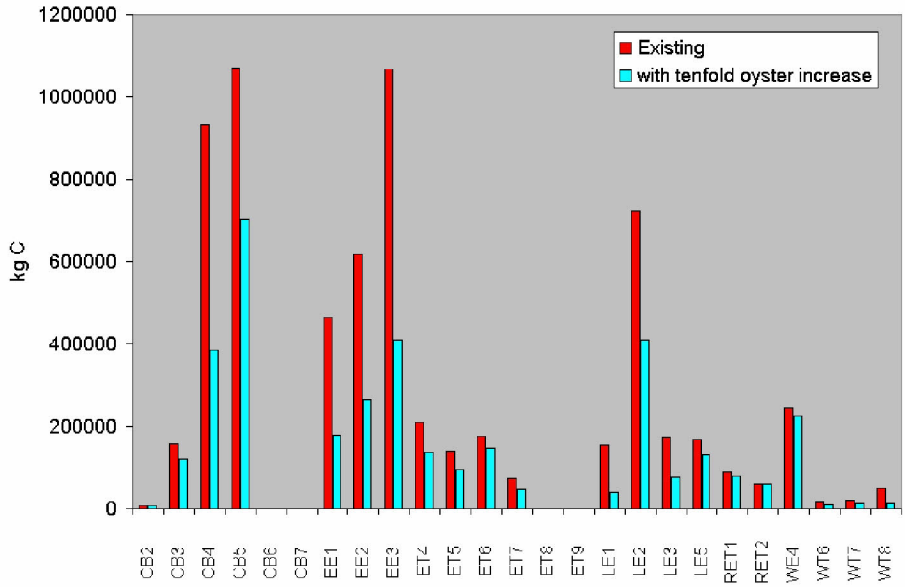

Figure 11. Effect of tenfold increase in oyster biomass on biomass of other bivalve filter feeders

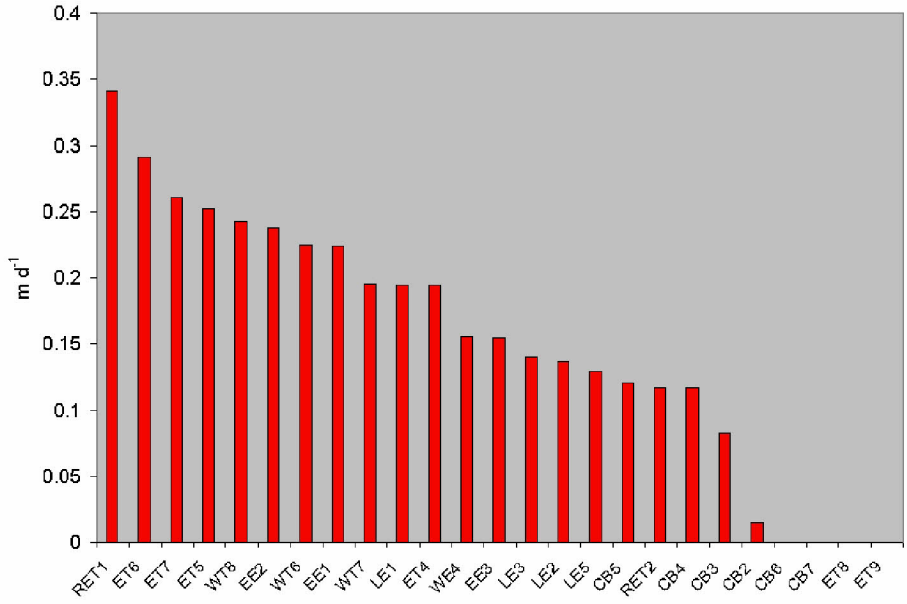

Figure 12. Equivalent settling rate from bivalve filter feeders under existing conditions

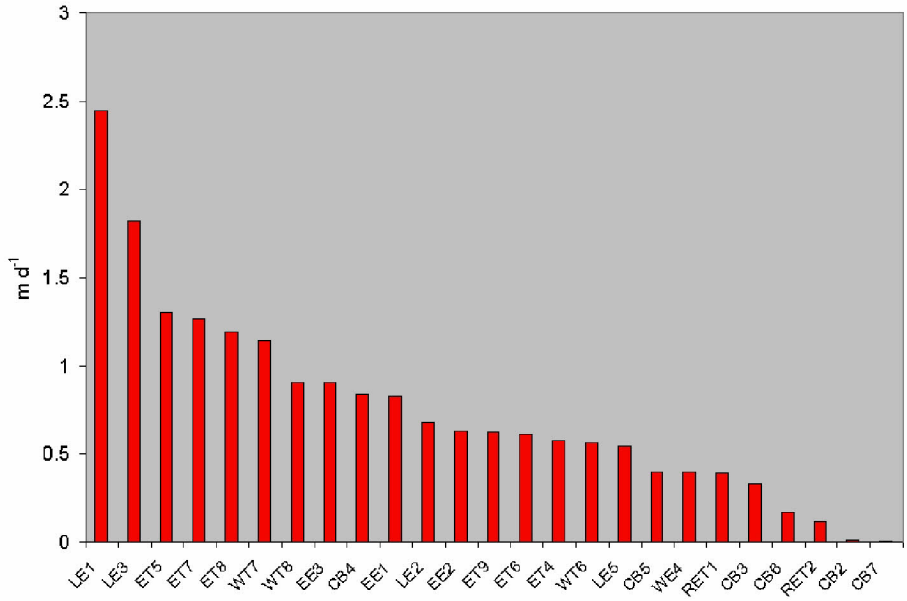

Figure 13. Equivalent settling rate from oysters and bivalve filter feeders under the tenfold increase in oyster biomass

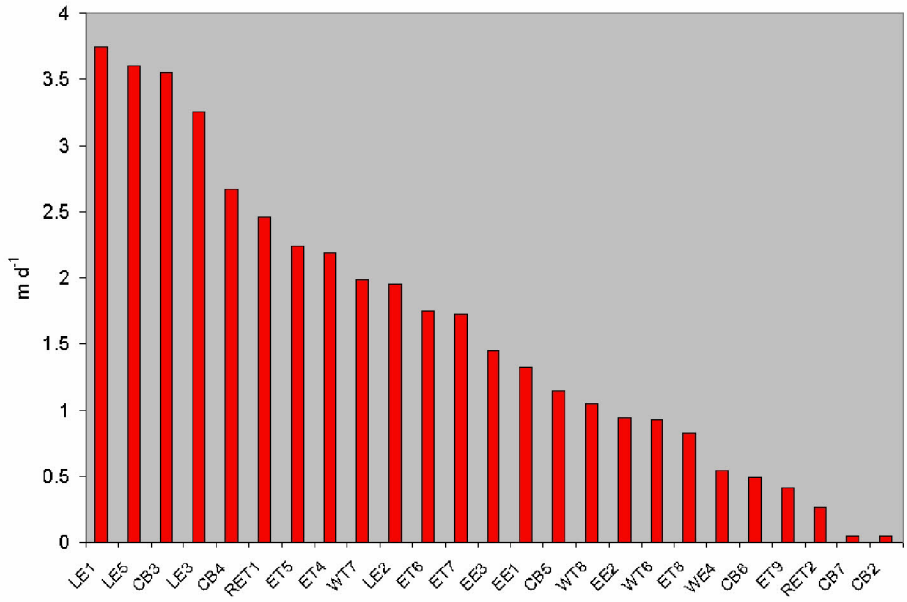

Figure 14. Equivalent settling rate from oysters and bivalve filter feeders under historic conditions

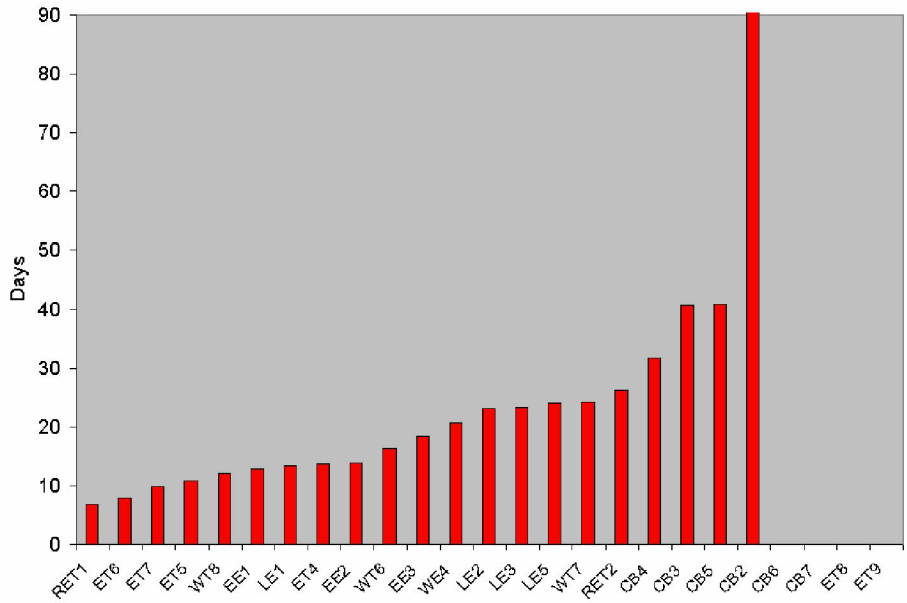

Figure 15. Time for bivalves to filter the water column under existing conditions

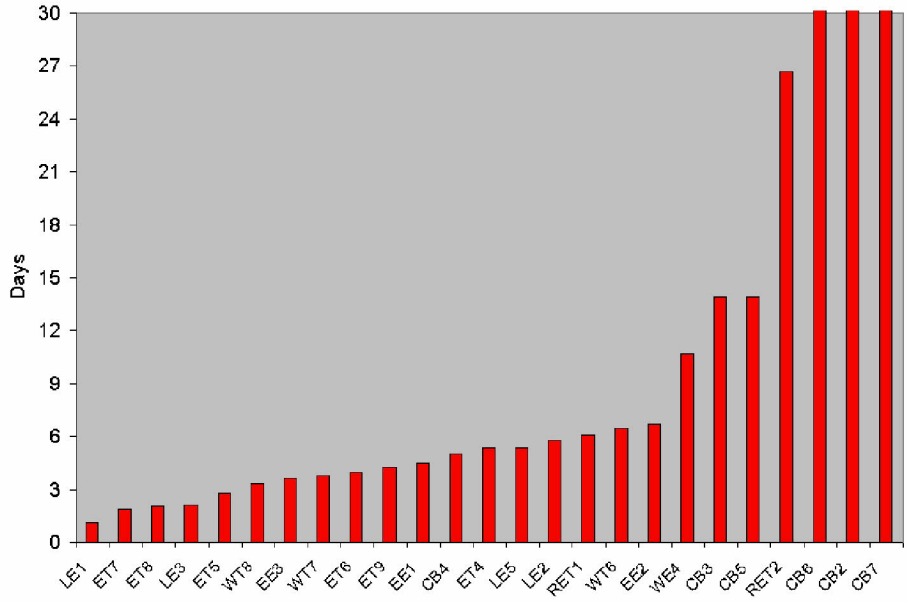

Figure 16. Time for oysters and bivalves to filter the water column under the tenfold increase in oyster biomass

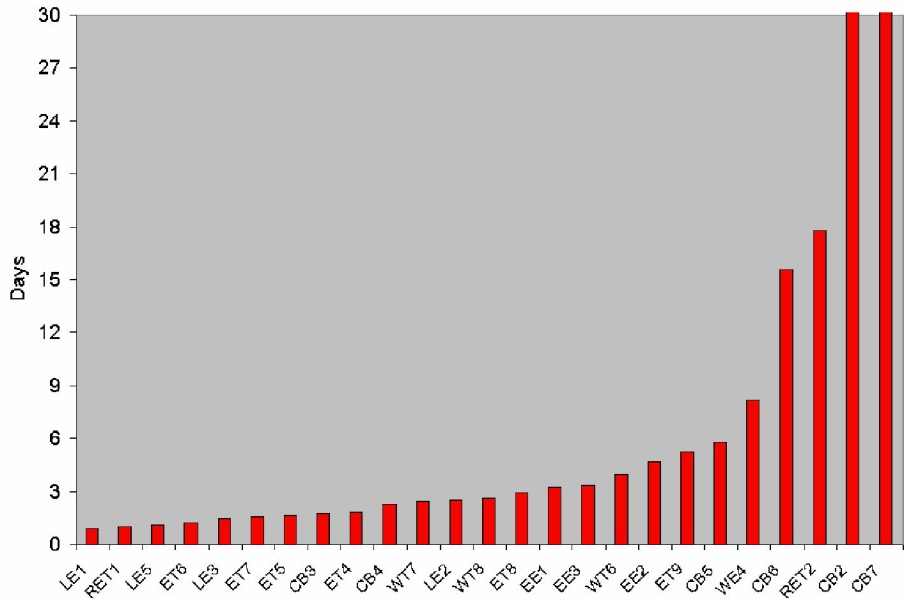

Figure 17. Time for oysters and bivalves to filter the water column under historic conditions

4 Oyster Effects on Water Quality

Introduction

Oysters affect the environment on a variety of spatial scales ranging from their immediate surroundings outwards to the entire water body. The effects are considered here on three scales. The first is the smallest that can be resolved in the model, the model cell. Cell areas are ~ 10^6 m^2, an order of magnitude larger than typical Maryland oyster bars. Since modeled oysters are uniformly distributed within cells, however, the processes in cells occupied by oysters are comparable to processes in bars containing similar densities of oysters. The second spatial scale is the regional scale represented by Chesapeake Bay Program Segments (CBPS). Program segments (Figure 1) are subdivisions of the bay determined by mean salinity, natural boundaries, and other features. Median area is ~ 1.5×10^8 m^2, of which only a fraction is occupied by oyster bottom. The third scale is system-wide, an area of 1×10^{10} m^2, as represented by the model grid.

We selected three of the 35 CBPS for detailed examination of oyster effects on the regional scale. The selected segments (Figure 1) provide a range of geometry (Table 1) and environmental conditions. CB4 is a mainstem bay segment with the greatest volume, surface area, and depth of the selected segments. Due to the depth, only 70% of the area is suitable for oyster habitat, as determined by the historic Yates surveys. Perhaps the most significant characteristic of the segment is the regular occurrence of summer bottom-water anoxia. EE2 is an eastern embayment that encompasses the mouth of the Choptank River. Volume is an order of magnitude less and depth is half of the selected mainstem segment. Virtually all of EE2 is suitable oyster habitat. Minimum dissolved oxygen concentration in bottom water occasionally falls below 3 g m^{-3} but persistent anoxia does not occur. Segment ET9 is the Big Annemessex River, located on the Maryland eastern shore. Despite the name, the Big Annemessex is the smallest of the three selected segments, separated by an order of magnitude in volume and area from EE2. Average depth is roughly half the depth in the lower Choptank River. Virtually all the segment provides suitable oyster habitat and minimum dissolved oxygen concentration exceeds 6 g m^{-3}.

Table 1 Regional Characteristics				
Region	Volume, 10^9 m^3	Area, km^2	Mean Depth, m	Fraction oyster bottom
CB4	10.8	966	11.2	0.71
EE2	1.8	334	5.3	1.00
ET9	0.1	33	2.8	0.8

Local Effects

Biomass-Specific Effects

Effects on the local scale can be normalized by oyster biomass or by surface area. Biomass-specific results allow comparisons to published rates in Chesapeake Bay and elsewhere. For examination of biomass-specific effects, we selected a cell at a depth of 6.7 m within the lower Choptank River, CBPS EE2 (Figure 1). This region supports a viable oyster population and represents the environment from which oysters were drawn for the experiments of Jordan (1987) and Newell and Koch (2004).

Biomass-specific filtration rates, computed within the model based on the simulated environment, agree closely with the experiments on which the rates were based as well as with other independent measures and calculations (Table 1). Order-of-magnitude similarity prevails between modeled and measured respiration and ammonium excretion (Table 1). An interesting contrast occurs with carbon deposition (Table 1). The model agrees well with Jordan's measures but departs from other reports. The modeled and measured filtration and respiration measures are comparable across systems because these are primarily functions of oyster physiology. Carbon deposition is influenced by local organic carbon concentration as well as by physiological processes and, consequently, can only be compared when local organic carbon concentrations are similar.

Areal-Based Effects

The regional and system-wide effects of oyster restoration are best understood by first isolating the local impacts of oysters. This is accomplished by examining sediment diagenetic processes and fluxes between the bottom sediments, oysters, and water column for a range of oyster densities. The basis for comparison is the 2002 version of the model (Cerco and Noel 2004), which included no oysters. This is compared to multiple model runs with oysters, conducted at various mortality rates, that produced a range of oyster densities. Three cells are considered, one each from CB4, EE2, and ET9. All values are annual averages across the ten simulated years.

Benthic Algae. Benthic algae (Figure 2) are non-existent in the CB4 (3.7 m depth) and EE2 (6.7 m depth) cells in the absence of oysters. The shallow ET9 cell (2.1 m depth) supports viable benthic algae at zero oyster density. Density of benthic algae increases in all cells concurrent with oyster density as oysters clear the water column of suspended solids. The enhancement of benthic algae is consistent with experimental results (Newell et al. 2002, Porter et al. 2004)

although only the ET9 cell sustains algal density we calculate is sufficient to influence nutrient exchange at the sediment-water interface (Cerco and Noel 2004). The model state variable is algal carbon. Most observations are of

Table 1
Modeled and Observed Biomass-Specific Oyster Effects

Property	Rate	Source	Comments
Filtration rate, $m^3\ g^{-1}$ oyster C d^{-1}	0.24	Model	Summer average
	0.22	Jordan (1987)	Mean value, T $\geq$ 20 °C
	0.26	Newell and Koch (2004)	Average of measures at 20 and 25 oC
	0.027 to 0.33	Epifanio and Ewart (1977)	For algal suspensions > 1 g C m^{-3}
	0.27	Riisgard (1988)	Calculated for a 2.1 g DW oyster at 27 to 29 °C
Respiration rate, g DO g^{-1} oyster C d^{-1}	0.04	Model	Summer average
	0.03 to 0.06	Boucher and Boucher-Rodini (1988)	Spring and summer rates
	0.017	Dame et al. (1992)	Annual average
	0.02	Dame (1972)	1 g DW oyster at 20 to 30 °C
Ammonium excretion, mg N g^{-1} oyster C d^{-1}	1.43	Model	Summer average
	< 0.1	Hammen et al. (1966)	Ammonium plus urea
	2.8 to 3.88	Boucher and Boucher-Rodini (1988)	Spring and summer rates, includes urea
	0.8	Srna and Baggaley (1976)	1 g DW oyster at 20 °C
	4.8 to 7.9	Magni et al (2000)	*Ruditapes* and *musculista*
Carbon deposition, g C g^{-1} oyster C d^{-1}	0.088	Model	Summer average
	0.099	Jordan (1987)	Mean value, T $\geq$ 20 °C
	0.03	Haven and Morales-Alamo (1966)	
	0.002 to 0.012	Tenore and Dunstan (1973)	Depends on C concentration, range is 0.1 to 0.7 g C m^{-3}

chlorophyll. Using a carbon-to-chlorophyll ratio of 50 (Gould and Gallagher 1990) indicates annual-average computed benthic algal chlorophyll is 30 to 40 mg m^{-2} in the ET9 cell.

Carbon and Oxygen Fluxes. The introduction of oysters results in biodeposition of carbon to the sediments (Figure 3). Carbon deposition due to gravitational settling (Figure 4) is simultaneously diminished as particulate carbon that previously settled is instead filtered. Total carbon deposition (Figure 5) is diminished by the introduction of oysters indicating that the minimum computed density is sufficient to reduce net production of particulate carbon in the water column. The amount of carbon removed by filtering (Figure 6) levels off as oyster densities increase beyond the initial value. Several cells indicate diminished filtration at the highest oyster densities. We attribute the level filtration to an equilibrium between carbon supplied, through transport and production, and carbon removed. As oyster density increases, biodeposition decreases. At higher densities, larger fractions of the carbon filtered are lost through respiration or retained as biomass. Total carbon deposition, through settling and biodeposition, decreases continually in response to increased oyster density.

Increasing oyster densities are accompanied by continual increases in respiration (Figure 7) and decreases in diagenetic sediment oxygen consumption (Figure 8). As noted in the biomass-specific results, respiration is largely a function of oyster density, independent of location. The increased respiration is more than offset by decreased sediment oxygen consumption so that total oxygen consumption decreases as oyster density increases (Figure 9).

Nitrogen. Fluxes of particulate nitrogen reproduce the pattern established for carbon. The introduction of oysters produces biodeposits to the sediments. As oyster density increases, both biodeposition and settling decrease. Biodeposition decreases because a greater fraction of nitrogen filtered is lost through respiration or retained as biomass. Settling decreases because formation of particulate nitrogen in the water column, through algal activity, is diminished by oyster predation.

The introduction of oysters diminishes the release of diagenetically-produced sediment ammonium (Figure 10). Diminished ammonium release is partially offset by excretion from oysters but the net impact of oysters is reduced net release to the water column, especially at highest densities (Figure 11). Two processes contribute to the reduction in diagenetic ammonium release. The role of reduced nitrogen deposition is obvious. Enhanced sediment nitrification to nitrate is also apparent, as evidenced by enhanced sediment denitrifiction of nitrate to nitrogen gas (Figure 12). Denitrification is also enhanced by the flux of nitrate from the water column into the sediments; nitrate no longer used in algal production diffuses into the sediments instead. The net effect of oysters on total nitrogen is removal from the water column via enhanced denitrification and retention in the sediments (Figure 13).

Phosphorus. Oyster effects on particulate phosphorus follow the pattern established for carbon and nitrogen. Introduction of oysters results in biodeposition, which is partially offset by diminished gravitational settling. As

oyster density increases, both biodeposition and settling decrease. Biodeposition decreases because a greater fraction of phosphorus filtered is lost through respiration or retained as biomass. Settling decreases because formation of particulate phosphorus in the water column, through algal activity, is diminished by oyster predation.

The net effect of oysters on dissolved phosphorus contrasts with nitrogen and is site-specific. At two sites, release of diagenetically-produced phoshorus diminishes as oyster density increases while at the third site release of diagenetic phosphorus is largely independent of oyster density (Figure 14). The two sites at which release diminishes support the largest densities of benthic algae so interception of diagenetic phosphorus release is suggested. At the site with least benthic algae, EE2, oyster phosphorus excretion adds to the constant diagenetic flux so that net release of dissolved phosphorus to the water column increases (Figure 15) and net retention in the sediments decreases (Figure 16). At the other two sites, excretion offsets algal uptake so the net flux is nearly constant and retention in the sediments increases as a non-linear function of oyster density.

Regional Effects

Three model runs are considered: 1) no oyster restoration, derived from the 2002 version of the model; 2) a tenfold increase in oyster biomass; and 3) historic oyster density. Quantities selected for analysis include:

- Summer-average bottom dissolved oxygen,
- Summer-average surface chlorophyll,
- Summer-average light attenuation,
- Summer-average SAV biomass,
- Annual-average surface algal carbon,
- Annual-average net primary production,
- Annual-average particulate carbon deposition,
- Annual-average sediment oxygen demand,
- Annual-average surface total nitrogen,
- Annual-average particulate nitrogen deposition,
- Annual-average sediment diagenetic ammonium flux,
- Annual-average net nitrogen removal (denitrification plus burial),
- Annual-average surface total phosphorus,
- Annual-average particulate phosphorus deposition,
- Annual-average sediment diagenetic phosphorus release, and
- Annual-average net phosphorus removal

Our convention for surface concentration is the average over the upper 6.7 m of the water column, roughly the depth of the surface mixed layer in the mid-bay. Bottom dissolved oxygen is represented by all waters below 12.9 m in CB4 and below 6.7 m in EE2. Due to shallow depth, the surface mixed layer coincides with the bottom in ET9. Results are averaged across the entire regional area and across all model years.

CB4

Water quality standards in Chesapeake Bay are based on dissolved oxygen, chlorophyll, and water clarity. The ten-fold oyster increase improves summer-average, bottom, dissolved oxygen in this mainstem segment by less than 0.5 g m^{-3} (Figure 17). Simulation of historic oyster densities improves dissolved oxygen by roughly 1 g m^{-3}. Computed surface chlorophyll is reduced by 30% for a ten-fold increase in oyster density and is halved when oysters are restored to historic densities (Figure 18). Light attenuation is reduced by roughly 20% for a ten-fold increase in oyster densities and by roughly 40% when oysters are restored to historic densities (Figure 19).

The improvements in dissolved oxygen and chlorophyll are effected by reductions in net primary production (Figure 20). A 20% reduction in production accompanies the ten-fold increase in oyster density. A reduction of nearly 40% results from restoration of historic densities. The water clarity improvements, effected by removal of phytoplankton and other solids from the water column, produce increases in computed SAV biomass of 33% to more than 100% (Figure 21).

Restoration of oysters increases net nitrogen removal (Figure 22), through denitrification and sediment retention, by 20% to 50% although the reduction in surface total nitrogen concentration is only 10% to 15% (Figure 23). When averaged over the region, the effect of oyster restoration is increased phosphorus retention in the sediments (Figure 24). Net removal increases by a third for a ten-fold increase in oyster density and doubles when oysters are restored to historic densities. Phosphorus concentration in the water column corresponds with net removal rates more closely than nitrogen (Figure 25). Surface total phosphorus concentration is reduced by 20% to 40%.

EE2

Improvements in summer-average, bottom, dissolved oxygen at the mouth of the Choptank are consistent with the mainstem segment: less than 0.5 g m^{-3} for a ten-fold increase in oyster density and roughly 1 g m^{-3} for restoration to historic densities (Figure 26). Percentage reductions in surface chlorophyll (Figure 27) and light attenuation (Figure 28) also correspond closely with the adjacent mainstem segment as do the reductions in net primary production (Figure 29) and improvements in SAV (Figure 30).

ET9

Computed dissolved oxygen concentration in the eastern shore embayment declines by 0.5 g m^{-3} as a consequence of oyster restoration (Figure 31). The decline in dissolved oxygen reflects diminished dissolved oxygen production associated with the 40% to 60% reduction in net primary production (Figure 32). Reductions in summer surface chlorophyll exceed the reductions in annual net production (Figure 33). The ten-fold increase in oyster density induces a 60% decrease in summer surface chlorophyll while restoration to historic densities induces a greater then 70% decrease. Light attenuation in this region decreases by a third to nearly a half (Figure 34). Corresponding increases

in SAV greatly exceed the responses in other segments (Figure 35). SAV biomass nearly triples for a ten-fold increase in oyster density and increases by greater than a factor of four for restoration to historic oyster densities.

Regional Budgets

Nutrient budgets were constructed for each of the regions for the three subject model runs. Results are annual averages across all model years. Terms in the budgets are:

- Point Source – Direct inputs from municipal and industrial facilities
- Distributed – Loads to the region from the adjacent watershed
- Atmospheric – Loads to the water surface
- Transport – Net loads from the upstream region. For CB4, this is adjacent mainstem region CB2. For EE2, this is the Choptank River segment ET5. No upstream segment exists for ET9.
- Net Removal – Accumulation in the bottom sediments plus denitrification
- Incremental – Increase in net removal due to oysters

Nitrogen transport down the mainstem of the bay dwarfs all other sources and sinks in CB4 (Figure 36). In view of the enormity of nitrogen transported in relative to the amount removed by oysters, the ability of oyster restoration to impact this segment at all is remarkable. This budget suggests the impact of oysters on phytoplankton is through direct grazing rather than through nutrient removal that results in limits to phytoplankton growth. Although nutrient removal can be viewed as an ecosystem service, direct grazing should be regarded as the primary service. More phosphorus is removed in CB4 than flows in from upstream and local sources (Figure 37). The deficit is made up by net phosphorus transport from downstream, as indicated by our earliest model (Cerco and Cole 1994) and by bay nutrient budgets (Boynton et al. 1995). As with nitrogen, the incremental nutrient removal by oysters is small relative to the net transport along the bay axis.

Incremental nutrient removal by oysters in EE2 is significant relative to other regional sources and sinks. Under the restoration scenarios, net nitrogen (Figure 38) and phosphorus (Figure 39) removal exceed the local sources indicating nutrient import from the adjacent mainstem segment.

Nitrogen loading and net removal in segment ET9 are closely balanced under existing conditions (Figure 40). As with EE2, enhanced removal via oyster restoration results in nitrogen import from the adjacent Tangier Sound. This segment imports phosphorus under existing conditions (Figure 41). Net import is enhanced under conditions of oyster restoration.

System-Wide Effects

The methods, properties examined, and budgeting from the regional analyses are extensible to the entire system. We consider the system to extend from the fall lines of major tributaries to the mouth of the bay. We were

requested to make two supplementary model runs for the sponsor. These combined the 2002 model (Cerco and Noel 2004) with the nutrient and solids loads from the recent allocation. One run was completed without oysters. The second run incorporated the ten-fold oyster restoration. Since the results of those runs have not been documented, we summarize them here.

Summer-average dissolved oxygen concentration is considered for all portions of the bay greater than 12.9 m depth. Dissolved oxygen increases by 0.25 g m^{-3} for the ten-fold oyster restoration and by 0.8 g m^{-3} for restoration to historic levels (Figure 42). By way of comparison, the dissolved oxygen improvement attained by the allocation loads exceeds the improvement attained by oyster restoration to historic levels. Allocation loads combined with ten-fold oyster restoration provide the greatest level of improvement, more than 1 g m^{-3} over current levels. System-wide, summer, surface chlorophyll concentration declines by more than 1 mg m^{-3} for a ten-fold increase in oyster biomass and by 2.5 mg m^{-3} for restoration to historic levels (Figure 43). As with dissolved oxygen, the allocation loads provide greater benefit than oyster restoration with improved benefits from both load reductions and oyster restoration.

The improvements in dissolved oxygen and chlorophyll are effected by reductions in net primary production (Figure 44). A 14% reduction in system-wide production accompanies the ten-fold increase in oyster density. A reduction of 25% results from restoration of historic densities. The allocation loads provide greater reductions in algal production than any level of oyster restoration and greatest reductions accompany load reductions and oyster restoration.

The water clarity improvements that accompany oyster restoration (Figure 45) produce increases in computed system-wide SAV biomass of 25% to more than 60% (Figure 46). The historic levels of oysters result in the greatest improvements in SAV, suggesting local solids removal can be more effective than indirect controls on organic solids effected through nutrient controls. Still, the allocation loads produce larger improvements than the proposed ten-fold increase in oyster biomass.

Load reductions produce greater reductions in total nutrients than oyster restoration. The allocation loads diminish system-wide surface total nitrogen by 0.27 g m^{-3} (Figure 47) and total phosphorus by 0.011 g m^{-3} (Figure 48) with marginal additional reductions accomplished by load reductions combined with oyster restoration. The maximum nutrient reductions accomplished by oyster restoration are 0.11 g m^{-3} total nitrogen and 0.009 g m^{-3} total phosphorus. These results contrast the different strategies for phytoplankton control. The allocation loads reduce phytoplankton through nutrient reductions. Oyster restoration controls phytoplankton by direct grazing; nutrient reductions are a by-product of algal removal.

System-wide nutrient budgets can be constructed that parallel the regional budgets. In this case, transport is the net flux at the mouth of the bay. Negative transport indicates nutrient loss to the ocean; positive transport indicates nutrient import from the ocean. Ten-fold oyster restoration removes 30,000 kg d^{-1} total nitrogen from the system (Figure 49). Oysters at historic levels remove 54,000 kg d^{-1}. Ten-fold oyster restoration removes 4,000 kg d^{-1}

total phosphorus from the system (Figure 50). Oysters at historic levels remove 5,000 kg d^{-1}. By way of comparison, the ten-fold restoration removes loading roughly equivalent to direct atmospheric deposition. These are 25,000 kg d^{-1} total nitrogen and 1,900 kg d^{-1} total phosphorus.

References

Boucher, G., and Boucher-Rodoni, R. (1988). "In situ measurement of respiratory metabolism and nitrogen fluxes at the interface of oyster beds," *Marine Ecology Progress Series*, 44, 229-238.

Boynton, W., Garber, J., Summers, R., and Kemp, W. (1995). "Inputs, transformations, and transport of nitrogen and phosphorus in Chesapeake Bay and selected tributaries," *Estuaries*, 18(1B), 285-314.

Cerco, C., and Cole, T. (1994). "Three-dimensional eutrophication model of Chesapeake Bay," Technical Report EL-94-4, US Army Engineer Waterways Experiment Station, Vicksburg, MS.

Cerco, C., and Noel, M. (2004). "The 2002 Chesapeake Bay eutrophication model," EPA 903-R-04-004, Chesapeake Bay Program Office, US Environmental Protection Agency, Annapolis, MD.

Dame, R., (1972). "Comparison of various allometric relationships in intertidal and subtidal American oysters," *Fishery Bulletin*, 70(4), 1121-1126.

Dame, R., Spurrier, J., and Zingmark, R. (1992). "In situ metabolism of an oyster reef," *Journal of Experimental Marine Biology and Ecology*, 164, 147-159.

Epifanio, C., and Ewart, J. (1977). "Maximum ration of four algal diets for the oyster *Crassostrea virginica* Gmelin," *Aquaculture*, 11, 13-29.

Gould, D., and Gallagher, E. (1990). "Field measurements of specific growth rate, biomass, and primary production of benthic diatoms of Savin Hill Cove, Boston," *Limnology and Oceanography*, 35, 1757-1770.

Hammen, C., Miller, H., and Geer, W. (1966). "Nitrogen excretion of *Crassostrea virginica*," *Comparative Biochemistry and Physiology*, 17, 1199-2000.

Haven, D., and Morales-Alamo, R. (1966). "Aspects of biodeposition by oysters and other invertebrate filter feeders," *Limnology and Oceanography*, 11, 487-498.

Jordan, S. (1987). "Sedimentation and remineralization associated with biodeposition by the American oyster *Crassostrea virginica* (Gmelin)," Ph.D. diss., University of Maryland, College Park.

Magni, P., Montani, S., Takada, C., and Tsutsumi, H. (2000). "Temporal scaling and relevance of bivalve nutrient excretion on a tidal flat of the Seto Inland Sea, Japan," *Marine Ecology Progress Series*, 198, 139-155.

Newell, R., and Koch, E. (2004). "Modeling seagrass density and distribution in response to changes in turbidity stemming from bivalve filtration and seagrass sediment stabilization," *Estuaries*, 27(5), 793-806.

Riisgard, H. (1988). "Eficiency of particle retention and filtration rate in 6 species of Northeast American bivalves," *Marine Ecology Progress Series*, 45, 217-223.

Srna, R., and Baggaley, A. (1976). "Rate of excretion of ammonia by the hard clam *Mercenaria mercenaria* and the American oyster *Crassostrea virginica*," *Marine Biology*, 36, 251-258.

Tenore, K., and Dunstan, W. (1973). "Comparison of feeding and biodeposition of three bivalves at different food levels," *Marine Biolo gy*, 21, 190-195.

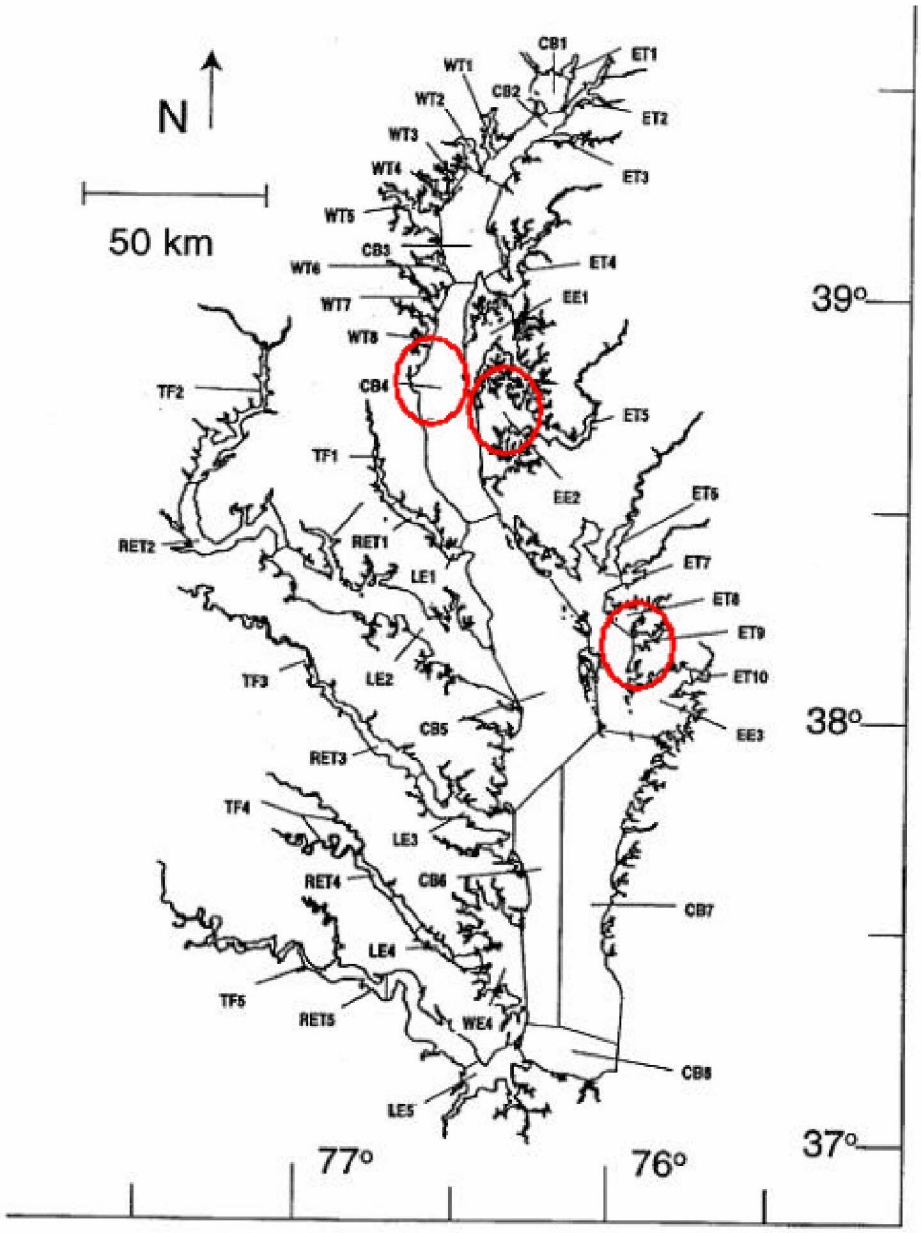

Figure 1. Chesapeake Bay program segments.

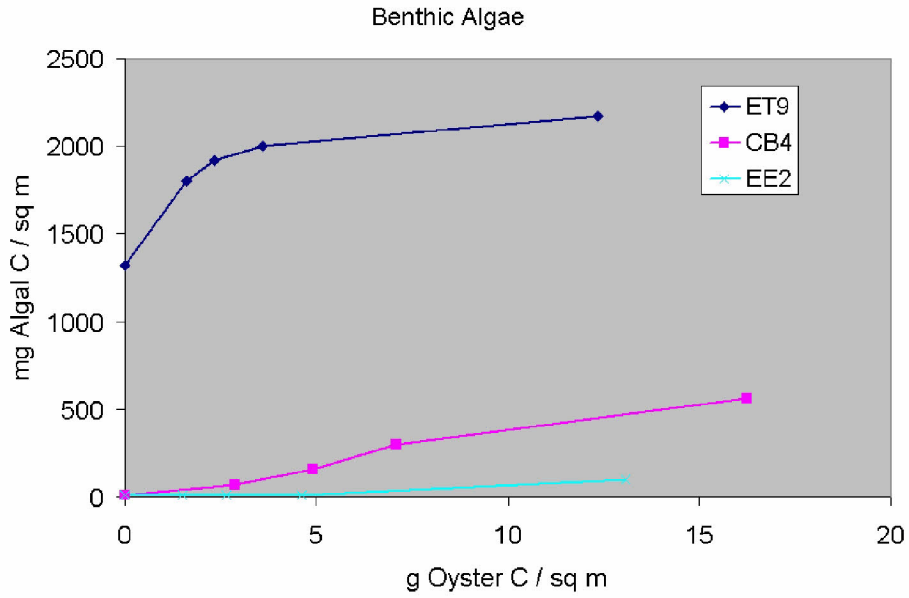

Figure 2. Effect of oysters on benthic algae.

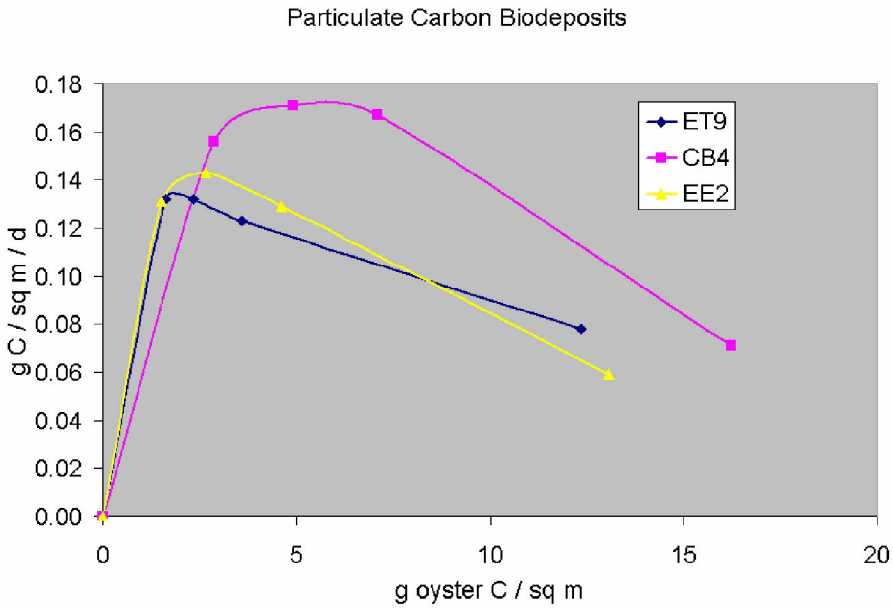

Figure 3. Effect of oysters on particulate carbon biodeposition.

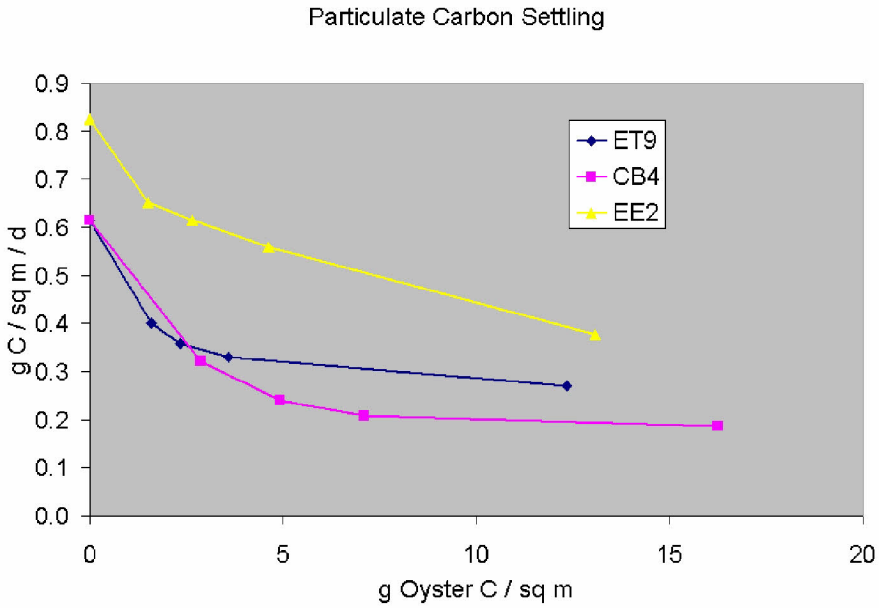

Figure 4. Effect of oysters on gravitational settling of particulate carbon.

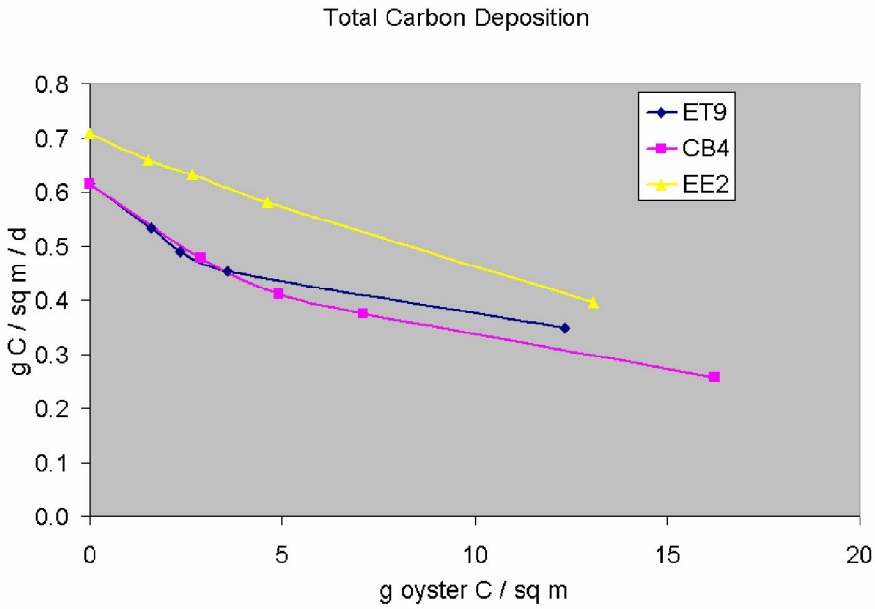

Figure 5. Effect of oysters on total carbon deposition.

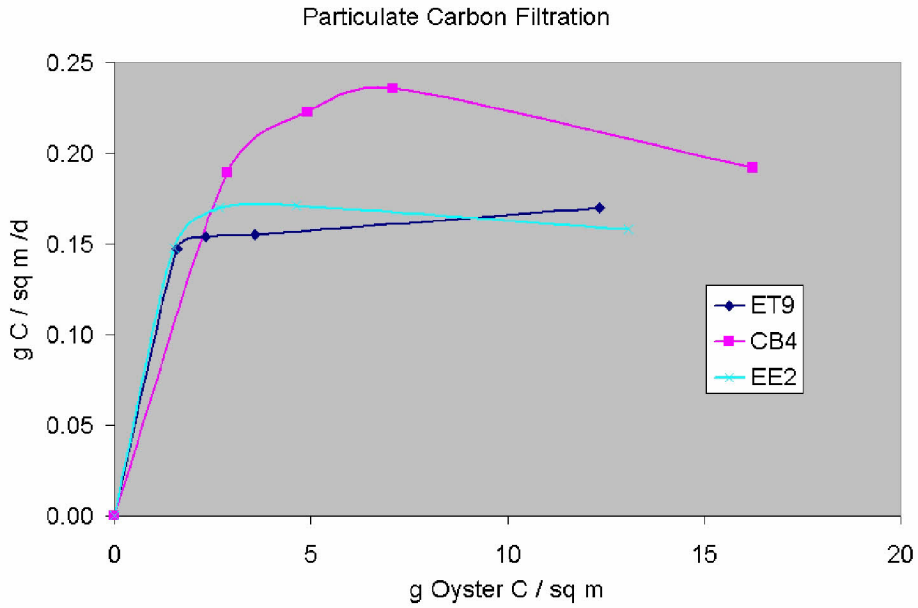

Figure 6. Effect of oysters on particulate carbon filtration.

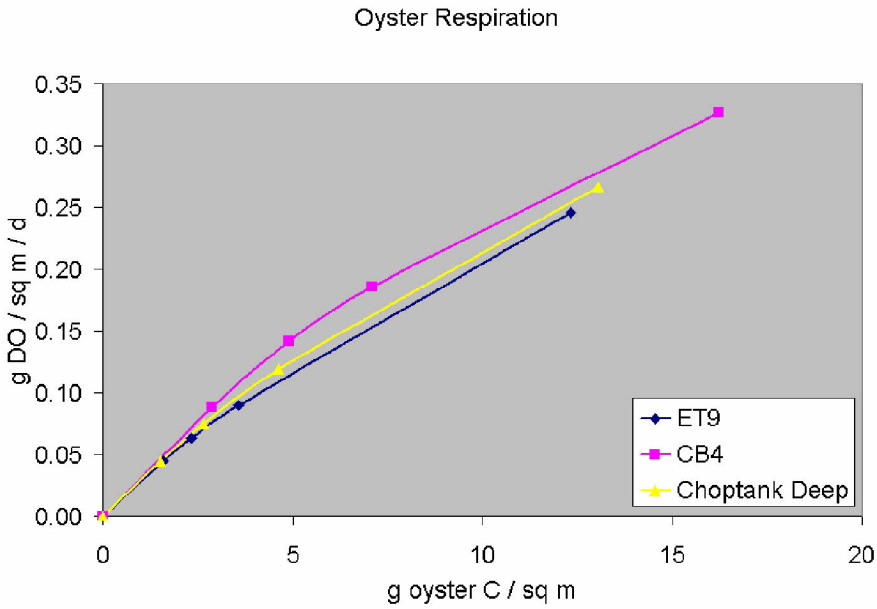

Figure 7. Effect of oysters on areal respiration.

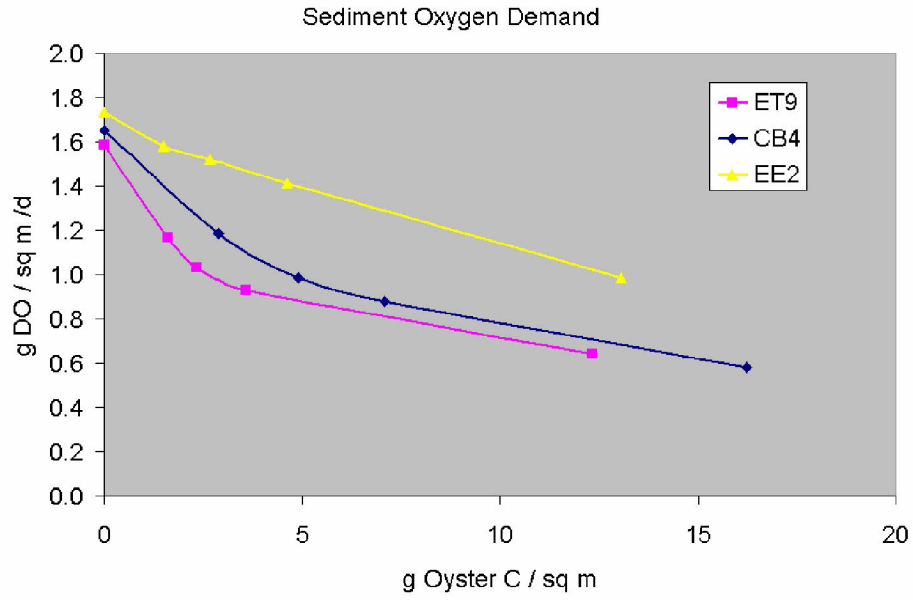

Figure 8. Effect of oysters on sediment oxygen demand.

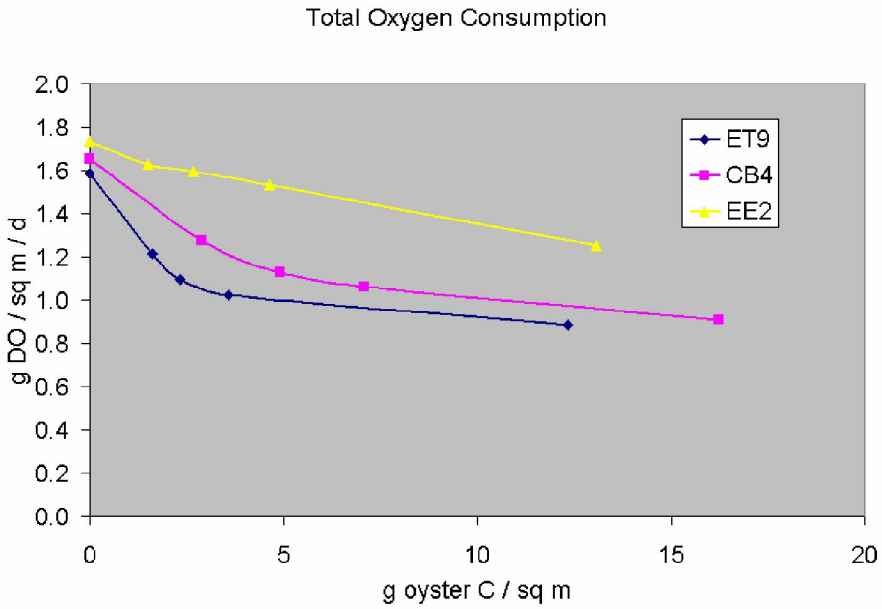

Figure 9. Effect of oysters on total benthic oxygen consumption.

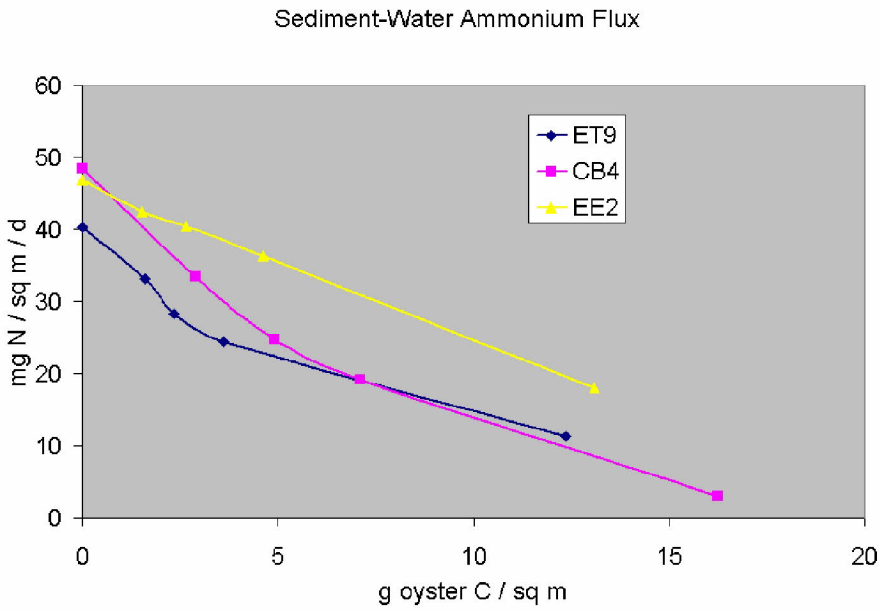

Figure 10. Effect of oysters on sediment-water ammonium flux.

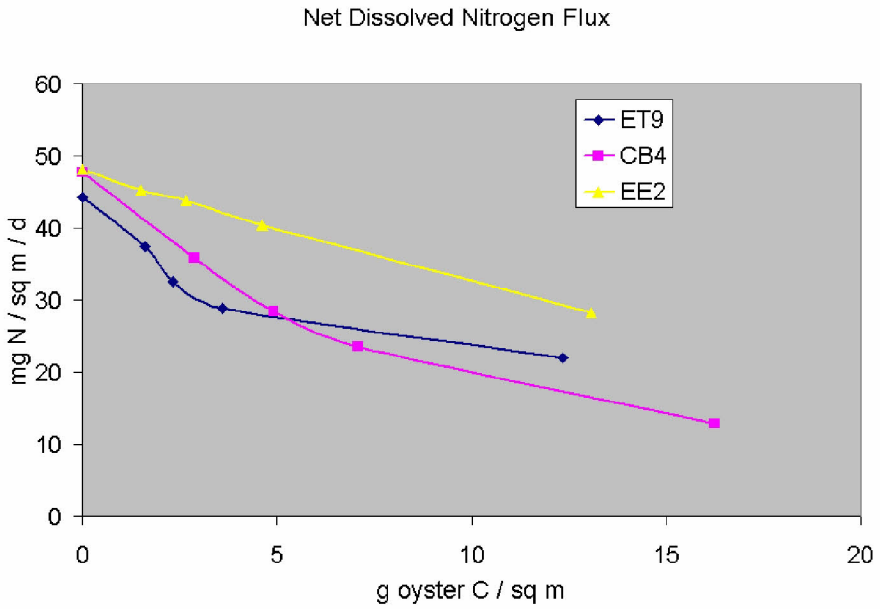

Figure 11. Effect of oysters on net benthic dissolved nitrogen flux.

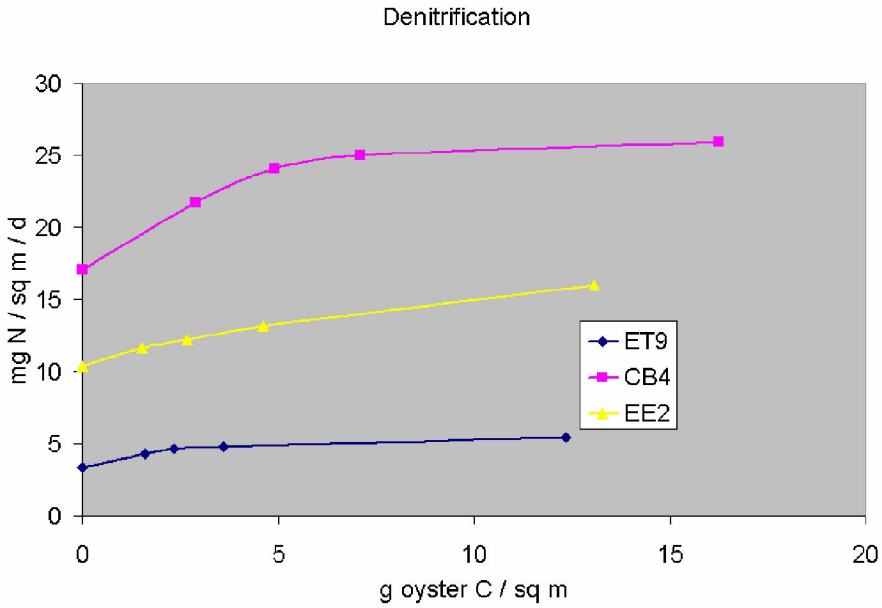

Figure 12. Effect of oysters on sediment denitrification.

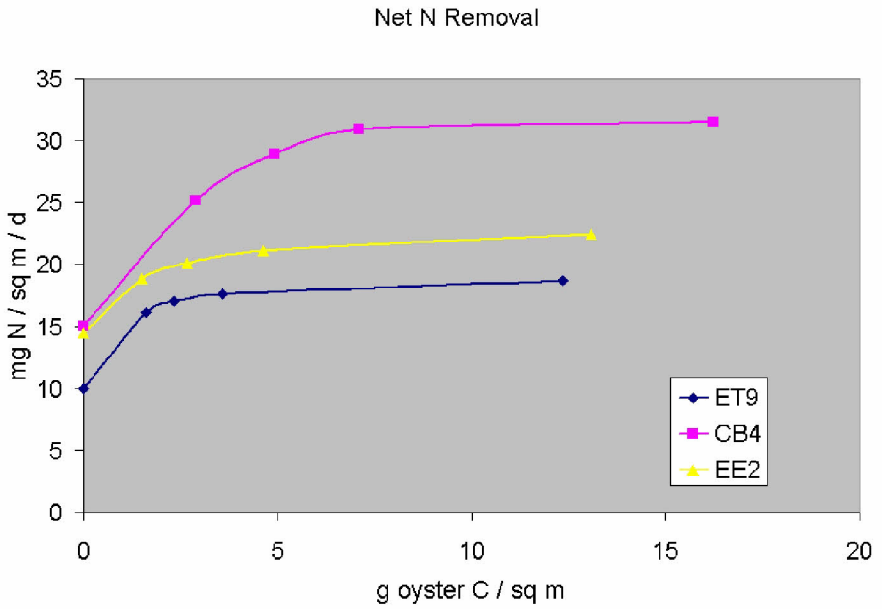

Figure 13. Effect of oysters on net sediment nitrogen removal.

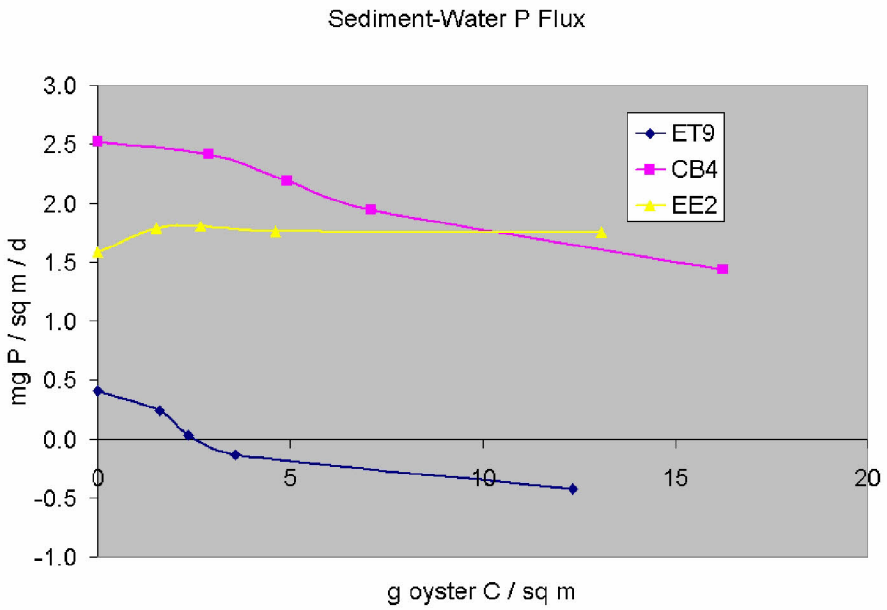

Figure 14. Effect of oysters on sediment-water dissolved phosphorus flux. Positive flux is release to the water column.

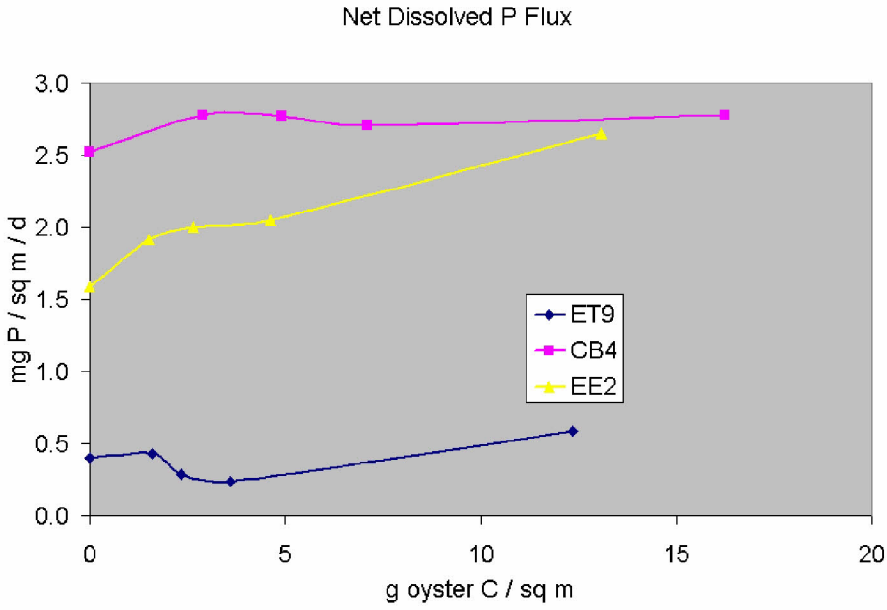

Figure 15. Effect of oysters on net benthic dissolved phosphorus flux.

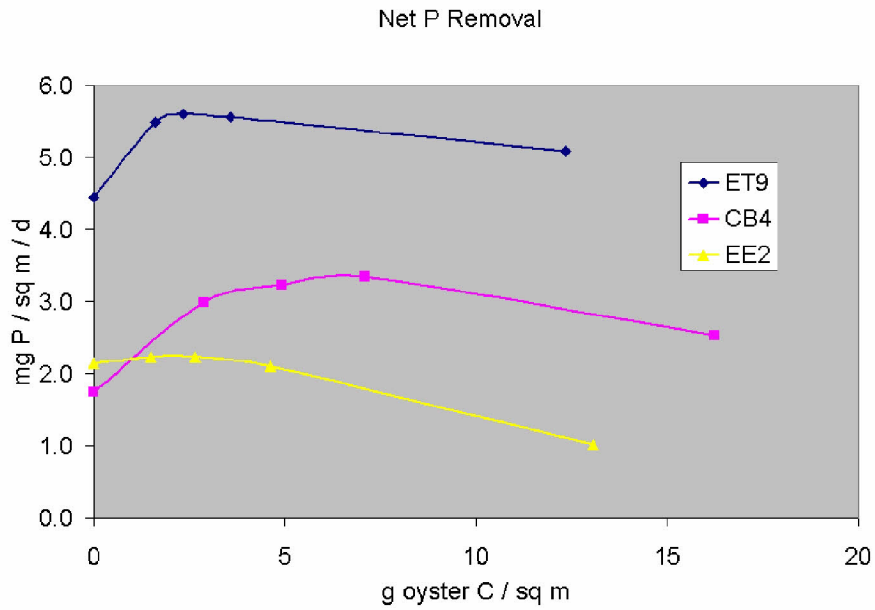

Figure 16. Effect of oysters on net sediment phosphorus removal.

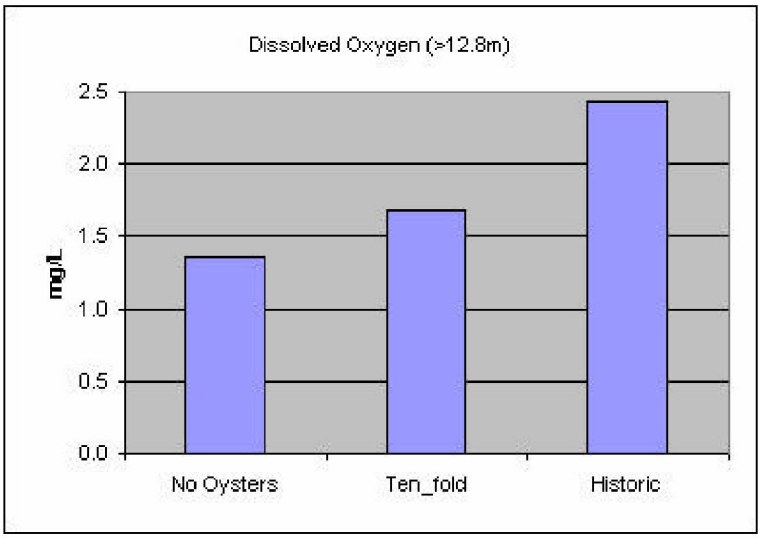

Figure 17. Effect of oysters on summer-average, bottom, dissolved oxygen in CB4.

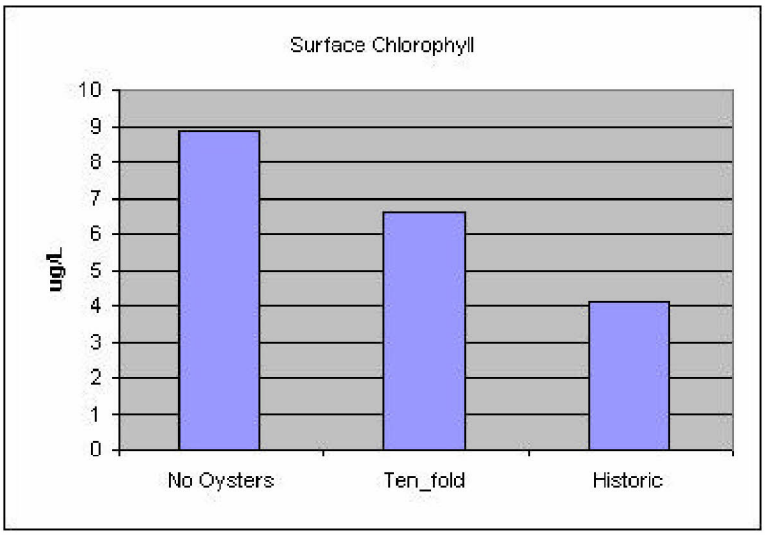

Figure 18. Effect of oysters on summer-average, surface, chlorophyll in CB4.

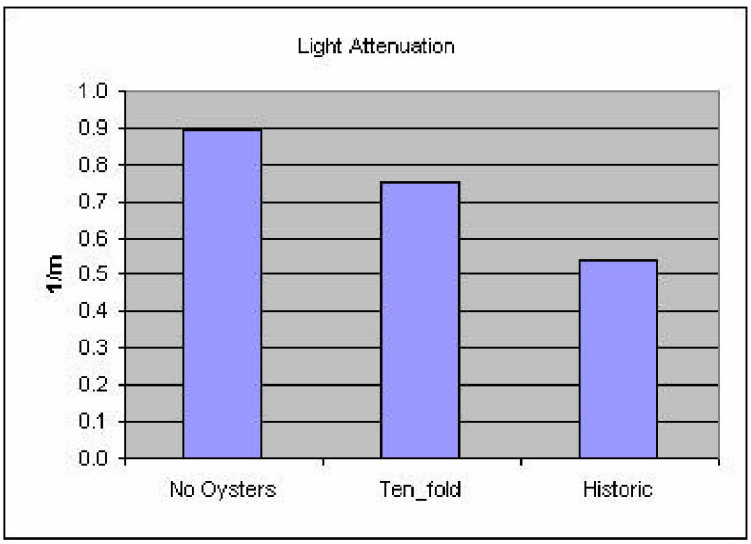

Figure 19. Effect of oysters on summer-average light attenuation in CB4.

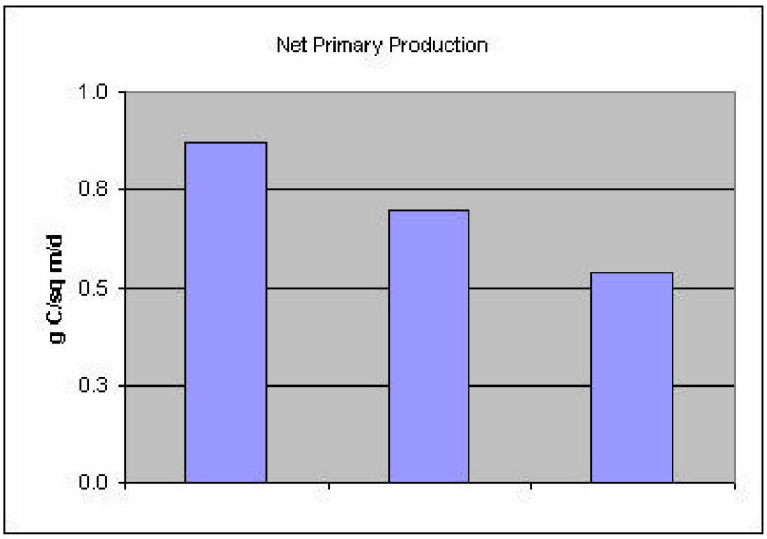

Figure 20. Effect of oysters on annual-average net phytoplankton primary production in CB4.

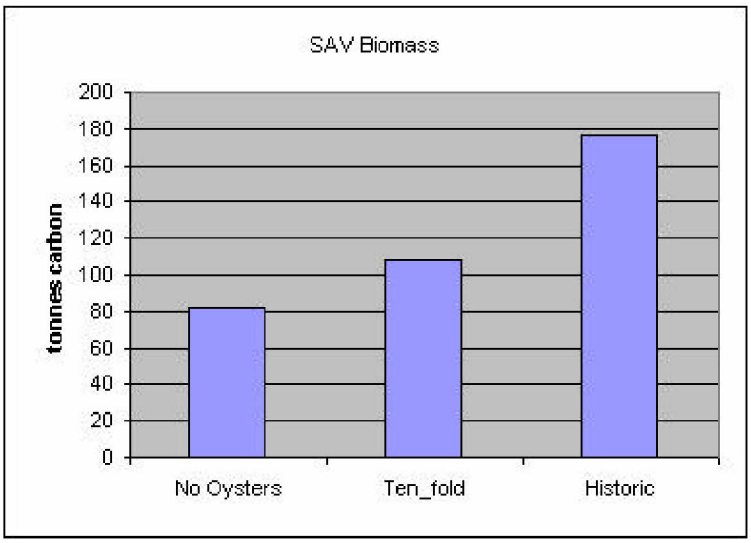

Figure 21. Effect of oysters on summer-average SAV biomass in CB4.

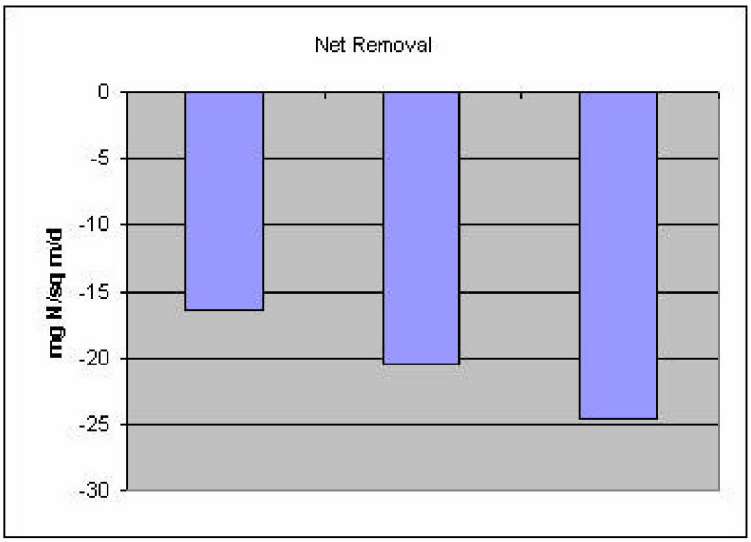

Figure 22. Effect of oysters on net benthic nitrogen removal in CB4.

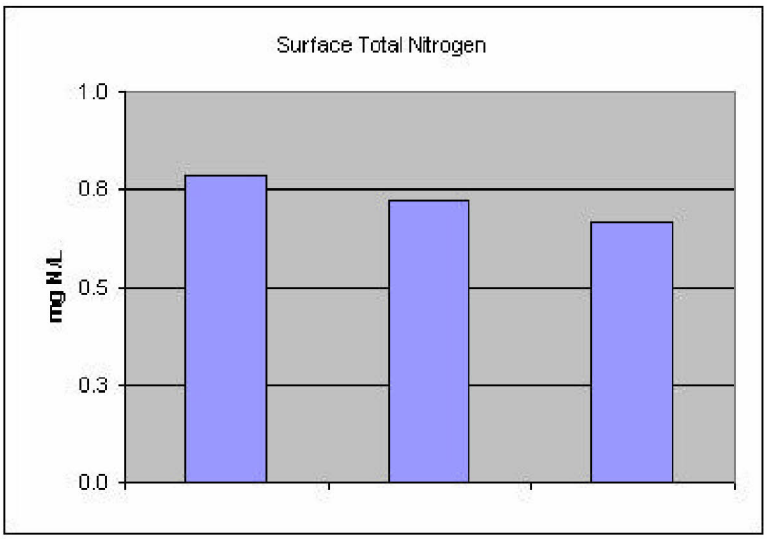

Figure 23. Effect of oysters on annual-average, surface, total nitrogen in CB4.

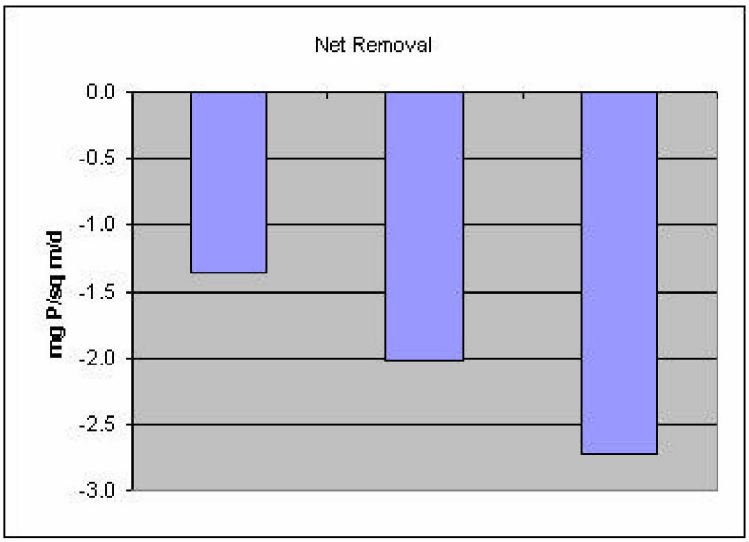

Figure 24. Effect of oysters on net benthic phosphorus removal in CB4.

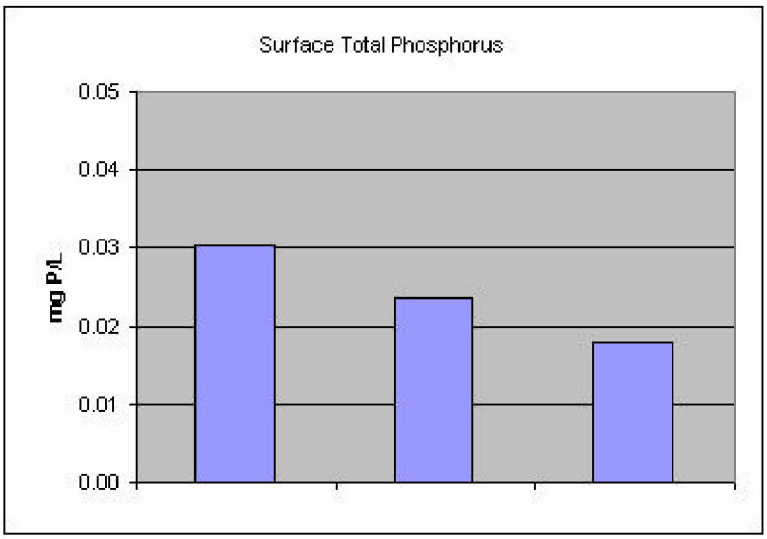

Figure 25. Effect of oysters on annual-average, surface, total phosphorus in CB4.

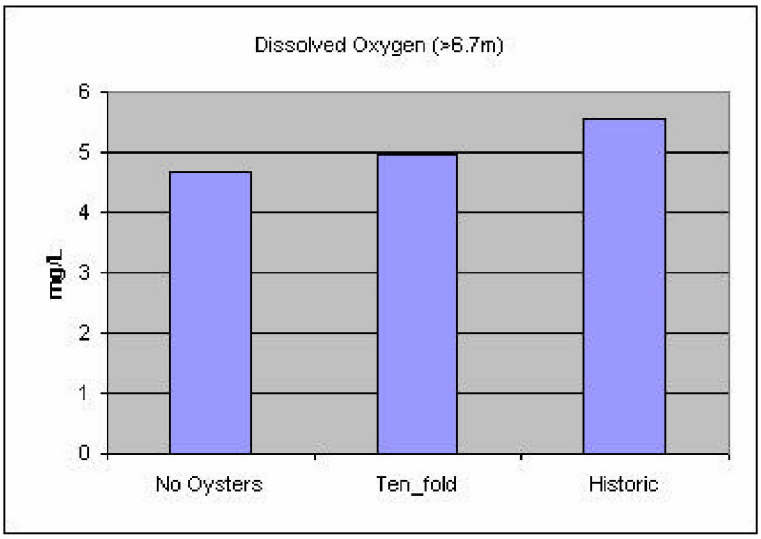

Figure 26. Effect of oysters on summer-average, bottom, dissolved oxygen in EE2.

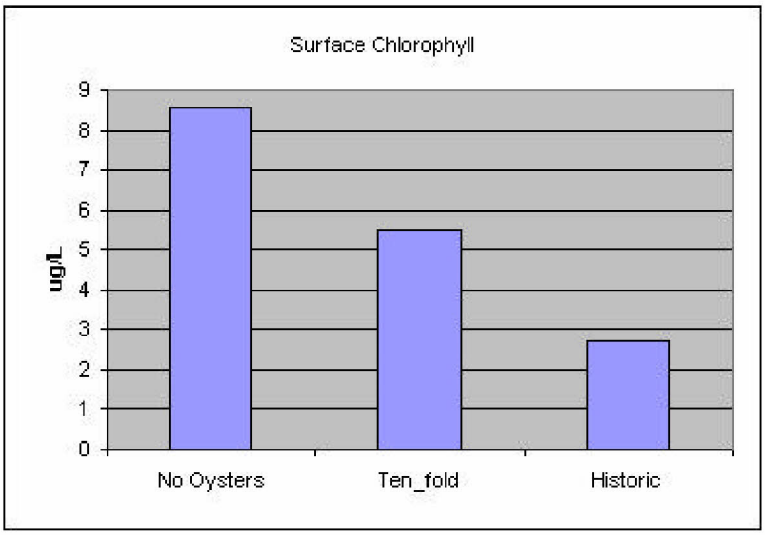

Figure 27. Effect of oysters on summer-average, surface, chlorophyll in EE2.

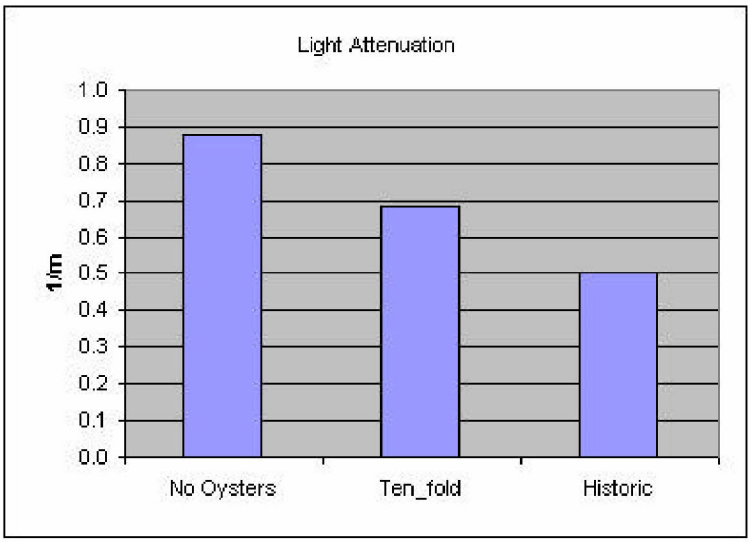

Figure 28. Effect of oysters on summer-average light attenuation in EE2.

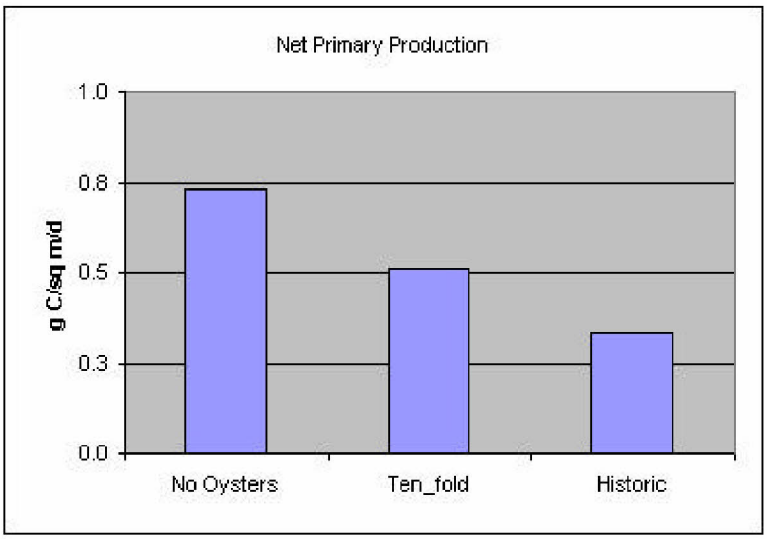

Figure 29. Effect of oysters on annual-average net phytoplankton primary production in EE2.

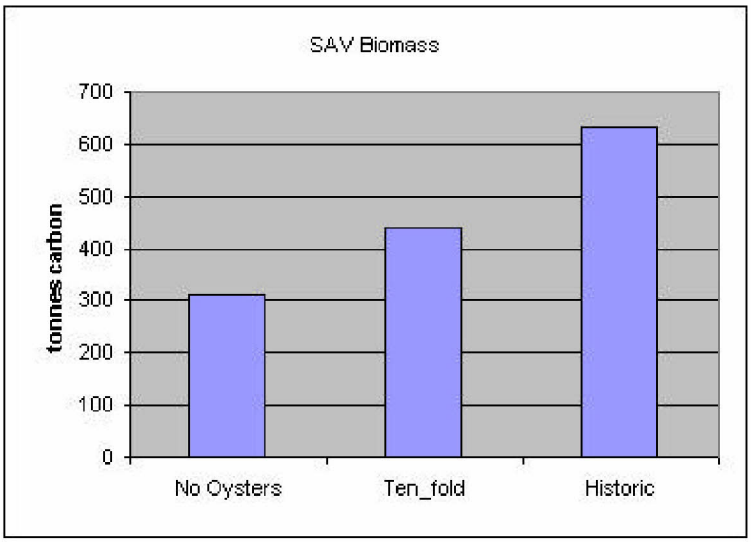

Figure 30. Effect of oysters on summer-average SAV biomass in EE2.

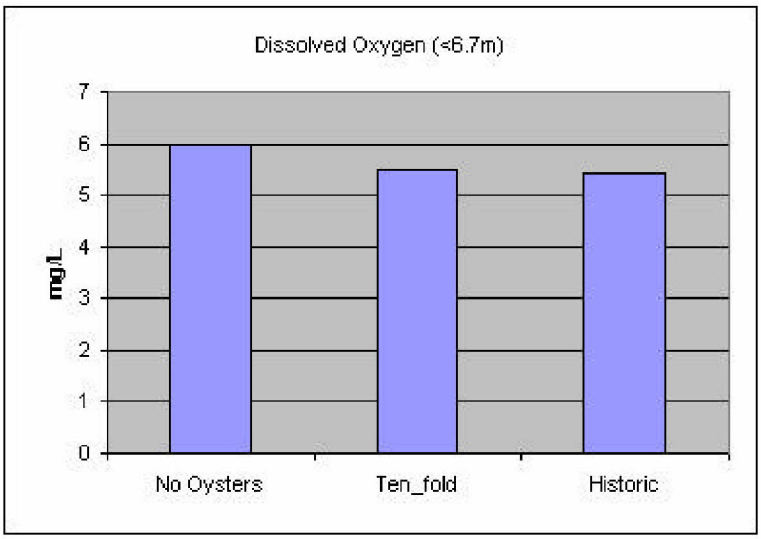

Figure 31. Effect of oysters on summer-average dissolved oxygen in ET9.

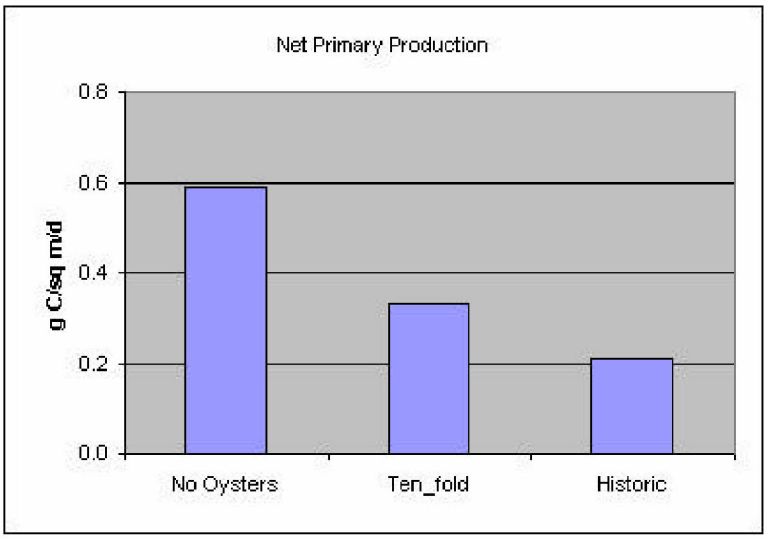

Figure 32. Effect of oysters on annual-average net phytoplankton primary production in ET9.

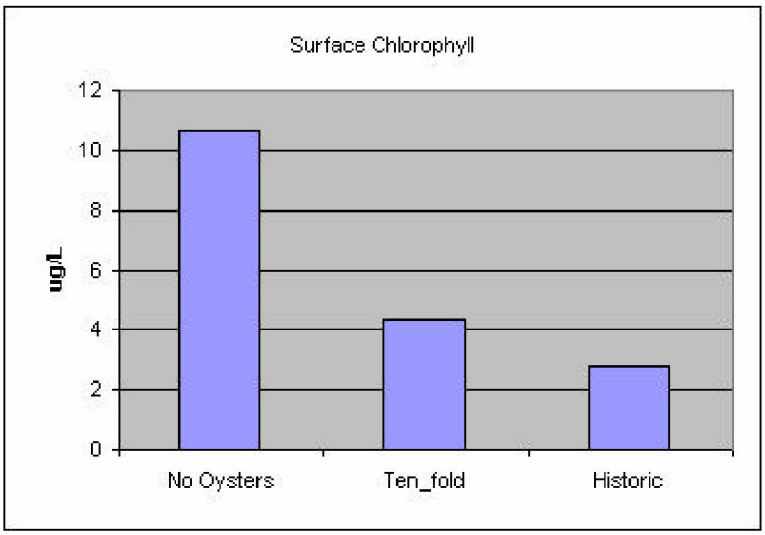

Figure 33. Effect of oysters on summer-average chlorophyll in ET9.

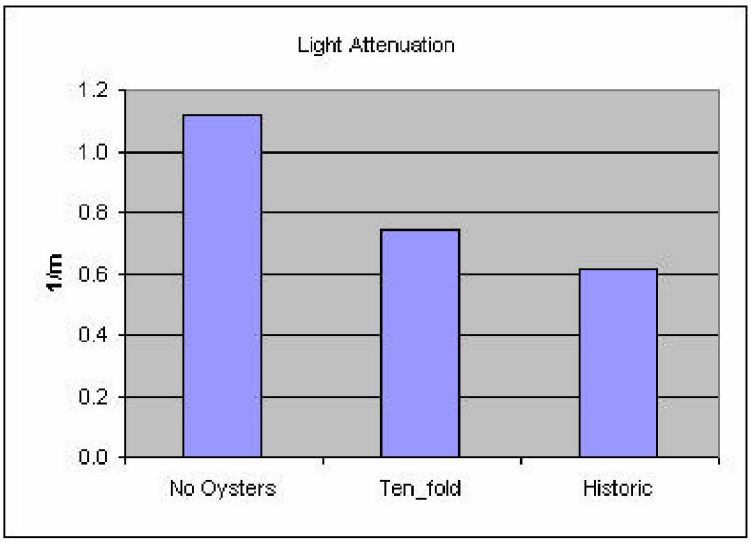

Figure 34. Effect of oysters on summer-average light attenuation in ET9.

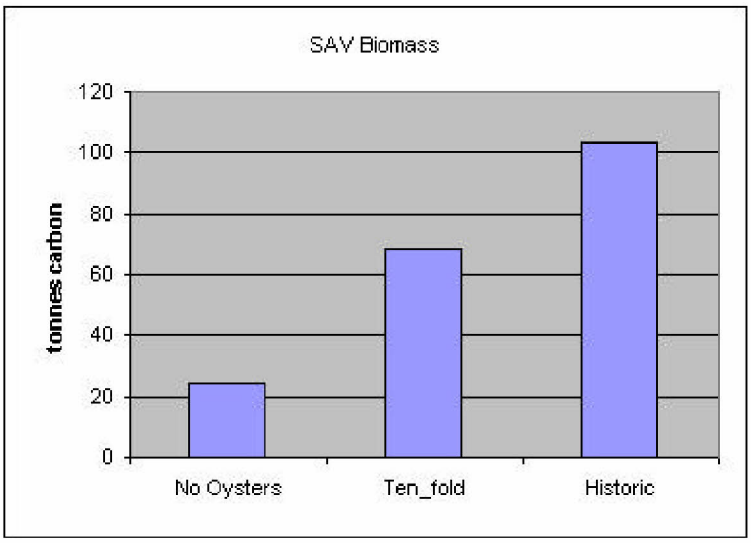

Figure 35. Effect of oysters on summer-average SAV biomass in ET9.

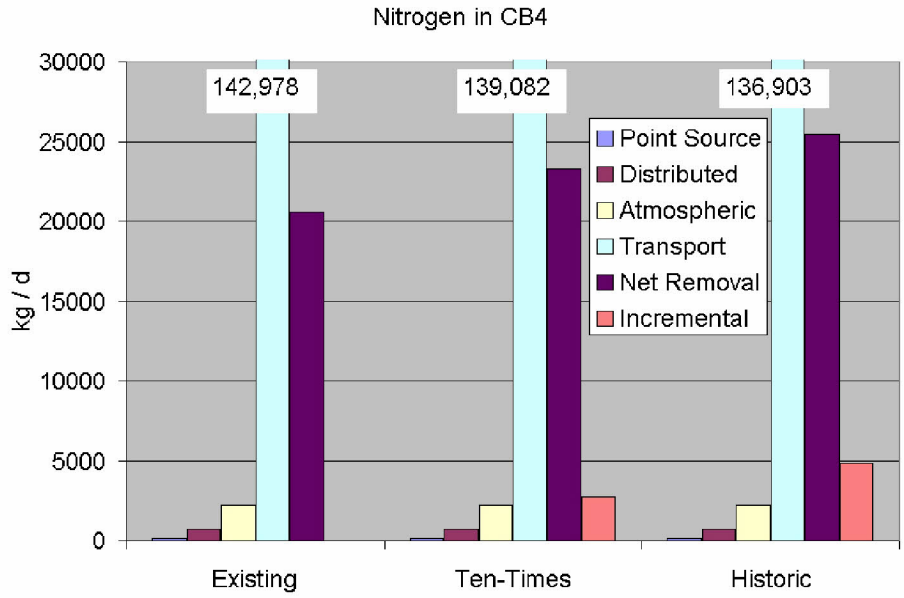

Figure 36. Effect of oysters on nitrogen budget in CB4.

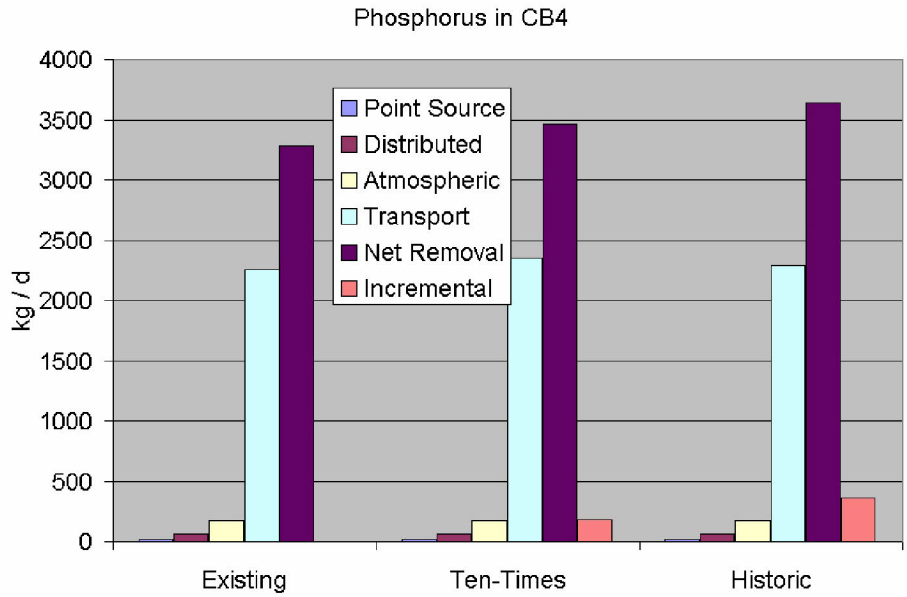

Figure 37. Effect of oysters on phosphorus budget in CB4.

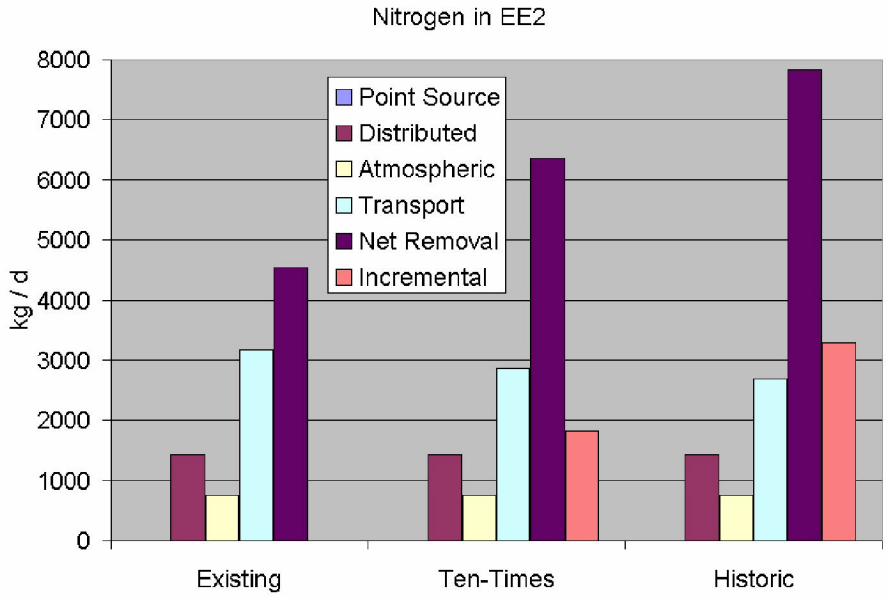

Figure 38. Effect of oysters on nitrogen budget in EE2.

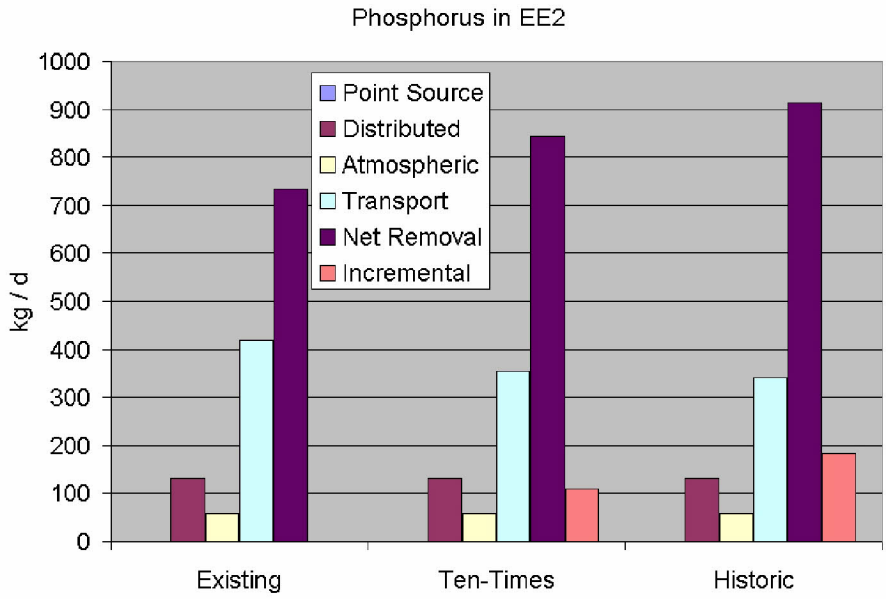

Figure 39. Effect of oysters on phosphorus budget in EE2.

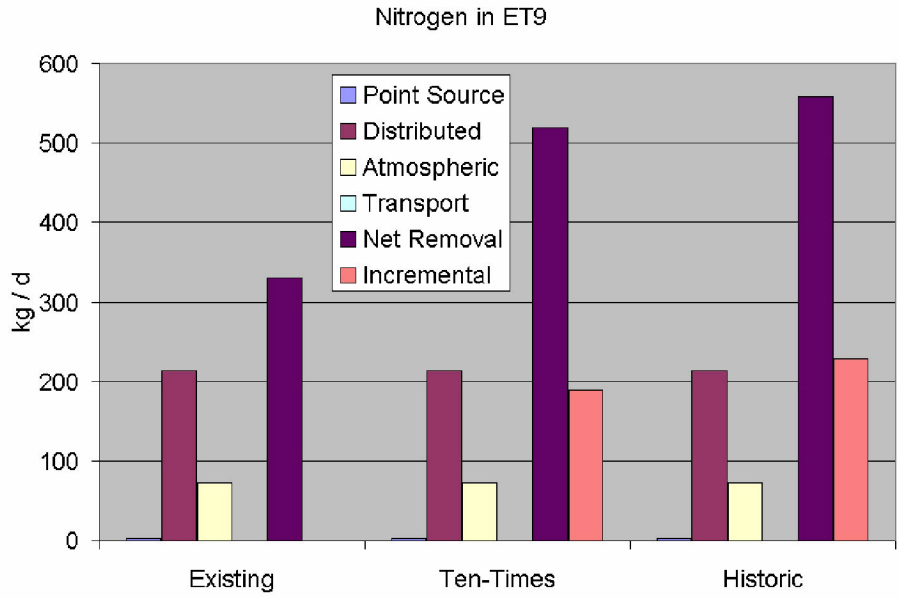

Figure 40. Effect of oysters on nitrogen budget in ET9.

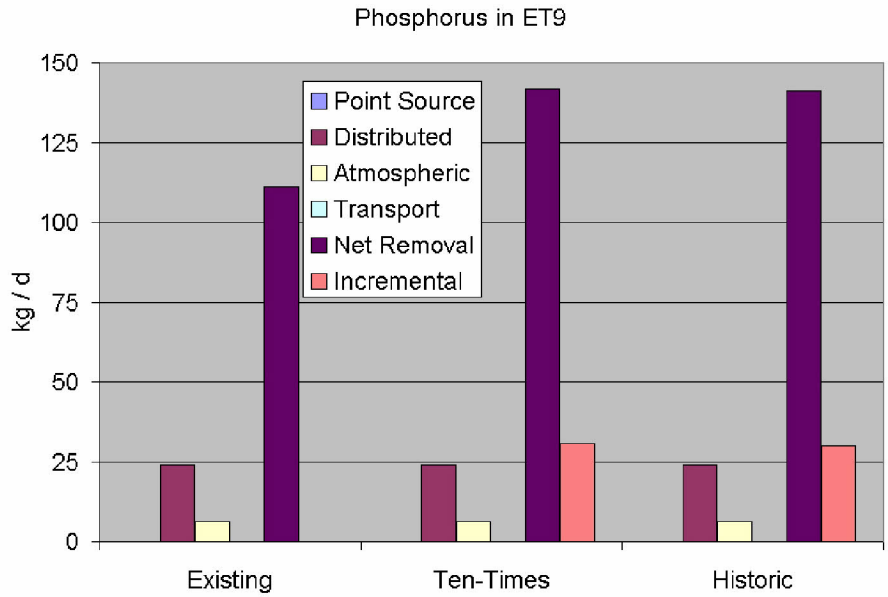

Figure 41. Effect of oysters on phosphorus budget in ET9.

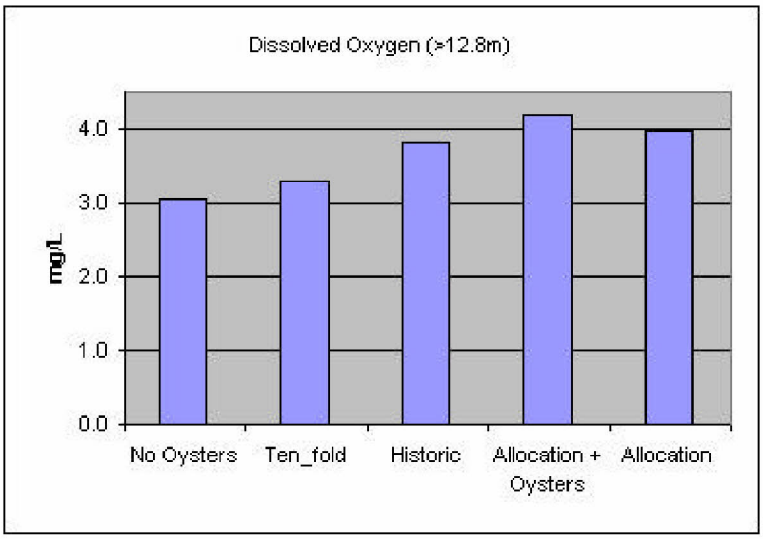

Figure 42. Effect of oysters on system-wide summer-average, bottom, dissolved oxygen.

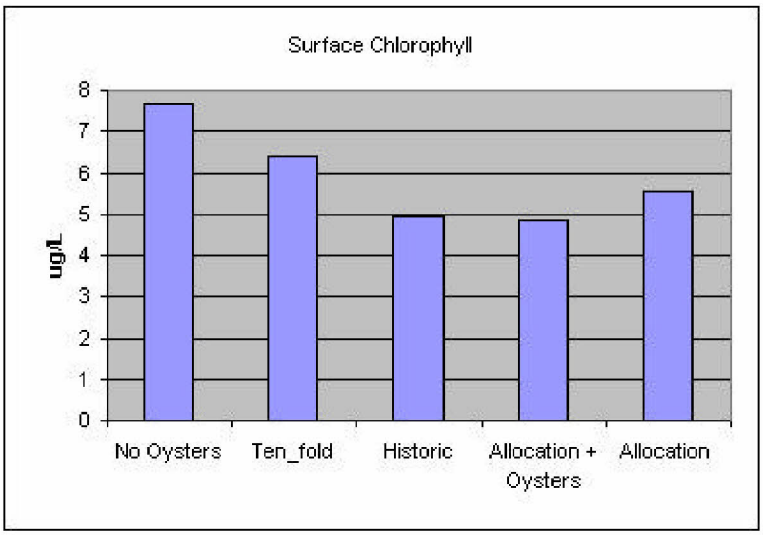

Figure 43. Effect of oysters on system-wide, summer-average, surface chlorophyll.

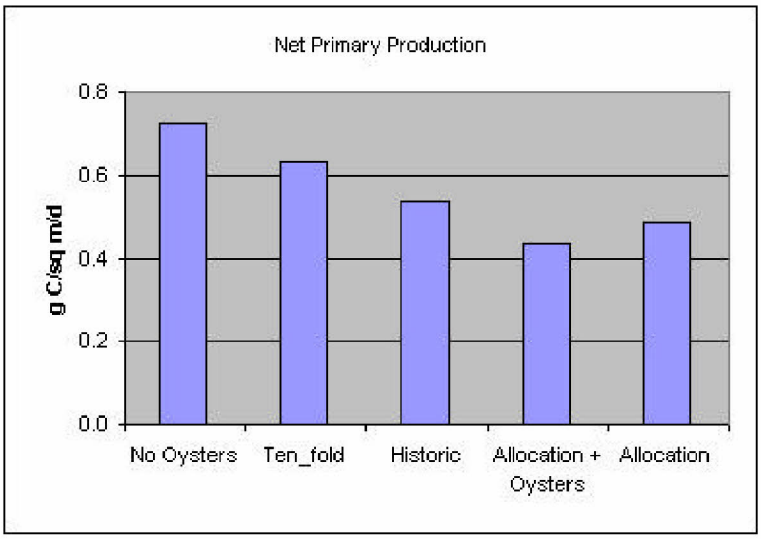

Figure 44. Effect of oysters on system-wide, annual-average, net phytoplankton primary production.

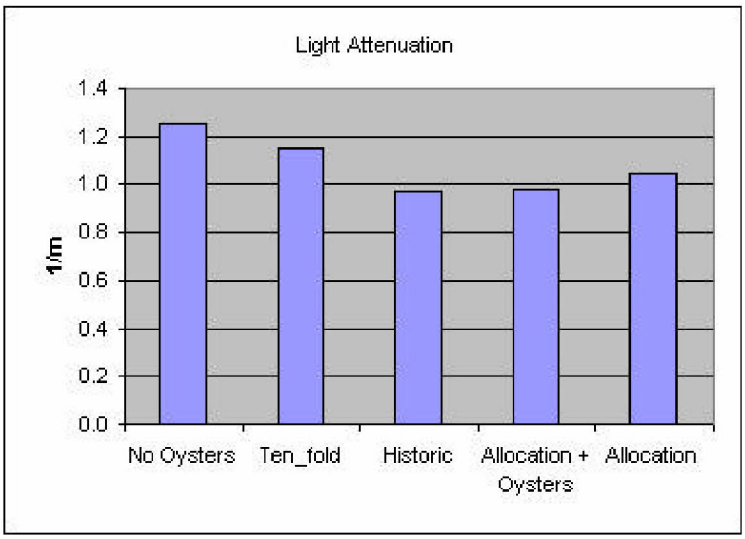

Figure 45. Effect of oysters on system-wide, summer-average, light attenuation.

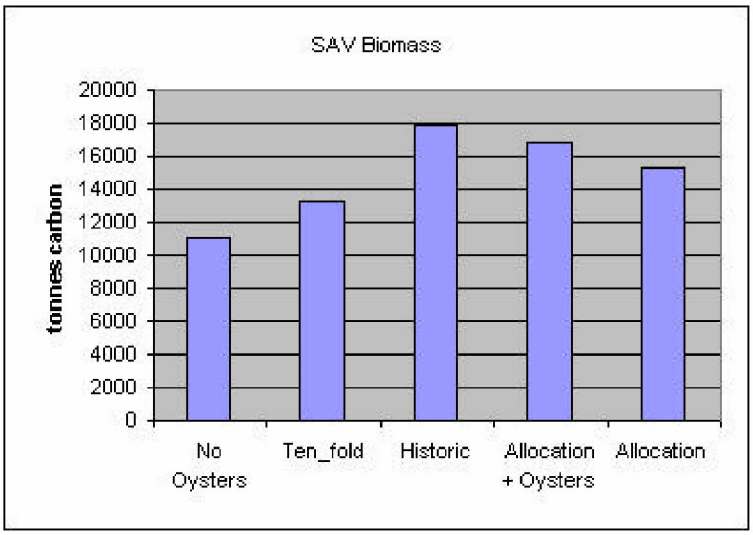

Figure 46. Effect of oysters on system-wide, summer-average, SAV biomass.

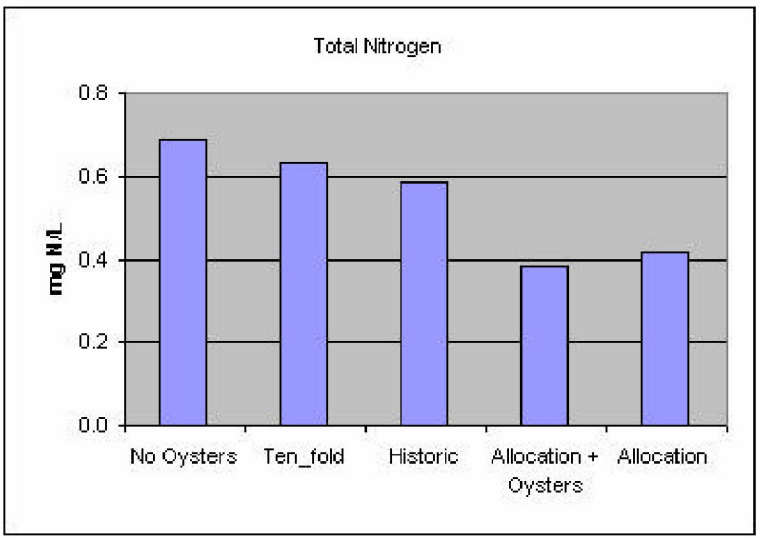

Figure 47. Effect of oysters on system-wide, annual-average, surface, total nitrogen.

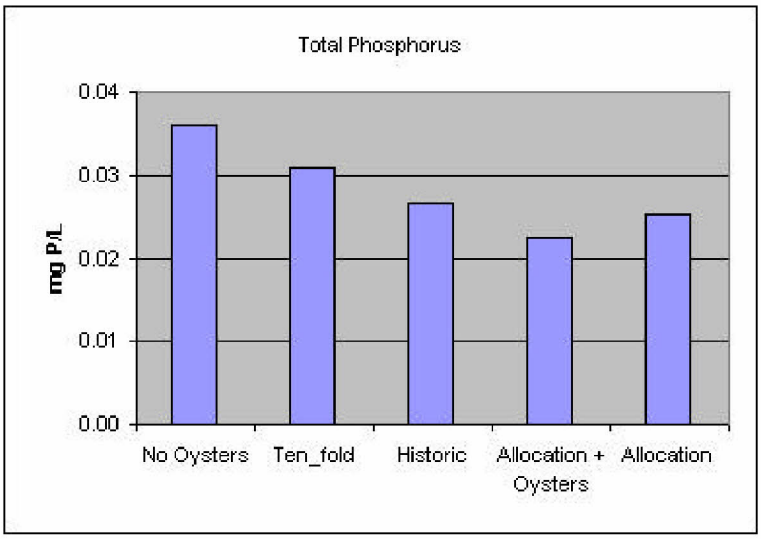

Figure 48. Effect of oysters on system-wide, annual-average, surface, total phosphorus.

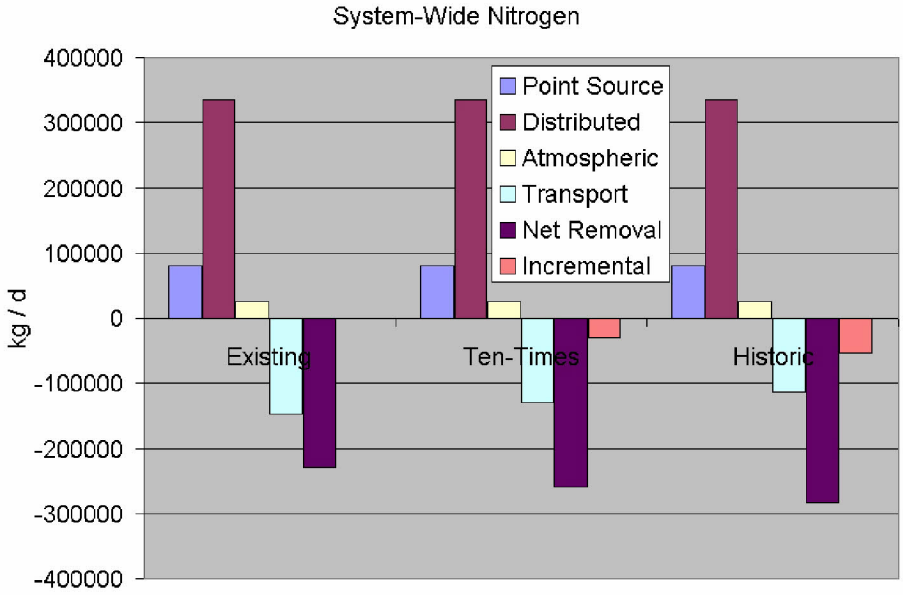

Figure 49. Effect of oysters on system-wide nitrogen budget.

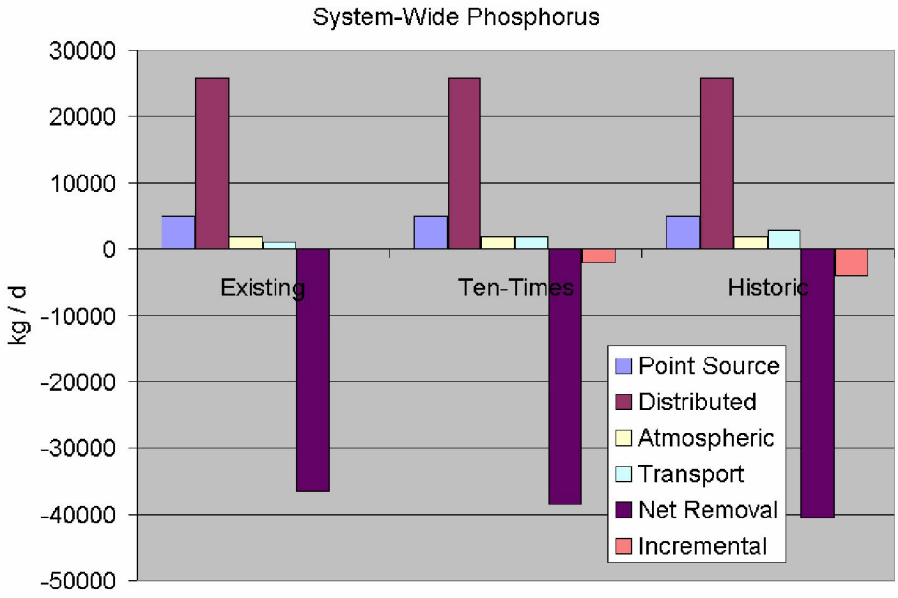

Figure 50. Effect of oysters on system-wide phosphorus budget.

5 Discussion and Conclusions

Analysis of the oyster modeling is like peeling the proverbial onion. There's always another layer to be examined. Every insight produces two more questions. Sufficient model runs have been conducted to resolve the oyster issue raised by the Chesapeake Bay 2000 Agreement:

> By 2004, assess the effects of different population levels of filter feeders such as menhaden, oysters and clams on Bay water quality and habitat.

Additional examination of the runs can be conducted and fruitful insights remain to be obtained. The production of this report is motivated by the need to produce tangible, citable, documentation of the work completed to date.

Oyster restoration will, no doubt, benefit the bay environment. Our analyses indicate the chief benefit will be restoration of SAV, brought about by filtration of solids from the water column. The most significant conclusion from our work, however, is that oyster restoration is no panacea for the host of environmental problems that plague the bay. Oyster restoration should be viewed as one of many contributions to remediation of the bay's problems.

Our work did not target specific regions of the bay with specific levels of restoration. Rather, target levels for system-wide biomass were attained and the spatial distribution of oysters was calculated dynamically based on computed environmental factors including salinity, suspended solids, and available food. Potential spatial distribution was limited to historic oyster beds. As a result of our approach, the modeled ten-fold increase in oyster biomass multiplied oysters in the Maryland portion of the bay by 50 times while the Virginia portion of the bay received only a four-fold increase, primarily in the lower James and Rappahannock Rivers. Consequently, our ten-fold increase probably exaggerates the benefits to be obtained by ten-fold increases in local oyster densities in the northern bay.

Our work indicates a ten-fold oyster increase will improve summer-average, bottom, dissolved oxygen by ~ 0.3 g m^{-3} in the portion of the mainstem plagued by the worst anoxia. Oyster restoration alone is not likely to bring the deep channel of the mainstem into compliance with dissolved oxygen standards. A dissolved oxygen increase of 0.3 g m^{-3} has economic value when traded off against the costs of nutrient controls. Some portions of the bay that marginally violate dissolved oxygen standards will marginally meet the standards when improved by 0.3 g m^{-3}. System-wide, the combination of oyster restoration

and the recent nutrient allocations are calculated to increase summer-average, bottom, dissolved oxygen by ~ 1.1 g m^{-3}.

Multiple reasons can be offered for the absence of more significant dissolved oxygen response to oyster restoration. The obvious explanation is that oysters are found in the shoals rather than over the deep trench. Phytoplankton production over the trench remains free to settle to bottom waters and contribute to anoxia. A more subtle explanation lies in the origins of mainstem anoxia. Oxygen depletion in the upper bay does not originate solely with excess production in the overlying waters. Rather, oxygen depletion is accumulated as net circulation moves bottom water up the channel from the mouth of the bay. This mechanism was originally proposed by Kuo et al. (1991) for the Rappahannock River and has been shown to apply to the mainstem bay as well (Cerco 1995). Improvement in upper bay dissolved oxygen requires reduction in lower bay oxygen demand. The oyster restoration strategy does nothing to diminish oxygen demand in the lower bay and, consequently, has limited impact on the upper bay.

Our work indicates oyster restoration removes both nitrogen and phosphorus from the bay water column. Nitrogen removal is more significant than phosphorus removal since nitrogen is the nutrient that contributes to excess algal production in the portions of the bay occupied by oysters (Fisher et al. 1992, Malone et al. 1996). We calculate the ten-fold increase in oyster biomass removes 30,000 kg d^{-1} total nitrogen from the system via enhanced denitrification and retention in the sediments. This removal can be put into perspective by noting the Susquehanna River provides ~ 150,000 kg d^{-1} total nitrogen to the mainstem while point sources in the Baltimore vicinity provide ~ 15,000 kg d^{-1} (Cerco and Noel 2004). Oyster restoration may substitute for a major upgrade in point-source controls but does not offset the larger distributed loading from the watershed.

The comparison above does not address timing. Loads from the watershed arrive largely during spring runoff and occasionally as autumn tropical storms. Removal via oysters occurs during the warm months concurrent with peak algal production. This issue introduces the question of primary "services" provided by oysters. We suggest the primary service is direct grazing on algae. Rather than quantifying the amount of nitrogen removed by oysters, we should ask what load reductions produce reductions in algal biomass equivalent to the reductions from grazing. Nutrient removal is a byproduct of grazing. In order for nutrient removal to have value, it must be shown that the removal enhances limits to algal production. The model can provide insights in this regard and additional examination is warranted.

Our model provides unique capability to address oyster restoration in the bay. We believe ours is the first approach to combine detailed representation of the bay geometry with mechanistic representations of three-dimensional transport, water-column eutrophication processes, sediment diagenetic processes, and dynamic computation of oyster biomass. Due to the large number of computed interactions, exact quantification of benefits such as SAV biomass improvement involves uncertainty. We believe, however, our basic findings regarding the nature and magnitude of restoration benefits are valid. Our results

are consistent with the earlier findings of Officer et al (1992) and Gerritson et al. (1994) and with the recent findings of Newell and Koch (2004). Benthic controls of algal production are most effective in shallow, spatially-limited regions. In these shallow regions, oyster removal of solids from the water column enhances adjacent SAV beds. The ability to influence deep regions of large spatial extent is limited by the location of oysters in the shoals and by exchange processes between the shoals and deeper regions.

The potential improvements obtained by oyster restoration are also limited by factors not considered in the model. Disease is an obvious limitation. Habitat destruction has also been suggested as an impediment (Rothschild et al. 1994). We recommend that oyster restoration be targeted to specific areas with suitable environments and that resulting environmental improvements be viewed on similar, local scales.

References

Cerco, C. (1995). "Response of Chesapeake Bay to nutrient load reductions," *Journal of Environmental Engineering*, 121(8), 549-557.

Cerco, C., and Noel, M. (2004). "The 2002 Chesapeake Bay eutrophication model," EPA 903-R-04-004, Chesapeake Bay Program Office, US Environmental Protection Agency, Annapolis, MD.

Fisher T, Peele E, Ammerman J, Harding L (1992). Nutrient limitation of phytoplankton in Chesapeake Bay. Mar Ecol Prog Ser 82:51-63

Gerritsen, J., Holland, A., and Irvine, D. (1994). "Suspension-feeding bivalves and the fate of primary production: An estuarine model applied to Chesapeake Bay," *Estuaries*, 17(2), 403-416.

Kuo, A., Park, K., and Moustafa, Z. (1991). "Spatial and temporal variabilities of hypoxia in the Rappahannock River, Virginia," *Estuaries*, 14(2), 113-121.

Malone T, Conley D, Fisher T, Glibert P, Harding, Sellner K (1996). Scales of nutrient-limited phytoplankton productivity in Chesapeake Bay. Estuaries 19:371-385

Newell, R., and Koch, E. (2004). "Modeling seagrass density and distribution in response to changes in turbidity stemming from bivalve filtration and seagrass sediment stabilization," *Estuaries*, 27(5), 793-806.

Officer, C., Smayda, T., and Mann, R. (1982). "Benthic filter feeding: A natural eutrophication control," *Marine Ecology Progress Series*, 9, 203-210.

Rothschild, B., Ault, J., Goulletquer, P., and Heral, M. (1994). "Decline of the Chesapeake Bay oyster population: a century of habitat destruction and overfishing," Marine Ecology Progress Series, 111, 29-39.